

University of Windsor

## Scholarship at UWindor

---

Electronic Theses and Dissertations

Theses, Dissertations, and Major Papers

---

8-27-2019

# Design and Preparation of Stretchable Semiconductors Through Polymer Blending

Mariia Selivanova  
*University of Windsor*

Follow this and additional works at: <https://scholar.uwindsor.ca/etd>

---

### Recommended Citation

Selivanova, Mariia, "Design and Preparation of Stretchable Semiconductors Through Polymer Blending" (2019). *Electronic Theses and Dissertations*. 7788.  
<https://scholar.uwindsor.ca/etd/7788>

This online database contains the full-text of PhD dissertations and Masters' theses of University of Windsor students from 1954 forward. These documents are made available for personal study and research purposes only, in accordance with the Canadian Copyright Act and the Creative Commons license—CC BY-NC-ND (Attribution, Non-Commercial, No Derivative Works). Under this license, works must always be attributed to the copyright holder (original author), cannot be used for any commercial purposes, and may not be altered. Any other use would require the permission of the copyright holder. Students may inquire about withdrawing their dissertation and/or thesis from this database. For additional inquiries, please contact the repository administrator via email ([scholarship@uwindsor.ca](mailto:scholarship@uwindsor.ca)) or by telephone at 519-253-3000ext. 3208.

# **DESIGN AND PREPARATION OF STRETCHABLE SEMICONDUCTORS THROUGH POLYMER BLENDING**

By

Mariia Selivanova

A Thesis  
Submitted to the Faculty of Graduate Studies  
Through the Department of Chemistry and Biochemistry  
in Partial Fulfillment of the Requirements for  
the Degree of Masters of Science  
at the University of Windsor

Windsor, Ontario, Canada

2019

© 2019 Mariia Selivanova

**DESIGN OF EXTRINSICALLY STRETCHABLE SEMICONDUCTORS THROUGH  
POLYMER BLENDING**

by

Mariia Selivanova

APPROVED BY:

---

J. Ahamed

Department of Mechanical, Automotive and Materials Engineering

---

T. Carmichael

Department of Chemistry & Biochemistry

---

S. Rondeau-Gagné, Advisor

Department of Chemistry & Biochemistry

August 27, 2019

## DECLARATION OF CO-AUTHORSHIP/PREVIOUS PUBLICATION

### I. Co-Authorship

I hereby declare that this thesis incorporates material that is result of joint research, as follows:

Chapter 3 of the thesis was co-authored with Ching-Heng Chuang, Blandine Billet, Aleena Malik, Peng Xiang, Eric Landry, and Yu-Cheng Chiu under the supervision of Prof. Simon Rondeau-Gagné. The key ideas, primary contributions, experimental designs, data analysis, interpretation, and writing were performed by the author, and the contribution of co-authors was primarily through device fabrication and characterization. Blandine Billet and Aleena Malik contributed to the characterization of the polymer blend systems; Yu-Hsuan Chen and Ching-Heng Chuang completed transistor fabrication and measurements; Peng Xiang and Eric Landry provided a branched polyethylene (BPE) derivative from PolyAnalytik company. All authors provided feedback and editions to the published manuscript. All authors have given approval to the final version of the manuscript. Chapter III was adapted with permission from Ref. 29. (Chapter IV) copyright 2019 American Chemical Society.

Chapter 4 of the thesis was co-authored with Blandine Billet, Song Zhang, Audithya Nyayachavadi, Aleena Malik, Peng Xiang, Eric Landry, Xiaodan Gu, under the supervision of Prof. Simon Rondeau-Gagné. The main ideas and contributions, as well as writing were performed by the author, while the significant input of the co-authors was primarily through the data analysis and characterization. Blandine Billet and Aleena Malik helped to study the stretchability of the polymer blend systems; Audithya Nyayachavadi helped to acquire the grazing incidence X-ray diffraction (GIXRD) data at the Canadian Light source at beamline HXMA; Zhang Song

completed the determination of the Young's modulus as well as processed the GIXRD data; Peng Xiang and Eric Landry provided a branched polyethylene (BPE) derivative from PolyAnalytik company. All authors provided feedback and editions to the published manuscript.

I am aware of the University of Windsor Senate Policy on Authorship and I certify that I have properly acknowledged the contribution of other researchers to my thesis and have obtained written permission from each of the co-author(s) to include the above material(s) in my thesis.

I certify that, with the above qualification, this thesis, and the research to which it refers, is the product of my own work.

## II. Previous Publications

This thesis includes one original paper that have been previously published in peer reviewed journal of *ACS Applied Materials and Interfaces*, as follows:

Thesis Chapter	Publication title/full citation	Publication status*
<i>Chapter 3</i>	<b>Selivanova, M.; Chuang, C.; Billet, B.; Malik, A.; Xiang, P.; Landry, E.; Chiu, Y.; Rondeau-Gagné, S. Morphology and Electronic Properties of Semiconducting Polymer and Branched Polyethylene Blends. <i>ACS Appl. Mater. Interfaces</i> 2019, <i>11</i>, 12723–12732.</b>	<i>Published</i>
<i>Chapter 4</i>	<b>Branched Polyethylene as a Plasticizing Additive to Modulate the Mechanical Properties of <math>\pi</math>-conjugated Polymers, 2019</b>	<i>Submitted</i>

I certify that I have obtained a written permission from the copyright owner(s) to include the above published material(s) in my thesis. I certify that the above material describes work completed during my registration as a graduate student at the University of Windsor.

### III. General

I declare that, to the best of my knowledge, my thesis does not infringe upon anyone's copyright nor violate any proprietary rights and that any ideas, techniques, quotations, or any other material from the work of other people included in my thesis, published or otherwise, are fully acknowledged in accordance with the standard referencing practices. Furthermore, to the extent that I have included copyrighted material that surpasses the bounds of fair dealing within the meaning of the Canada Copyright Act, I certify that I have obtained a written permission from the copyright owner(s) to include such material(s) in my thesis.

I declare that this is a true copy of my thesis, including any final revisions, as approved by my thesis committee and the Graduate Studies office, and that this thesis has not been submitted for a higher degree to any other University or Institution.

## ABSTRACT

A new strategy for influencing the solid-state morphology of conjugated polymers was developed through physical blending with a low molecular weight branched polyethylene (BPE). This non-toxic and low boiling point additive was blended with a high charge mobility diketopyrrolopyrrole (DPP)-based conjugated polymer and a detailed investigation of both electronic (Chapter III) and mechanical (Chapter IV) properties was performed. The new blended materials were characterized by various techniques, including X-ray diffraction, UV-Vis spectroscopy and atomic force microscopy (AFM). Interestingly, the branched additive was shown to reduce the crystallinity of the conjugated polymer, while promoting aggregation and phase separation in the solid-state. The performance of the new branched polyethylene/conjugated polymer blends was also investigated in organic field-effect transistors, which showed a stable charge mobility, independent of the blending ratio. Furthermore, by using the new BPE additive, the amount of conjugated polymer required for the fabrication of organic field-effect transistor devices was reduced down to 0.05 wt.%, without affecting charge transport, which is very promising in a large-scale fabrication of organic-field effect transistors (OFET) devices. Moreover, BPE additive acts as a plasticizer, thus drastically decreasing the crystallinity of conjugated polymers which is beneficial for the development of stretchable and flexible electronic devices. The incorporation of BPE amount to the conjugated polymer leads to an increase of the crack onset strain of polymer blends and decrease in the number of cracks, as well as their width. Our results demonstrate that the physical blending of conjugated polymer with non-toxic, low-molecular weight BPE is a promising strategy for the modification and fine-tuning of the solid-state morphology of conjugated polymers without sacrificing their charge transport properties, thus creating new opportunities for the large-scale processing of organic semiconductors.

## **DEDICATION**

This thesis is dedicated to my beloved parents, brother and my boyfriend who have always been a constant source of support, encouragement, inspiration and gave me strength when I thought of giving up, who continually provided me with moral, emotional and financial support.



## ACKNOWLEDGEMENTS

I would first like to thank my thesis supervisor Dr. Rondeau-Gagné for inviting me to join his research group. It has been a great opportunity and pleasure to do the research within his lab and learn many useful skills as well as gain tremendous experience working with various characterization techniques. He was always open and ready to answer any question or give a piece of advice whenever I was struggling with any issue about my research, even though he was very busy during the day. He taught me to solve problems, never give up, try to do the experiments once again if something was not working and most importantly, he was leading me in the right direction throughout the past two years. I would also like to thank all members of the Rondeau-Gagné Research Group, particularly Michael Ocheje who has been very helpful with introducing me to the research of the group and sharing his gained skills since I joined the group. To all the members of SRG Research Group: Julia, Blake, Gage, Nazir and Adit, thank you for your support, encouragement, help, and enjoyable experience we have shared together.

I would also like to acknowledge Dr. Tricia Breen Carmichael as an internal second reader of this thesis, and I am grateful for her very valuable comments on this thesis and great suggestions for the future work during the committee meetings. Additionally, I want to thank her for providing a great course about surface chemistry that was very useful and helpful in the field of my research. I also want to thank Dr. Jalal Ahamed as my external second reader from the Department of Mechanical, Automotive, and Materials Engineering for the comments on this thesis.

Finally, I want to express a very special gratitude to my parents, brother and boyfriend for providing me with very needed support and continuous encouragement throughout these hard years of studying, working and doing my research. To my parents and brother, thank you for working long hours to pay the tuition which I know is very expensive for international students.

You did everything so that I have an opportunity to succeed in life and this accomplishment would not have been possible without you. To my dad, thank you for being a role model for me, you always encouraged me to study abroad and have a better life. Since I was a kid you motivated me to learn English language and I knew you were spending last money on our education without having a vocation for yourself. Thank you.

With that said, I would like to once again thank Dr. Simon Rondeau-Gagné for giving me the opportunity to join his group I will always be grateful for.

## TABLE OF CONTENTS

<b>DECLARATION OF CO-AUTHORSHIP/PREVIOUS PUBLICATION.....</b>	<b>iii</b>
<b>ABSTRACT.....</b>	<b>vi</b>
<b>ACKNOWLEDGEMENTS .....</b>	<b>viii</b>
<b>LIST OF TABLES .....</b>	<b>xii</b>
<b>LIST OF FIGURES .....</b>	<b>xiii</b>
<b>LIST OF ABBREVIATIONS .....</b>	<b>xxii</b>
<b>CHAPTER I. INTRODUCTION .....</b>	<b>1</b>
1.1. Organic Electronics and their Applications .....	1
1.2. Organic Electronics in Comparison to Inorganic Electronics .....	2
1.3. Semiconducting Conjugated Polymers .....	5
1.4. Determination of the Electronic and Mechanical Properties of Conjugated Polymers..	10
1.4.1. Evaluation of the Electronic Properties.....	10
1.4.2. Key Methods for the Evaluation of Mechanical Properties .....	13
1.5. Approaches toward Stretchability .....	18
1.5.1. Strain Engineering.....	19
1.5.2. Molecular Design .....	19
1.5.3. Physical Blending Between Conjugated Polymer and Soft Elastomers.....	22
1.6. Scope of Thesis .....	27
<b>REFERENCES.....</b>	<b>29</b>
<b>CHAPTER II. EXPERIMENTAL PROCEDURE AND CHARACTERIZATION</b>	
<b>METHODS .....</b>	<b>47</b>
2.1. Materials .....	47
2.2. Experimental Procedure .....	47
2.3. Sample Preparation.....	49
2.4. Measurements and Characterization.....	49
2.4.1. FET Device Fabrication and Characterization .....	50
2.4.2. Film-on-water (FOW) procedure .....	51
2.4.3. Atomic Force Microscopy (AFM) .....	52
2.4.4. Grazing Incidence X-Ray Diffraction (GIXRD).....	53
2.4.5. Dichroic Ratio Measurements .....	55

2.4.6. Crack onset strain .....	55
2.4.7. Film-on-Water (FOW) Tensile Pull Test .....	56
<b>REFERENCES</b> .....	57
<b>CHAPTER III. MORPHOLOGY AND ELECTRONIC PROPERTIES OF SEMICONDUCTING POLYMER AND BRANCHED POLYETHYLENE BLENDS</b> .....	59
3.1. Introduction .....	59
3.2. Results and Discussion .....	62
3.3. Conclusion.....	77
<b>REFERENCES</b> .....	79
<b>CHAPTER IV. BRANCHED POLYETHYLENE AS A PLASTICIZING ADDITIVE TO MODULATE THE MECHANICAL PROPERTIES OF MORPHOLOGY AND ELECTRONIC PROPERTIES OF <math>\pi</math>-CONJUGATED POLYMERS</b> .....	86
4.1. Introduction .....	86
4.2. Results and Discussion .....	89
4.3. Conclusion.....	99
<b>REFERENCES</b> .....	100
<b>CHAPTER V</b> .....	105
5.1. Conclusion.....	105
5.2. Future Work and Perspectives .....	106
<b>APPENDICES</b> .....	108
APPENDIX A. CHAPTER III SUPORTING INFORMATION .....	108
APPENDIX B. CHAPTER IV SUPPORTING INFORMATION .....	118
APPENDIX C. COPYRIGHT PERMISSIONS .....	118
<b>VITA AUCTORIS</b> .....	140

## LIST OF TABLES

<b>Table 3. 1.</b> Average and maximum hole mobility ( $\mu_h^{\text{ave}}$ , $\mu_h^{\text{max}}$ ), threshold voltages ( $V_{\text{th}}$ ), $I_{\text{on}}/I_{\text{off}}$ , and ratios for OFETs fabricated from polymer blends of 0 wt.% to 90 wt.% BPE before and after thermal annealing. The device performances were averaged from 12 devices, from three different batches. Thickness was evaluated by profilometry. ....	71
<b>Table 3. 2.</b> Average and maximum hole mobility ( $\mu_h^{\text{ave}}$ , $\mu_h^{\text{max}}$ ), threshold voltages ( $V_{\text{th}}$ ), $I_{\text{on}}/I_{\text{off}}$ , and ratios for OFETs fabricated from diluted solution of various conjugated polymers blended with 98 wt.% BPE before and after thermal annealing. The device performances were averaged from 12 devices, from three different batches. Thickness was evaluated by profilometry. ....	73
<b>Table B1.</b> Average and maximum hole mobility ( $\mu_h^{\text{ave}}$ , $\mu_h^{\text{max}}$ ), threshold voltages ( $V_{\text{th}}$ ), $I_{\text{on}}/I_{\text{off}}$ , and ratios for OFETs fabricated from polymer blends of 0 wt.% to 90 wt.% BPE before and after thermal annealing. The device performances were averaged from 12 devices, from three different batches. Thickness was evaluated by profilometry. ....	118
<b>Table B2.</b> Parameters used for AFM-IR imaging of the polymer blends .....	120

## LIST OF FIGURES

<b>Figure 1. 1.</b> Most common applications in the field of organic electronics.....	2
<b>Figure 1. 2.</b> Comparison between characteristics of organic and inorganic electronics .....	3
<b>Figure 1. 3.</b> Formation of the $\pi$ -conjugation in polyacetylene polymer by the delocalization of $\pi$ -electron cloud along the polymer chain.....	6
<b>Figure 1. 4.</b> The chemical structures of most common conjugated polymers in organic electronics: a) Polyacetylene (PA); b) Polythiophene (PT); c) Polypyrrole (PP); d) Polyisothianaphthene (PPy); e) Polyethelene-dioxythiophene (PEDOT); f) Poly(3-hexyl)thiophene(P3HT); g) Polyparaphenylene vinylene (PPV); h) Poly(2,5-dialkyloxy)-paraphenylenevinylene; i) Polyparaphenylene (PPP); j) Polyheptadiyne. ....	6
<b>Figure 1. 5.</b> Charge transport in a conjugated polymer: a) intramolecular; b) intermolecular. <sup>32</sup> ...	8
<b>Figure 1. 6.</b> Microstructure of conjugated polymer thin films. a) Semi-crystalline ordered domains are favourable for good charge transport; b) semi-crystalline disordered aggregates, ideal morphology for balanced electronic and mechanical properties; c) completely amorphous film favorable for mechanical properties. <sup>40</sup> .....	9
<b>Figure 1. 7.</b> Schematic illustration of an organic field-effect transistor device .....	11
<b>Figure 1.8.</b> Schematic representation of four configurations of organic field-effect transistors: (a) bottom-gate top-contact (BG/TC); (b) bottom-gate bottom-contact (BG/BC), (c) top-gate top-contact (TG/TC), (d) top-gate bottom-contact (TG/BC) structures. <sup>46</sup> .....	11
<b>Figure 1. 9.</b> Schematic illustration of pseudo free-standing thin-film tensile tester for measuring mechanical property of floated ultrathin conjugated polymer films. ....	14
<b>Figure 1. 10.</b> The schematic illustration of tensile strain on film-on-elastomer of the thin film (red) upon releasing the strain of the substrate, where d is the wavelength of the wrinkling	

instability, $h_f$ is thickness of the thin film, $E_f$ and $E_s$ are the modulus of the film and substrate, respectively <sup>136</sup> .....	15
<b>Figure 1.11.</b> The schematic representation of the nanoindentation experiment: (a) there is no contact between the tip and sample; (b) the cantilever deflects by bending in the opposite direction ( $x$ ); (c) the deformation of the sample by the tip ( $\sigma$ ). <sup>75,76</sup> .....	17
<b>Figure 1.12.</b> Comparing main three approaches to stretchable semiconducting conjugated polymers: <b>a)</b> strain engineering; <sup>78</sup> <b>b)</b> physical blending; <sup>80</sup> <b>c)</b> backbone engineering. <sup>79</sup> .....	18
<b>Figure 1. 13.</b> Schematic illustration of molecular design strategy for the developments of the intrinsically stretchable semiconducting polymers: <b>a)</b> backbone approach which involves introducing soft and flexible blocks into the polymer backbone; <b>b)</b> side-chain approach which is based on the incorporation of various side-chains onto the polymer backbone, which can be terminated with X groups (siloxane, amide, urea groups, and others). .....	20
<b>Figure 1. 14.</b> Schematic illustrations of different spin-casted films: (a) vertically phase separated (bilayer); (b) laterally phase-separated. ....	23
<b>Figure 1. 15. a)</b> Chemical structures of semiconducting polymer poly(2,5-bis(2-octyldodecyl)-3,6-di(thiophen-2-yl)diketopyrrolo[3,4-c]pyrrole-1,4-dione-alt-thieno[3,2-b]thiophen) (DPPT-TT) and SEBS elastomer. A 3D schematic of the desired morphology composed of embedded polymer nanofibrils in elastomer matrix to achieve nanoconfinement effect; <b>b)</b> A 3D illustration of the morphology of the polymer/elastomer blend; AFM phase images of the top and bottom interfaces of the blended film with 70 wt.% of SEBS. <sup>110</sup> .....	26
<b>Figure 1. 16.</b> Chemical structure of branched polyethylene .....	28
<b>Figure 2.1.</b> Synthetic pathway towards P(DPPTVT) polymer.....	48

<b>Figure 2.2.</b> A schematic illustration of preparing a DPP-based polymer/BPE thin film under strain through film-on-water (FOW) method. ....	52
<b>Figure 2.3.</b> Schematic illustration of a typical AFM set up. ....	53
<b>Figure 2.4.</b> a) Representation of edge-on and face-on orientations of the P3HT backbone semiconducting polymer with respect to the substrate surface; Schematic illustration of the typical 2D GIXRD pattern which corresponds to b) edge-on orientation and c) face-on orientation. ....	54
<b>Figure 2.5.</b> Schematic diagram of polarized UV-vis characterization on stretched polymer blend films with the polarization direction of light a) parallel and b) perpendicular to the stretching direction. ....	55
<b>Figure 3.1.</b> Blending of low molecular weight branched polyethylene (BPE) with a DPP-based polymer for fine-tuning of the solid-state morphology. ....	61
<b>Figure 3.2.</b> a) Chemical structure of P(DPPTVT) conjugated polymer; b) chemical structure of branched polyethylene (BPE) utilized in polymer blends; c) UV-Vis spectra of P(DPPTVT) blended with 0 wt.% to 90 wt.% BPE (thin films) before thermal annealing, and d) UV-Vis spectra of P(DPPTVT) blended with 0 wt.% to 90 wt.% BPE (thin films) after thermal annealing. ....	64
<b>Figure 3.3.</b> UV-Vis spectra of P(DPPTVT) blended with 0 wt.% to 90 wt.% LPE (thin films) a) before thermal annealing, and b) after thermal annealing at 170°C. ....	65
<b>Figure 3.4.</b> UV-Vis spectra of conjugated polymer blended with a) 0 wt% LPE and b) 90 wt.% LPE before and after thermal annealing at 170°C. ....	66
<b>Figure 3.5.</b> Atomic force microscopy images (height) of 0, 50, 75 and 90 wt. BPE/P(DPPTVT) blends, before and after thermal annealing (170°C). Scale bar is 500 nm. ....	66



**Figure 3.6.** X-ray diffraction spectra (reflectance mode) of P(DPPTVT) blended with 0 to 90 wt.% BPE a) before thermal annealing and b) after thermal annealing at 170°C. The concentration of conjugated polymer was kept constant (1.5 mg/mL). ..... 69

**Figure 3.7.** Wide-angle grazing incident X-Ray diffractogram (GIXRD) of a) P(DPPTVT), b) P(DPPTVT) + 50 wt.% BPE, and c) P(DPPTVT) + 90 wt.% BPE. .... 70

**Figure 3.8.** UV-Vis spectra of P(DPPTVT) blended with 0 wt.% to 98 wt.% BPE (thin films) a) before and b) after thermal annealing; c) transfer curves for OFET devices built from P(DPPTVT) 0.05 wt.% in chlorobenzene and 98 wt.% BPE/P(DPPTVT). ..... 74

**Figure 3.9.** Wide-angle grazing incident X-Ray diffractogram (GIXRD) of a) P(DPPTVT) solution (0.05 wt.% in chlorobenzene) annealed at 170°C, b) P(DPPTVT) blended with 98 wt.% BPE after thermal annealing at 170 °C, and c) P(DPPTVT) blended with 98 wt.% BPE without thermal annealing; Atomic force microscopy (AFM) height images of thin films of d) P(DPPTVT) 0.05 wt.% in chlorobenzene, annealed at 170 °C; e) P(DPPTVT) blended with 98 wt.% BPE without thermal annealing; f) P(DPPTVT) blended with 98 wt.% BPE after annealing at 170°C. Scale bar is 200 nm. .... 76

**Figure 4.1.** Blending of low molecular weight branched polyethylene (BPE) with a DPP-based polymer for modulation of the mechanical properties..... 89

**Figure 4.2.** a) Crack on-set strain of P(DPPTVT)/BPE blends containing 0 wt.% and 90 wt.% of BPE before (left) and after (right) the formation of cracks, as observed by optical microscopy. Scale bars are 25µm; b) Crack onset strain versus the amount of BPE as determined by optical microscopy before thermal annealing..... 91

<b>Figure 4.3.</b> Atomic force microscopy – Fourier-transform infrared spectroscopy analysis of polymer blends prepared with a) 25 wt.%, b) 50 wt.%, c)75 wt.%, and d) 90 wt.% of BPE. DPP-based polymer is depicted in red/yellow and BPE is depicted in blue. ....	92
<b>Figure 4.4.</b> Atomic force microscopy images (height) of BPE/P(DPPTVT) blends containing 0 to 90 wt.% BPE at a) 10, b) 50 and c) 100% strain before thermal annealing. ....	94
<b>Figure 4.5.</b> Thin film crack width versus the amount of BPE additive for a) 25 %; b) 50%; c) 75%, and d) 100% strain elongation as determined by atomic force microscopy (AFM). ...	95
<b>Figure 4.6.</b> Elastic modulus of polymer blends with different weight ratios of BPE additive, determined by Film-On-Water tensile pull test a) before thermal annealing and b) after thermal annealing. ....	97
<b>Figure A1.</b> <sup>1</sup> H NMR spectrum of P(DPPTVT) in TCE-d <sub>2</sub> at 120°C.....	108
<b>Figure A2.</b> Boiling point of LPE and BPE additives, measured by the capillary tube method.	108
<b>Figure A3.</b> UV-Vis spectra of P(DPPTVT) blended with a) 0 wt.% BPE, b) 50 wt.% BPE, c) 75 wt.% HBPE and d) 90 wt.% BPE before and after thermal annealing for blending systems (thin films). ....	109
<b>Figure A4.</b> Atomic force microscopy images (phase) of 0, 50, 75 and 90 wt. BPE/P(DPPTVT) blends, before and after thermal annealing (170°C). Scale bar is 400 nm. ....	109
<b>Figure A5.</b> Atomic force microscopy images (height) of the top and bottom interfaces of the P(DPPTVT) film blended with 75 wt% BPE. Scale bar is 500 nm.....	110
<b>Figure A6.</b> Atomic force microscopy images (height) of 100 to 10 wt.% P(DPPTVT) solution in chlorobenzene (CB), before and after thermal annealing (200°C). Scale bar is 400 nm. ...	110
<b>Figure A7.</b> Atomic force microscopy images (phase) of 100 to 10 wt.% P(DPPTVT) solution in chlorobenzene (CB), before and after thermal annealing (200°C). Scale bar is 400 nm. ...	111

<b>Figure A8.</b> Atomic force microscopy images (height) of 0, 50 and 90 wt. LPE/P(DPPTVT) blends, before and after thermal annealing (170°C). Scale bar is 500 nm. ....	111
<b>Figure A9.</b> Wide-angle grazing incident X-Ray diffractogram (GIXRD) of P(DPPTVT) blended with 0 to 90 wt.% BPE in a) z axis, and b) x-y axis.....	112
<b>Figure A10.</b> Transfer curves for OFET devices built from 0 wt.% BPE to 90 wt.% BPE, before thermal annealing. $V_d = -60V$ .....	112
<b>Figure A11.</b> Transfer curves for OFET devices built from 0 wt.% BPE to 90 wt.% BPE, after thermal annealing. $V_d = -60V$ .....	113
<b>Figure A12.</b> Charge mobility of P(DPPTVT) diluted in chlorobenzene after annealing at 170°C (black curve) and P(DPPTVT) blended with LPE at different ratios (red curve). ....	113
<b>Figure A13.</b> Transfer curves for OFET devices built from a) highly diluted solution of P(DPPTVT) in chlorobenzene, annealed at 170 °C; b) 98 wt.% BPE, annealed at 100 °C, and c) 98 wt.% BPE annealed at 170 °C. $V_d = -60V$ .....	114
<b>Figure A14.</b> Charge mobility of P(iITVT) diluted in chlorobenzene after annealing at 170°C (black curve), P(iITVT) blended with BPE at different ratios (red curve) annealed at 170°C, and P(iITVT) blended with BPE at different ratios (blue curve) annealed at 100°C.....	114
<b>Figure A15.</b> Transfer curves for OFET devices built from pure P(iITVT) annealed at 170°C (black curve), 0.05 wt.% P(iITVT) in chlorobenzene annealed at 170°C (red curve), 98 wt.% BPE/P(iITVT) after thermal annealing at 170°C, 98 wt.% BPE/P(iITVT) after thermal annealing at 100°C. ....	115
<b>Figure A16.</b> Atomic force microscopy height images of thin film of P(DPPTVT) a) 2 wt.% solution in chlorobenzene; b) blended with 98 wt.% BPE without annealing, c) blended with	

98 wt.% BPE after annealing at 100 °C, and d) blended with 98 wt.% BPE after annealing at 170 °C.....	116
<b>Figure A17.</b> Atomic force microscopy phase images of thin film of P(DPPTVT) a) 2 wt.% solution in chlorobenzene; b) blended with 98 wt.% BPE without annealing, c) blended with 98 wt.% BPE after annealing at 100 °C, and d) blended with 98 wt.% BPE after annealing at 170 °C.....	117
<b>Figure B1.</b> A schematic illustration of preparing a DPP-based polymer/BPE thin film under strain through film-on-water (FOW) method. ....	118
<b>Figure B2.</b> Crack on-set strain of P(DPPTVT)/BPE blends containing from 25 wt.% to 75 wt.% of BPE obtained by observing the formation of cracks under optical microscope (right) and before appearance of cracks (left). Scale bars are 50µm. ....	119
<b>Figure B3.</b> Atomic force microscopy images (height) of BPE/P(DPPTVT) blends containing 0 to 90 wt.% BPE at 10% strain before thermal annealing. ....	120
<b>Figure B4.</b> Atomic force microscopy images (height) of BPE/P(DPPTVT) blends containing 0 to 90 wt.% BPE at 25% strain before thermal annealing. ....	121
<b>Figure B5.</b> Atomic force microscopy images (height) of BPE/P(DPPTVT) blends containing 0 to 90 wt.% BPE at 50% strain before thermal annealing. ....	121
<b>Figure B6.</b> Atomic force microscopy images (height) of BPE/P(DPPTVT) blends containing 0 to 90 wt.% BPE at 75% strain before thermal annealing. ....	122
<b>Figure B7.</b> Atomic force microscopy images (height) of BPE/P(DPPTVT) blends containing 0 to 90 wt.% BPE at 100% strain before thermal annealing. ....	122
<b>Figure B8.</b> Atomic force microscopy images (height) of BPE/P(DPPTVT) blends containing 0 to 90 wt.% BPE at 50% strain after thermal annealing. ....	123

**Figure B9.** Schematic diagram of polarized UV-vis characterization on stretched polymer blend films with the polarization direction of light a) parallel and b) perpendicular to the stretching direction. .... 123

**Figure B10.** Polarized UV-vis spectra of BPE/P(DPPTVT) blended system with 0 wt.% BPE stretched at different percent strains, with the polarization direction of light parallel (0°, red curve) and perpendicular (90°, black curve) to the stretching direction. .... 124

**Figure B11.** Polarized UV-vis spectra of BPE/P(DPPTVT) blended system with 25 wt.% BPE stretched at different percent strains, with the polarization direction of light parallel (0°, red curve) and perpendicular (90°, black curve) to the stretching direction. .... 124

**Figure B12.** Polarized UV-vis spectra of BPE/P(DPPTVT) blended system with 50 wt.% BPE stretched at different percent strains, with the polarization direction of light parallel (0°, red curve) and perpendicular (90°, black curve) to the stretching direction. .... 125

**Figure B13.** Polarized UV-vis spectra of BPE/P(DPPTVT) blended system with 75 wt.% BPE stretched at different percent strains, with the polarization direction of light parallel (0°, red curve) and perpendicular (90°, black curve) to the stretching direction. .... 126

**Figure B14.** Polarized UV-vis spectra of BPE/P(DPPTVT) blended system with 90 wt.% BPE stretched at different percent strains, with the polarization direction of light parallel (0°, red curve) and perpendicular (90°, black curve) to the stretching direction. .... 126

**Figure B15.** Dichroic ratios of the BPE/P(DPPTVT) blends containing a) 0 wt.%; b) 25 wt.%; c) 50 wt.%; d) 75 wt.%; and e) 90 wt.% of BPE in function of strain determined by polarized UV-Vis spectroscopy..... 127

**Figure B16.** Observations of a brittle freestanding thin film above 25 wt.% BPE obtained by Film-On-Water tensile test. .... 127

**Figure B17.** Wide-angle grazing incident X-Ray diffractogram (GIXRD) of a) P(DPPTVT), b) P(DPPTVT) + 50 wt.% BPE, and c) P(DPPTVT) + 90 wt.% BPE. .... 128

## LIST OF ABBREVIATIONS

AFM	Atomic Force Microscope
MeAN	Acetonitrile
BG-BC	Bottom-Gate Bottom-Contact
BG/TC	Bottom-Gate Top-Contact
BPD	Benzopyrrolodione
BPE	Branched Polyethylene
CB	Chlorobenzene
CBS	Conjugation-break spacer
CHCl <sub>3</sub>	Chloroform
CHN	Cyclohexanone
DBB	Dibutylbenzene
DCB	Dichlorobenzene
DPP	Diketopyrrolopyrrole
E	Elastic Modulus
FOW	Film-on-Water Tensile Test
GIXRD	Grazing-Incidence X-ray Diffraction
IDT	Indacenodithiophene
NWs	Nanowires

OFET	Organic Field-Effect Transistor
OLED	Organic Light Emitting Diode
OPV	Organic Photovoltaic
OSC	Organic Solar Cells
PA	Polyacetylene
PBA	poly(butyl acrylate)
PDCA	2,6-pyridine dicarboxamide
PDMS	Polydimethylsiloxane
PE	polyethylene
PEDOT	Polyethelene-dioxythiophene
PEDOT:PSS	poly(3,4ethylenedioxythiophene):poly(styrenesulfonate)
PET	poly(ethylene terephthalate)
PI	Poly(isoprene)
PMMA	Poly(methylmethacrylate)
PP	Polypyrrole
PPP	Polyparaphenylene vinylene
PPV	Polyparaphenylene
PPy	Polypyrrole
PS	Polystyrene
PT	Polyisothianaphthene
PTAA	Poly(triarylamine)
P3HT	Poly(3-hexyl)thiophene
SEBS	poly(styrene-ethylene-butylene-styrene)



TFT	Thin-Film Transistor
TG	Top-Gate
Tg	Glass transition temperature
THF	Tetrahydrofuran
$V_{GS(thr)}$	Threshold Voltage

## CHAPTER I. INTRODUCTION

### 1.1. Organic Electronics and their Applications

People live in an electronic world, using electronic devices in their every day life such as laptops, smartphones, digital cameras, cooking stoves and others. Due to the rapid technological advances, the market of electronic devices is currently growing towards the wearable electronics. One of the most interesting applications of these devices in a daily life are smart watches, fitness bands, sensors, however, the limitation of these electronic devices is their softness to fit the human body and move towards bioelectronics.<sup>1</sup> Therefore, the solution is the development of new organic electronic devices, using organic materials which are promising candidates due to their intrinsic softness, synthetic tunability for specific device applications with desired electronic and mechanical properties.

The field of organic electronics has attracted much attention in the scientific community and recent literature due to its large-area of applications. Nowadays, organic electronics see use in many applications including smart phones, televisions, sensors, batteries, photodetectors, organic lasers, devices which utilize light-emitting diode (OLED) displays among many others.<sup>2,3</sup> Although they offer a plethora of applications, the most interest is focused on main three types: OLEDs for displays and lighting, organic field-effect transistors (OFETs) and organic solar cells (OSC) (Figure 1.1).

In recent years the major focus of research has been done towards potential future applications of organic electronics. One of the growing and interesting area of research is development of new generation of organic electronics devices with desired properties such as flexibility, stretchability and softness that allow them to be bent, folded, twisted and stretched.

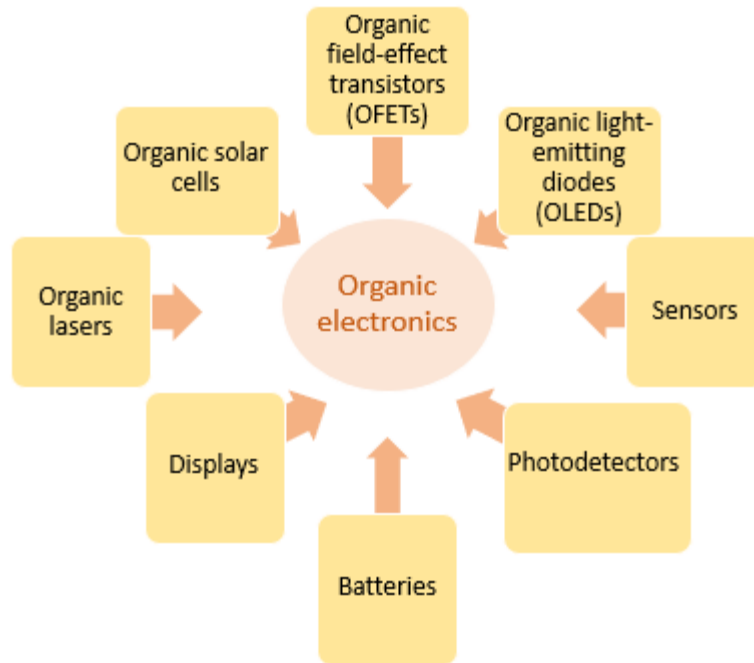


Figure 1. 1. Most common applications in the field of organic electronics

## 1.2. Organic Electronics in Comparison to Inorganic Electronics

Currently, most electronics devices are silicon-based. The main limitation of inorganic electronics is their low tolerance to mechanical stress which makes them potentially unsuitable for the development of flexible and stretchable electronic devices.<sup>4</sup> Not only do silicon-based devices possess low mechanical compliance, they also have high manufacturing costs, complex processing, small areas of fabrication that is not ideal for printed electronics.

These challenges have led to the increased development of organic electronics which promise low manufacturing costs, simple processing, and the ability to be made flexible, stretchable and solution-processed over large areas of fabrication (Figure 1.2.).

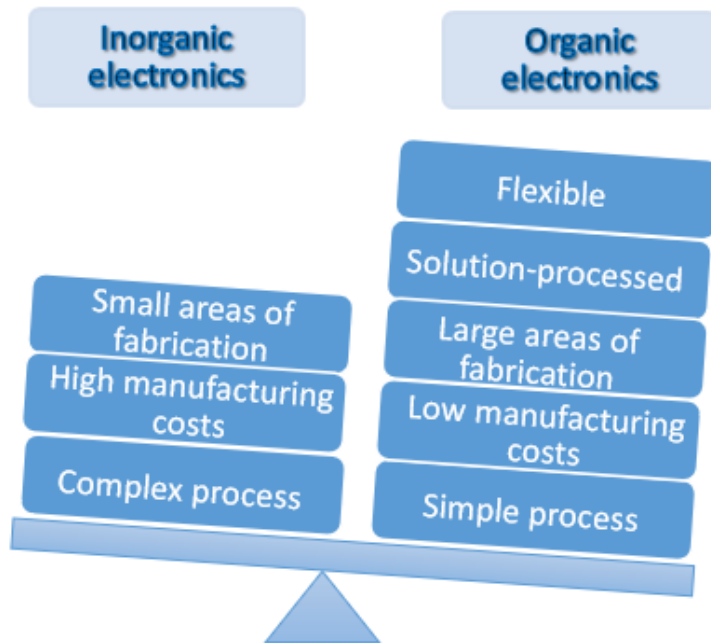


Figure 1. 2. Comparison between characteristics of organic and inorganic electronics

The development of new organic electronic materials with better performance and desired properties is a growing field of research. One novel feature of this new generation of organic electronics is flexibility.<sup>5</sup> Flexible devices must have high strain tolerance and at the same time high electronic performance which is unaffected by applied strain. It is important to realize that the term flexible can mean a range of various deformations such as bendable, foldable, rollable, permanently shaped, or non-breakable.<sup>6,7</sup>

The history of flexible electronics is longer than one may expect. The development of flexible electronics began in the 1960s. The first flexible solar cell arrays were made by shrinking silicon wafer cells to around 100 $\mu$ m and then assembling them on a plastic substrate to achieve flexibility.<sup>8</sup> The first thin-film transistor (TFT) was reported in 1968. Brody and colleagues made a TFT of tellurium on a strip of paper and subsequently designed TFTs on such flexible substrates as polyethylene and anodized aluminum foil. Interestingly, the TFTs maintained their performance

while bent to a  $1/16''$  radius. Moreover, they could be cut in two halves along the channel directions and continued to function.<sup>9,10</sup> One major breakthrough was the discovery and development of conductive polymers by Alan G. MacDiarmid, Alan J. Heeger and Hideki Shirakawa who were awarded the 2000 Nobel prize in Chemistry.<sup>11</sup>

The main three types of materials required for organic electronics are insulators, conductors and semiconductors.<sup>12</sup> One type of materials utilized in organic electronics is insulators (quartz, rubber) which do not allow the electric current to pass through them. Even though these materials remain non-conductive, they are no less critical for the operation of several electronic devices. For example, the dielectric material (glass, oxides of various metals) is a type of an insulator which becomes polarised in the presence of the electric field and used in OFETs to insulate the gate from the rest of the device.<sup>16</sup> Metals (silver, gold) are the best-known electronic conductors since it requires very little energy for the electrons to enter the conduction band. The conductivity of metallic films is around  $10^4$ - $10^6$  S/cm.<sup>6</sup> The key challenge of using conductors for the stretchable and flexible electronic devices is that metal films are often found to be mechanically inadequate.<sup>13,14</sup> This leads to the use of polymeric materials which naturally have some degree of mechanical compliance and represent another type of materials in organic electronics as semiconductors. One of the most used organic polymers in organic electronics is the polythiophene derivative poly(3,4-ethylenedioxythiophene):poly(styrenesulfonate) (PEDOT:PSS) with the conductivity greater than 1000 S/cm.<sup>15</sup>

In general, the control of the band gap of the semiconducting polymers has attracted much attention in the research of organic electronics and their use is growing towards the development of flexible, stretchable and highly conductive electronic devices.<sup>17</sup> Among other materials, semiconducting conjugated polymers possess the advantages of low cost, light weight, solution

processability and having naturally some degree of mechanical compliance, thus providing the opportunity to make the next generation of electronics devices.<sup>18</sup>

Despite all the progress, researchers continue to improve the synthesis of conjugated polymers towards the use in organic electronics that will lead to better performing solar cells, transistors, electronic displays and lights. The future researches aim to make flexible, stretchable electronic devices with long lifetimes that are recyclable or even biodegradable.

### **1.3. Semiconducting Conjugated Polymers**

One of the main building blocks for organic electronics are semiconductors.<sup>7</sup> Polymers are promising candidates for flexible organic electronics due to their low mechanical stiffness, large area fabrication, low temperature processing (lower cost), and most importantly the ability to be tuned for specific device applications.<sup>19,20</sup>

Organic semiconducting materials are classified as small molecules or conjugated polymers that have their backbone built through  $sp^2$  hybridization. In such configuration  $\pi$ -bonds are responsible for electronic properties of conjugated polymers since the  $\pi$ -electron clouds are delocalized throughout the polymer chain over the entire structure which in turn allows for fast charge-carrier movement along the polymer backbone.<sup>5</sup> The  $\pi$ -conjugation is illustrated on the polyacetylene polymer in Figure 1.3.<sup>21,22</sup> The most common conjugated polymers in organic electronics are illustrated in Figure 1.4.<sup>23</sup>

The great breakthrough in the field of organic electronics was the ability to decrease the band gap of conjugated polymers *via* alternating electron-rich (donor) and electron-deficient substituents (acceptor) along the conjugated backbone of semiconducting polymer. Interaction of the donor-acceptor building blocks enhances the nature of the double bond between the repeating units which leads to the stabilization of a low band gap within the polymer backbone.<sup>24,25</sup>

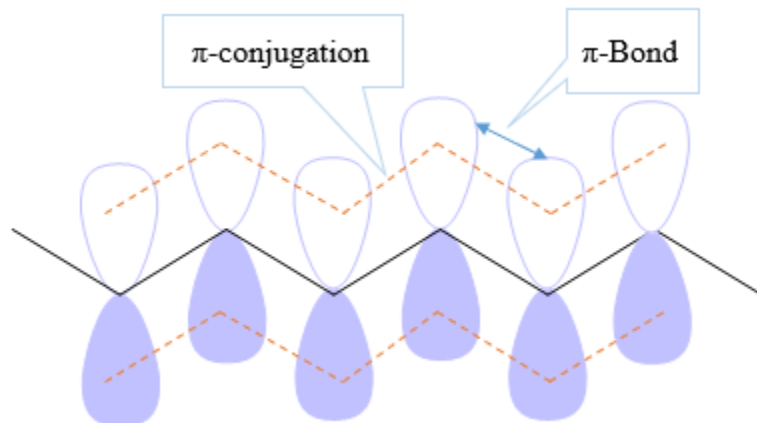


Figure 1. 3. Formation of the  $\pi$ -conjugation in polyacetylene polymer by the delocalization of  $\pi$ -electron cloud along the polymer chain.

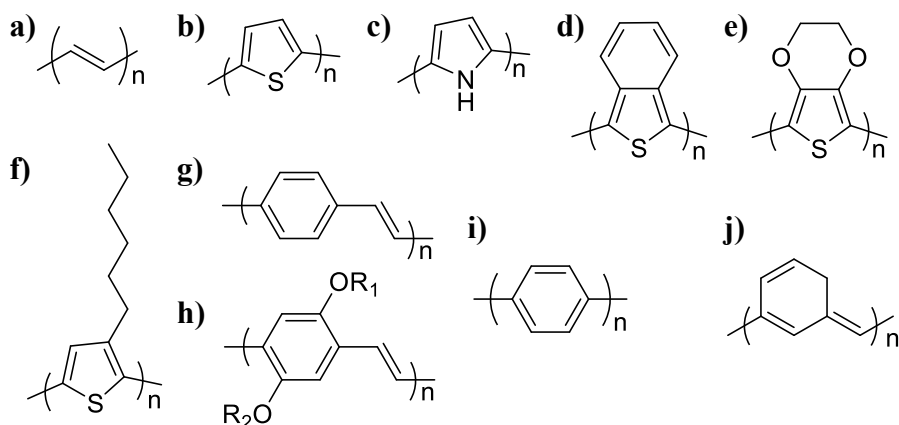


Figure 1. 4. The chemical structures of most common conjugated polymers in organic electronics: a) Polyacetylene (PA); b) Polythiophene (PT); c) Polypyrrole (PP); d) Polyisothianaphthene (PPy); e) Polyethelene-dioxythiophene (PEDOT); f) Poly(3-hexyl)thiophene(P3HT); g) Polyparaphenylene vinylene (PPV); h) Poly(2,5-dialkyloxy)-paraphenylenevinylene; i) Polyparaphenylene (PPP); j) Polyheptadiyne.

It is important to note that there are two kinds of extrinsic semiconductor: *p*-type (positively charged carries -holes); *n*-type (negatively charged carriers -electrons). *N*-type semiconductors

exhibit lower carrier mobility and are found to be more sensitive to surrounding conditions, especially to oxygen and humidity. As a result, the majority of semiconductors are *p*-type, but *n*-type are also available.<sup>26</sup> Pentacene is one of the most extensively studied *p*-type semiconductors for OFETs and displays one of the highest mobilities of  $1.5 \text{ cm}^2\text{V}^{-1}\text{s}^{-1}$  reported in the literature.<sup>27</sup> Among others, polythiophene<sup>28</sup>, poly(3-hexylthiophene)<sup>29</sup> and tetracene<sup>30</sup> are widely used organic semiconductors for OFETs applications. Various *n*-type semiconductors are based on oligothiophenes. Facchetti *et al* reported the perfluorohexylsubstituted thiophene oligomers with mobility as high as  $0.24 \text{ cm}^2\text{V}^{-1}\text{s}^{-1}$ .<sup>31</sup>

One of the main characteristics of semiconducting polymers is charge carrier mobility which determines how fast the charge carriers move through a semiconducting material. In conjugated polymers, the charge carriers (electrons or holes) can move in two ways: intramolecularly or intermolecularly. In the intermolecular charge transport manner (Figure 1.5., way 1) the charge carriers are moving by  $\pi$ -electron delocalization along the polymer backbone. In the intermolecular charge transport (Figure 1.5., way 2) the charge carriers are moving across the  $\pi$ - $\pi$ -stacking of the polymer backbones. It is found to provide the most sufficient charge transport in semiconducting polymers, however, it is dependent on the effective conjugation length of the polymer which is limited by the disorder along the polymer backbone and the presence of chemical defects.<sup>32</sup>

The researchers were mostly studying semiconducting conjugated polymers such as polyacetylene,<sup>33</sup> polypyrrole or polythiophenes as the main components in OFETs.<sup>29,34</sup> The charge-carrier mobilities for OFETs have increased dramatically from less than  $0.01 \text{ cm}^2/\text{Vs}$  in 2000 to more than  $1\text{-}3 \text{ cm}^2\text{V}^{-1}\text{s}^{-1}$  in 2012 which is as high as amorphous silica.<sup>35</sup> Later on, the performance of conjugated polymer-based OFET reached even  $21.3 \text{ cm}^2\text{V}^{-1}\text{s}^{-1}$ .<sup>36</sup>



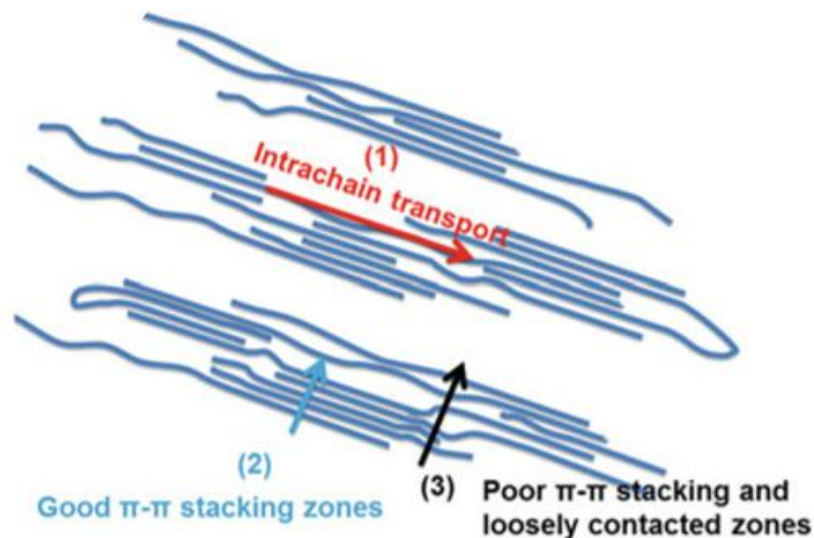


Figure 1. 5. Charge transport in a conjugated polymer: a) intramolecular; b) intermolecular.<sup>32</sup>

Although polymeric semiconductors are naturally flexible, they are typically not highly stretchable. A major challenge in developing flexible and stretchable semiconducting polymers is enhancing their mechanical properties without affecting their charge transport mobility. The competition between electronic and mechanical properties is dependent on the solid-state morphology.<sup>37-39</sup> Salleo *et al.* describe the multiple morphologies that co-exist in a solid-state conjugated polymer network.<sup>40</sup> Charge carriers typically move faster in crystalline regions than in amorphous regions in conjugated polymers because polymer chains adopt favourable  $\pi$ - $\pi$  stacking amongst the polymer chains in crystalline regions that result in high transport charge mobility, however, this morphology is inadequate with respect to mechanical compliance (Figure 1.6a).

In contrast, the random polymer chain orientation in amorphous regions hinders connectivity between conjugated backbones and leads to structural disorder which in turn limits charge transport in high-mobility conjugated polymers (Figure 1.6c). Since highly-crystalline conjugated polymers have proven to be inadequate for soft electronics applications and amorphous

morphology limits charge transport, the ideal morphology for stretchable semiconducting polymers is somewhere in between amorphous and crystalline with balanced electronic and mechanical properties. (Figure 1.6b).<sup>39</sup>

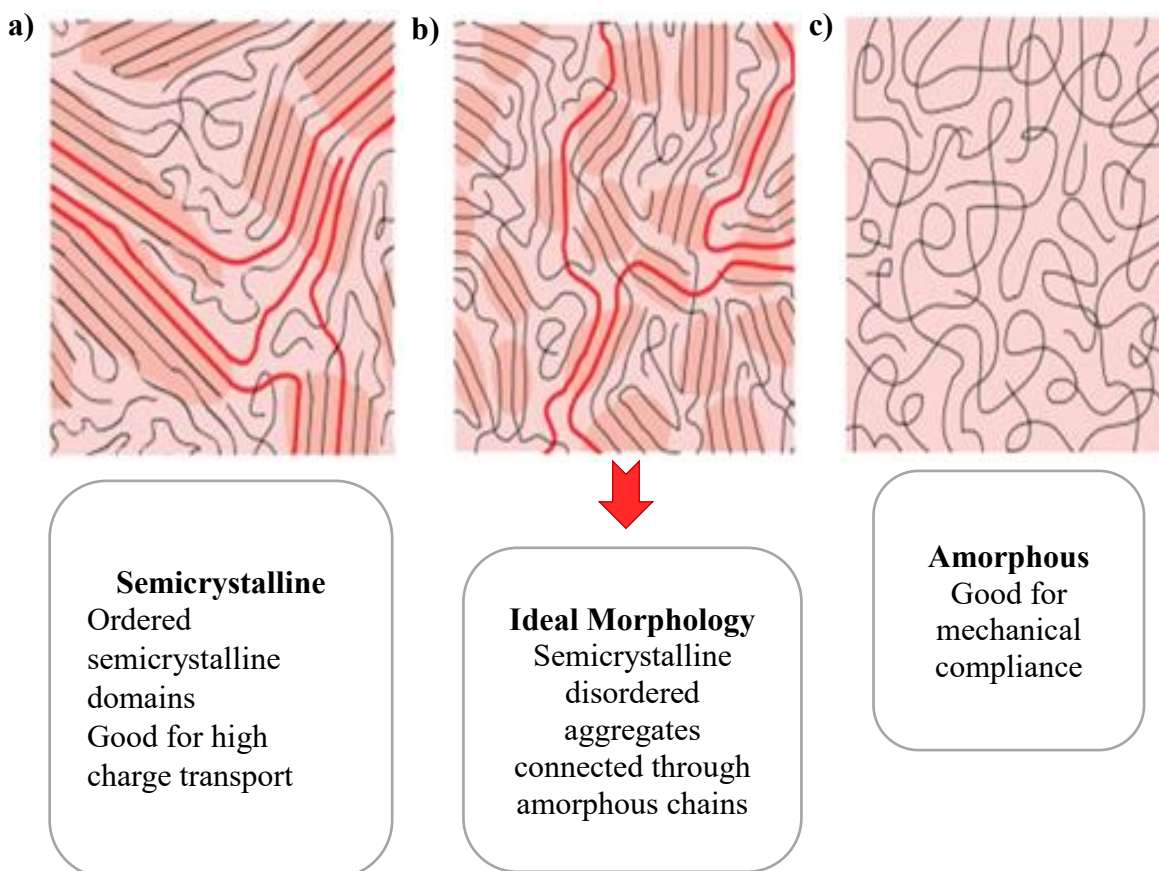


Figure 1. 6. Microstructure of conjugated polymer thin films. a) Semi-crystalline ordered domains are favourable for good charge transport; b) semi-crystalline disordered aggregates, ideal morphology for balanced electronic and mechanical properties; c) completely amorphous film favorable for mechanical properties. Adapted with permission from Ref. 40. Copyright 2013 Springer Nature.

## 1.4. Determination of the Electronic and Mechanical Properties of Conjugated Polymers

### 1.4.1. Evaluation of the Electronic Properties

The charge carrier mobility of organic semiconducting polymers has been improving tremendously over the past few years. A field-effect mobility as high as  $21.3 \text{ cm}^2\text{V}^{-1}\text{s}^{-1}$  has recently been measured by Luo and co-workers.<sup>36</sup> It has been found that polymers with a conjugation, an uninterrupted sequence of single and double bonds running through the whole molecule, are the most successful candidates for conducting polymers.<sup>41,42</sup>

Organic field-effect transistor is the main tool to probe the electronic properties of semiconducting polymers.<sup>43</sup> Nowadays, reports with mobility higher than  $1 \text{ cm}^2\text{V}^{-1}\text{s}^{-1}$  are common for OFET device's performance.<sup>44</sup> An OFET device consists of three terminals such as source, drain and gate. It is also composed of a semiconducting layer which is deposited on top of the dielectric layer.<sup>45</sup> The active semiconducting material is connected to two terminals (source and drain) and controlled at the third terminal (the gate) which is insulated from the rest of the device by the dielectric layer. When the voltage is applied to the gate, charge carriers are induced in the dielectric-semiconductor interface, creating a conductive channel. If a negative potential is applied to the gate, positive charges are formed at the interface between the semiconducting polymer and the dielectric layer. Then, due to the potential between the source electrode and the drain electrode, these positive charge carriers travel through the semiconducting layer, forming a *p*-type OFET device (Figure 1.7).<sup>46,47</sup>

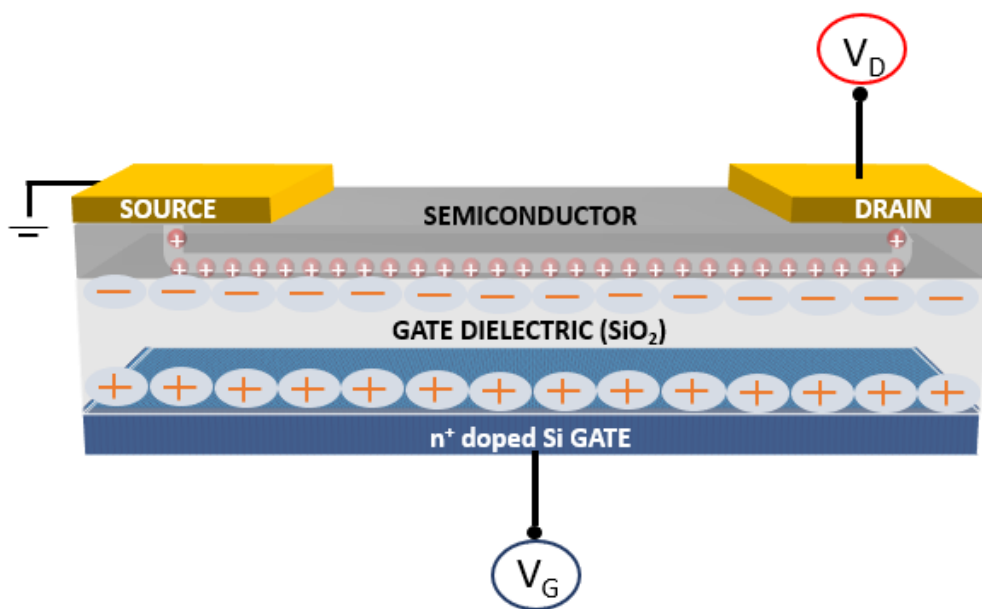


Figure 1. 7. Schematic illustration of an organic field-effect transistor device

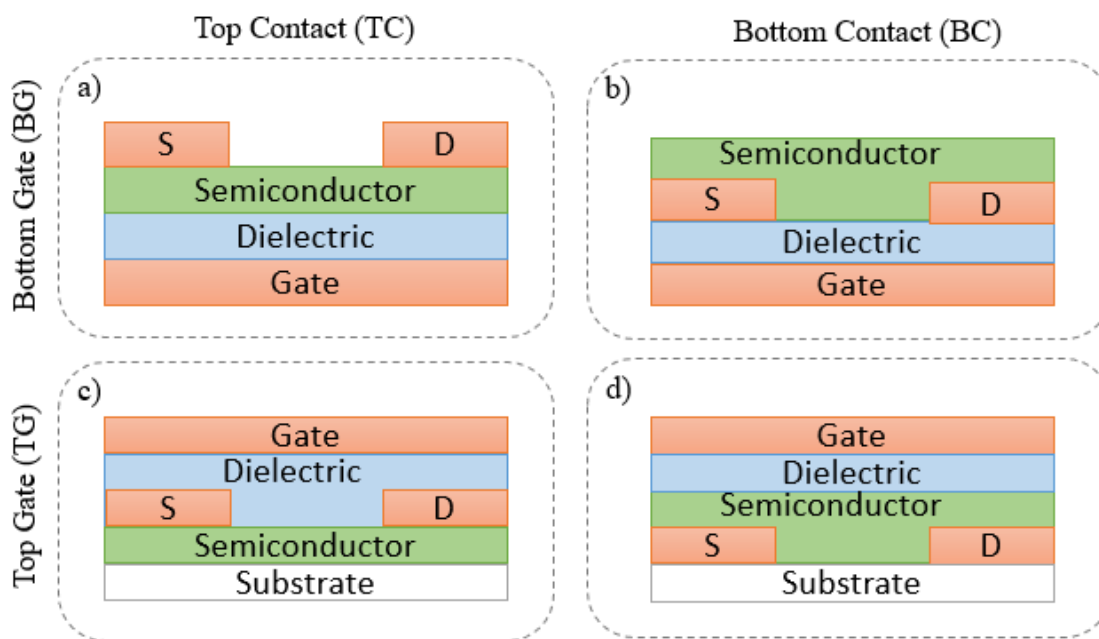


Figure 1.8. Schematic representation of four configurations of organic field-effect transistors: (a) bottom-gate top-contact (BG/TC); (b) bottom-gate bottom-contact (BG/BC), (c) top-gate top-contact (TG/TC), (d) top-gate bottom-contact (TG/BC) structures.

The possible configurations of OFET devices are shown in Figure 1.8.<sup>46</sup> In terms of gate configuration, (a) and (b) have bottom gate (BG) configurations, while (c) and (d) exhibit top-gate (TG) configurations. In terms of contact electrodes, there are top-contact (TC) (Figure 1.8a and c) and bottom-contact (BC) configurations (Figure 1.8b and d). The two most frequent structures are bottom-gate top-contact (BG/TC) and bottom-gate bottom-contact (BG-BC) because of their relatively simple fabrication. The advantages of bottom-gate configurations are commercially available doped silicon wafer with top layer of silicon oxide which act as electrode and dielectric, respectively. Moreover, the bottom-gate configurations is easier to fabricate comparing to the top-gate configurations.<sup>48,49</sup>

Charge carrier mobility is the main characteristic of the electronic properties of semiconducting polymers. It is the measure of the speed of charge carriers in a semiconductor material when electric field is applied and generally refers to both electrons and holes charge carriers called electron and hole mobility, respectively. Therefore, a great mobility value is essential for the generation of highly conductive electronic devices. The charge carriers in a semiconducting material are characterized by a velocity,  $v$ , hence, the mobility,  $\mu$ , is defined as a coefficient of proportionality between the drift velocity,  $v$ , of a charge carrier and the applied external electric field it experiences,  $E$ , where  $\mu = vE^{-1}$ . Consequently, the units of charge carrier mobility are  $\text{cm}^2 \text{V}^{-1}\text{s}^{-1}$ .<sup>50,51</sup> Another important parameter of OFET devices defines the turn-on of the device which means the conducting channel only forms after the gate voltage is beyond, so called threshold voltage. In other words, it is a minimum gate-to-source voltage ( $V_{\text{GS(thr)}}$ ) that is required to create a conducting path between source and drain terminals.<sup>52,53</sup>

#### 1.4.2. Key Methods for the Evaluation of Mechanical Properties

One of the important parameters for the development of flexible and stretchable devices is the mechanical compliance of semiconducting materials. Even though  $\pi$ -conjugated polymers are already flexible, they are typically not stretchable which is why the research is focused on the development of stretchable semiconducting materials with enhanced mechanical properties for the next generation of electronics.<sup>54</sup>

The main characteristics of the mechanical properties of semiconducting polymers are glass transition temperature ( $T_g$ ), degree of crystallinity, Young's modulus or also called elastic modulus, and crack onset strain. The  $T_g$  is described as a phase transition at which polymer chains have enough free volume to move relative to one another. It is very important characteristic since above this temperature polymer chains behave like soft and rubbery materials that is essential for their good mechanical properties.  $T_g$  is highly influenced by the effects of molar mass of semiconducting polymers as well as their structure.<sup>55</sup> As mentioned above the semiconducting polymers exist in such morphologies in a solid state as crystalline, semi crystalline or amorphous which affect their mechanical properties.<sup>40</sup> The degree of crystallinity is a fraction of the ordered domains in the polymer thin films. The most common method to measure the crystallinity of the semiconducting polymers is X-ray diffraction.<sup>56,57</sup> Another characteristic is Young's modulus which describes the resistance of semiconducting polymers to elastic deformation. The higher the Young's modulus is, the more rigid the polymer is. Organic semiconducting polymers have typical modulus in a GPa range.<sup>58</sup> Another parameter that describes the mechanical properties of semiconducting polymers is crack onset strain (COS). It provides an important perspective of film ductility and is a direct probe of stretchability.<sup>59</sup>

There are various methods to study the mechanical properties of semiconducting polymers. Every technique has its own advantages and limitations and can lead to important inconsistencies in terms of values and ranges. Therefore, it is crucial to get an overview of the different methods and techniques used to measure the mechanical properties of materials in order to get accurate values.

One way to examine the mechanical properties of  $\pi$ -conjugated polymers is measuring the elastic modulus or so-called Young's modulus by film-on-water tensile test (FOW).<sup>60</sup>

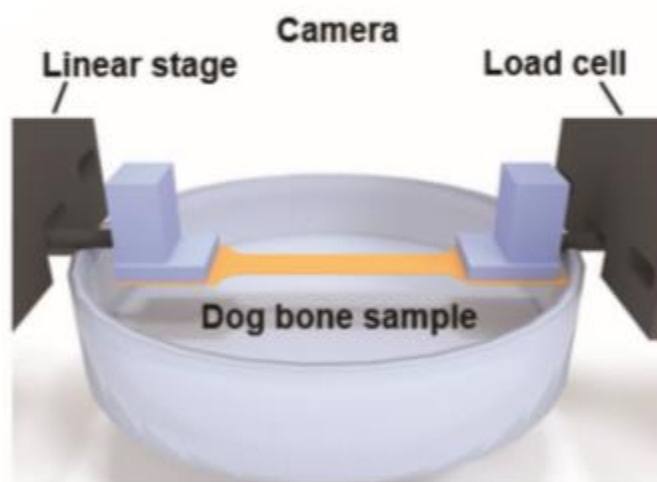


Figure 1. 9. Schematic illustration of pseudo free-standing thin-film tensile tester for measuring mechanical property of floated ultrathin conjugated polymer films. Adapted with permission from Ref. 60. Copyright 2018 John Wiley and Sons.

The FOW technique utilizes water as a surface with high surface tension of  $73 \text{ mN m}^{-1}$  to float thin films of semiconducting polymers. Once the dog-bone-shaped film is floated on the water surface, it is attached to the load grips using small PDMS slabs that make van der Waals adhesion with the load cell and the thin film. The tensile test was performed using motorized linear stage equipped with a digital encoder to obtain stress-strain curves (Figure 1.9).<sup>60,61</sup> This method

possesses the advantage of free-standing thin film tests comparing to the substrate-supported tests.<sup>61,62</sup>

The obtained stress-strain curve is an extremely important measure of a material's mechanical properties, providing such critical features as elastic and plastic zones, the elastic modulus, elastic limit or yield point, ultimate tensile strain, breaking stress or fracture point, and toughness.<sup>55,63</sup> The elastic modulus of a film ( $E$ ) is a slope of the stress-strain curve in the linear, elastic zone.<sup>54</sup>

Another technique to measure the elastic modulus of conjugated polymer thin films is tensile strain film-on-elastomer.<sup>64,65</sup> Briefly, the spincoated thin film is transferred onto the prestrained soft elastic substrate such as PDMS. Upon releasing the strain, the thin film on the elastomeric substrate buckles to form of a wavy and wrinkled surface due to the energetic competition and modulus mismatch between the film and substrate.<sup>66,67</sup> The schematic illustration of buckling of the thin film (red) upon releasing the strain of the substrate is shown in Figure 1.10.

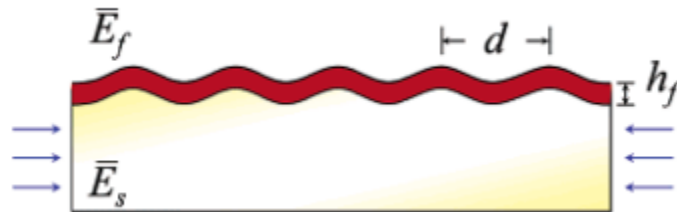


Figure 1. 10. The schematic illustration of tensile strain on film-on-elastomer of the thin film (red) upon releasing the strain of the substrate, where  $d$  is the wavelength of the wrinkling instability,  $h_f$  is thickness of the thin film,  $E_f$  and  $E_s$  are the modulus of the film and substrate, respectively. Adapted with permission from Ref. 136. Copyright 2015 Springer Nature.



The periodicity of the buckling pattern is mostly dependent on the modulus ratio between the film and substrate ( $E_f/E_s$ ) as well as the thickness of the thin film ( $hf$ ). The buckling wavelength is measured with either an optical microscope or AFM which can be directly correlated to the Young's modulus by using Stafford and coworkers' equation.<sup>68,69</sup> The advantage of the buckling method is that it does not require specialized equipment for measuring the elastic modulus of semiconducting polymer thin films. However, it possesses the disadvantage of being less accurate comparing to other techniques since the formation of surface buckles with uniform and periodic wavelength can be challenging. Moreover, this method provides only one value of the elastic modulus as a characteristic of the mechanical properties of semiconducting conjugated polymers, while FOW technique also includes the determination of the elastic limit and fracture points, elastic and plastic zones, as well as the toughness of the material.<sup>54,70</sup>

Another technique to measure the elastic modulus of semiconducting polymer thin films is called nanoindentation which is performed in the force mode using AFM by recording the interaction forces between the surface and a sharp tip mounted on a cantilever.<sup>71</sup>

In force mode, the tip is brought into contact with the surface, pushed to a maximum load, and then withdrawn. The voltage on the photodiode, recorded throughout the tip motion, is converted into force and then plotted against the distance which is commonly called the force curve.<sup>72</sup> However, this method applies the Hertz model<sup>73</sup> to assume nondeformable cantilever, the average contact area between point and base of the tip, as well as there are no additional interactions between the cantilever and sample.<sup>74,75</sup>

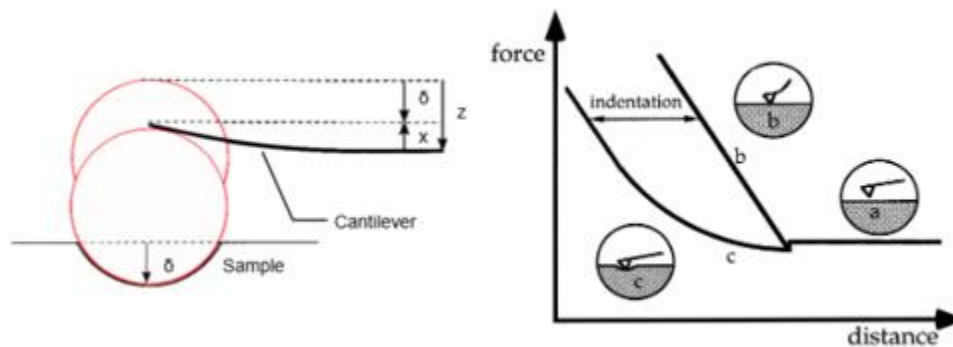


Figure 1.11. The schematic representation of the nanoindentation experiment: (a) there is no contact between the tip and sample; (b) the cantilever deflects by bending in the opposite direction ( $x$ ); (c) the deformation of the sample by the tip ( $\sigma$ ). Adapted with permission from Ref. 76. Copyright 1998 John Wiley and Sons.

As the tip is pushed into the sample by a distance  $z$  (height), the cantilever deflects, bending into the opposite direction ( $x$ ) and causing an increase in the voltage. The deformation of the sample by the tip ( $\sigma$ ) results in the deviation from the linearity between the force and distance. Finally,  $\sigma$  is calculated by subtracting the height distance ( $z$ ) from the cantilever deflection ( $x$ ). The schematic representation of the nanoindentation experiment is shown in Figure 1.11.<sup>75,76</sup>

The nanoindentation technique allows to study the mechanical properties of the material avoiding the transferring the sample onto the substrate for the further characterization, as well as the effects of the underlying substrate.<sup>77</sup> However, the properties of the probe, such as spring constant, sensitivity, and tip radius need to be known to obtain accurate results. Moreover, the surface forces, attractive forces (Van der Waals and electrostatic) can mask the onset of contact between the AFM probe and the specimen, which creates uncertainty in the location of the contact point.<sup>72,74</sup>

Another way to study the mechanical properties of conjugated polymers is measuring crack onset strain which is defined as minimum strain at which cracks start to propagate.<sup>54</sup> The film-on-

elastomer method is one of the most common approaches to measure crack onset strain by physically manipulating the films on a PDMS substrate. The formation of cracks under strain is simply observed by optical microscopy.<sup>59</sup>

## 1.5. Approaches toward Stretchability

Various strategies have been applied to achieve intrinsically stretchable semiconducting materials, which include covalent bonding, supramolecular chemistry (H-bonding, metal-ligand coordination, etc.), ionic interactions, and  $\pi$ - $\pi$  stacking. The main three approaches that have been used to achieve highly stretchable semiconducting polymers are strain engineering, physical blending and backbone engineering each of which has its own benefits and drawbacks (Figure 1.12.).<sup>78,80,86,88</sup>

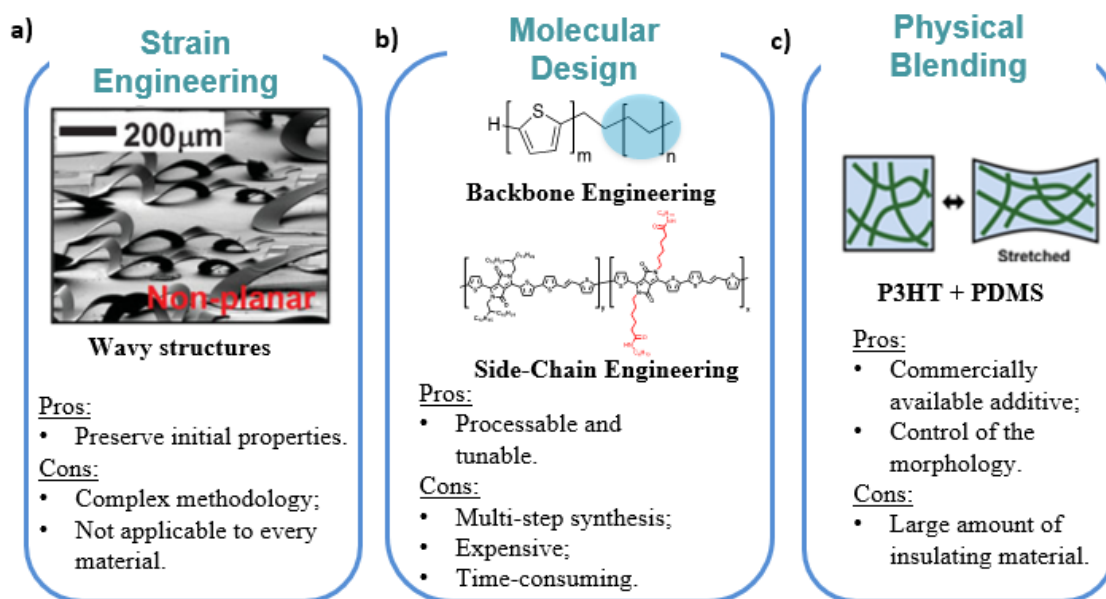


Figure 1.12. Comparing main three approaches to stretchable semiconducting conjugated polymers: **a)** strain engineering. Adapted with permission from Ref. 78. Copyright 2009 John Wiley and Sons. **b)** molecular design. Adapted with permission from Ref. 86. Copyright 2018 American Chemical Society and Ref. 88 Copyright 2007 John Wiley and Sons. **c)** physical blending. Adapted with permission from Ref. 80. Copyright 2016 John Wiley and Sons.

### **1.5.1. Strain Engineering**

The strain engineering approach or buckling method (also called “wrinkling”), is based on the placing of a rigid semiconductor thin film on a pre-strained elastomer substrate. The most common elastomeric substrate that has been used is polydimethylsiloxane (PDMS). When the film on the elastomer substrate is released, it generates wavy structures.<sup>81-83</sup>

Once Rogers and co-workers demonstrated highly stretchable devices using wrinkled Si nanoribbons,<sup>78</sup> many researchers became interested in this strategy to produce flexible and stretchable electronics.

The first stretchable organic device on a pre-strained PDMS substrate were reported by Bao and co-workers in 2011.<sup>84</sup> One year later, Someya and colleagues fabricated a photovoltaic (OPV) device on an ultrathin poly(ethylene terephthalate) (PET) substrate and then transferred it onto a pre-strained rubber substrate.<sup>85</sup> The wrinkles formed allowed the OPV to be folded and stretched to up to 50% tensile strain.

Even though the benefit of this approach is the ability to preserve the initial properties of semiconductor materials such as high performance, the major drawback is that it is not applicable to all materials. Moreover, buckling method is complicated to fabricate and might not be suitable for large area or mass production.

### **1.5.2. Molecular Design**

Molecular design is one of the common strategies to develop intrinsically stretchable semiconducting conjugated polymers. It consists of two main approaches as backbone and side-chain engineering. The concept of backbone engineering involves introducing chemical moieties

into the polymer backbone to modify its properties, while side-chain engineering is based on the incorporation of various side-chains onto the polymer backbone (Figure 1.13). These properties include: backbone planarity, lamellar spacing,  $\pi$ -stacking distances, crystallinity, glass transition temperature ( $T_g$ ), chain alignment and interchain interactions.<sup>86</sup>

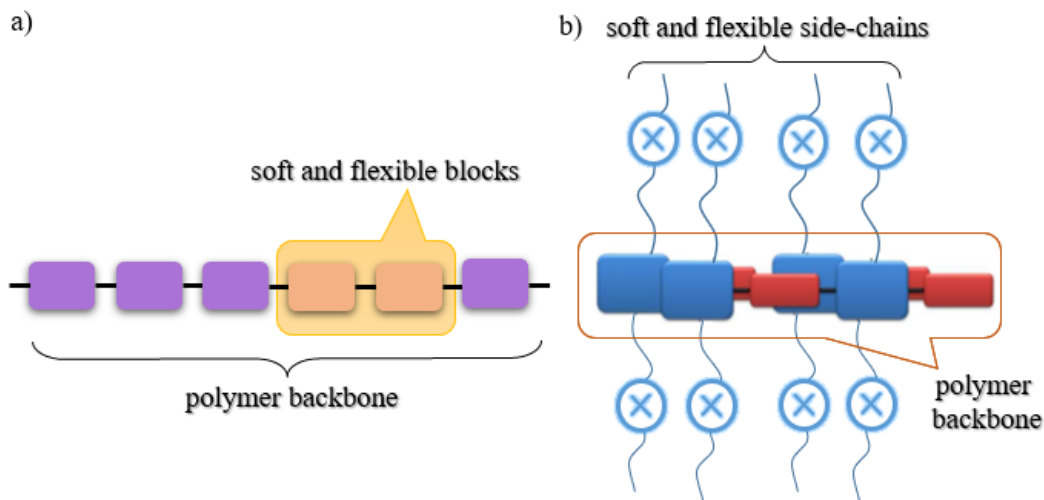


Figure 1. 13. Schematic illustration of molecular design strategy for the developments of the intrinsically stretchable semiconducting polymers: **a)** backbone approach which involves introducing soft and flexible blocks into the polymer backbone; **b)** side-chain approach which is based on the incorporation of various side-chains onto the polymer backbone, which can be terminated with X groups (siloxane, amide, urea groups, and others).

Among the different strategies used to enhance the mechanical properties of semiconducting polymers, the incorporation of soft blocks into the conjugated polymer backbone is an attractive approach to reduce the crystallinity in solid-state and increase the elongation at break without affecting the electronic properties.<sup>87</sup> The common flexible moieties that have been reported to improve the mechanical compliance of poly(3-hexyl)thiophene (P3HT) conjugated polymer are polyethylene (PE),<sup>88</sup> amorphous PMA,<sup>89</sup> and 2,6-pyridine dicarboxamide (PDCA).<sup>90</sup>

This strategy reduces the glass transition temperature, crystallinity and the elastic modulus which leads to an increase in stretchability of semiconducting polymers.<sup>91</sup>

The incorporation of conjugation-break spacers (CBSs) into the polymer backbone and the effect of broken conjugation of semiconducting polymers have also been studied to influence molecular interactions between polymer chains in order to improve stretchability. The results showed an increase in the crack-onset strain without drastically affecting charge transport mobility.<sup>54-94</sup>

Another approach to achieve highly stretchable and flexible semiconducting materials is side-chain engineering which is based on the incorporation of various side-chains onto the polymer backbone. The introduction of flexible and soft side-chains has found to break the aggregation of the polymer chains, increase in solubility, backbone planarity,  $\pi$ - $\pi$ -stacking interactions and lamellar distances, as well as decrease in crystallinity, Young's modulus and  $T_g$  of semiconducting polymers. Fundamental studies have been done to investigate the influence of side-chains on the mechanical properties of semiconducting conjugated polymers, and particularly the length of alkyl spacers.<sup>95</sup> It was found that long branched alkyl side-chains improve the solubility of polymers by increasing the chains' degrees of freedom.<sup>96,97,98</sup> In most reports, the polymers with a branched alkyl chain containing a greater number of carbons possessed higher charge mobility over  $1 \text{ cm}^2\text{V}^{-1}\text{s}^{-1}$ .<sup>99</sup> Interestingly, the bigger the distance of the branching position from the polymer backbone, the smaller the intermolecular  $\pi$ - $\pi$ -stacking distances which results in high charge mobility.<sup>100</sup> This strategy has been previously reported in the literature using such side-chains such as siloxane,<sup>101,102</sup> poly(butyl acrylate) (PBA),<sup>103</sup> amide-containing side-chains and others.<sup>86</sup> The incorporation of these side-chains onto the polymer backbone enhances charge transport mobility

of thin film transistors reaching the value of more than  $1.0 \text{ cm}^2 \text{ V}^{-1} \text{ s}^{-1}$  even upon stretching/releasing cycles.

Even though this approach is promising for the fabrication of stretchable electronic materials, it has some challenges including high expenses, being time-consuming, and difficulty in processing. Therefore, the physical blending approach has attracted the attention of researchers to achieve highly stretchable and conductive devices.

### **1.5.3. Physical Blending Between Conjugated Polymer and Soft Elastomers**

Physical blending is an attractive way to control polymer morphology and enhance mechanical compliance without affecting electronic performance. Phase separation plays a critical role in the performance of organic electronic devices. Semiconducting polymer blends are promising active layers in OFETs due to their solution-processability, high charge-carrier mobilities, good film formation capability, as well as the ability to tune their mechanical properties. It has been shown that phase separation strongly affects electronic properties of semiconducting polymers by inducing the confinement effect of polymer chains upon blending.<sup>104–107</sup> The fabrication of semiconducting polymer nanowires (NWs) for enhancing device performance has been previously reported.<sup>36,62–66,112</sup>

However, phase separation is a very complex phenomenon and is highly dependent on many factors such as solvent evaporation rate, the solubility parameters, solvent effect, the film-substrate interactions, the surface free energy of each component and the film thickness.<sup>113</sup> The factors are also interrelated. The phase separation *via* physical blending of semiconducting polymers and soft elastomers induces the confinement effect which is defined as a formation of

polymer nanofibers inside an elastomer matrix. As the film thickness increases, the confinement effect becomes weaker and the affinity between the substrate and film becomes the dominant cause of phase separation.<sup>114</sup>

Numerous thermodynamic and kinetic studies have been done to obtain a more complete picture of the phase separation phenomenon.<sup>115</sup> The first thermodynamic model of polymer blends was developed by Flory and Huggins in 1940's. Flory-Huggins theory explains how the Gibb's free energy of mixing can predict certain aspects of phase separation.<sup>116,117</sup> The second theory is Cahn-Hilliard theory which deals with the dynamics of phase separation.

Briefly, the Flory-Huggins model is derived from a polymer-solvent system where the Gibb's free energy of mixing ( $\Delta G_m$ ) is dependent on enthalpy of mixing ( $\Delta H_m$ ), temperature ( $T$ ) and entropy of mixing ( $\Delta S_m$ ). If  $\Delta G_m < 0$  then the enthalpic interactions between two species is favourable and the two components become miscible (homogeneous, one phase). If  $\Delta G_m > 0$  then mixing is unfavourable which leads to immiscibility of species (heterogeneous, two phases)<sup>116,117</sup>. The Flory-Huggins model has also been applied to two-polymer systems.

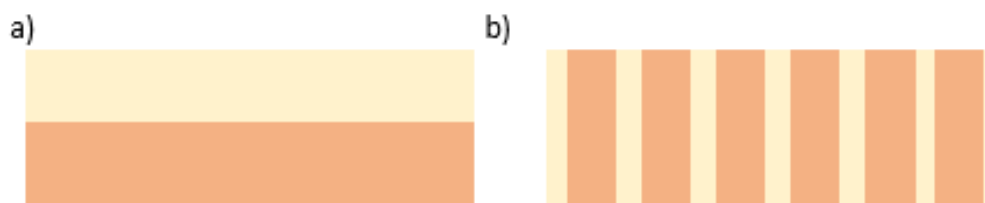


Figure 1. 14. Schematic illustrations of different spin-casted films: (a) vertically phase separated (bilayer); (b) laterally phase-separated.

There are two main types of phase separation between polymer blends: vertical phase separation and lateral phase separation. Vertical phase separation is defined as one phase being in



contact with a surface while lateral phase separation occurs when both phases are in contact with a surface (Figure 1.14.).<sup>118</sup>

Laterally phase-separated films are usually formed from vertically phase-separated films. In the first stage the spin-coated film undergoes vertical phase separation into a bilayer. In the second step the bilayer is distorted which is potentially caused by the solvent evaporation from the top surface, leading to the formation of a laterally phase-separated film. Varying the evaporation rate during spin-coating allows one to control the final phase separation to be either vertical or lateral.<sup>118–120,121</sup> Laterally phase-separated polymer blends are demonstrated to be efficient for different organic electronic devices.<sup>122,119,120,123</sup>

Vertical phase separation in polymer blends and its role in improving the performance of organic electronic devices has attracted much attention among researchers.<sup>124,125,126</sup> The use of vertical phase separation was demonstrated by depositing a P3HT and poly(methylmethacrylate) (PMMA) blend on a bare silicon substrate.<sup>127</sup> The reason for vertical separation to occur is preferential affinity of the relatively hydrophilic PMMA component of the blend to the hydrophilic substrate such as a bare silicon wafer or silicon-oxide (SiO<sub>2</sub>) resulting in a perfect P3HT-top and PMMA-bottom bilayer structure. Interestingly, the polymer blend showed better field-effect transistor performance of 0.002 cm<sup>2</sup>V<sup>-1</sup>s<sup>-1</sup> with a threshold voltage of -6.0V compared to a pure-P3HT film with a charge-carrier mobility of 0.0005 cm<sup>2</sup>V<sup>-1</sup>s<sup>-1</sup> and a threshold voltage of 29.7V.

The effect of the vertical phase separation on the electronic properties of conjugated polymers has been widely studied for organic field-effect transistor applications.<sup>128,129,130</sup> Moreover, vertical phase separation between polymer blends is a potential method to improve performance of solar cells<sup>131,132</sup> It can be achieved by solvent effect<sup>133,98,136</sup>, thermal annealing<sup>137–139,140,141</sup>, vapor annealing<sup>142,143</sup> and surface modification<sup>144</sup>.

The development of soft elastomer-conjugated polymer blends has shown to be a promising approach towards stretchable electronic materials. The challenge is to maintain the excellent charge transport characteristics of conjugated polymers while improving their mechanical properties. Recently, various elastomeric materials were added to control different properties of polymers such as backbone planarity, crystallinity, and morphology in the solid-state in order to improve their electronic and mechanical properties.<sup>145</sup>

The most common elastomers among various additives are high molecular weight PDMS, poly(styrene) (PS),<sup>146</sup> and poly(styrene-ethylene-butylene-styrene) (SEBS) have shown great results in achieving both high charge transport and good mechanical compliance. In 2015, Jeong *et al.* reported a blended system between P3HT and SEBS which was spin-coated onto the elastomeric substrate (PDMS). During spin-coating process, the P3HT nanofibers were phase-separated and spread out inside the SEBS matrix. The formation of semiconducting polymer nanowires is induced by phase separation between polymer elastomer components which result in an enhanced mechanical properties without affecting electronic performance of the fabricated devices.<sup>80,113,147-148</sup>

Another example of this approach has been reported by Bao *et al.* in 2017 which became a breakthrough in the field of stretchable electronics.<sup>110</sup> During blending, high charge-carrier mobility diketopyrrolopyrrole (DPP)-based conjugated polymers formed nanofibrils inside a soft and deformable elastomer, (SEBS), so called nanoconfinement effect (Figure 1.15a). The formation of polymer nanofibers inside a soft elastomer matrix was characterized by AFM and is illustrated in Figure 1.15c. The study shows that 70 wt.% of SEBS provides the highest mobility at 100% strain (a maximum value of  $1.32 \text{ cm}^2 \text{ V}^{-1} \text{ s}^{-1}$ ) which is a three orders of magnitude improvement compared to the neat film of the conjugated polymer. Good charge transport is

maintained due to the connectivity between the polymer nanofibrils while soft elastomer prevents crack propagation.

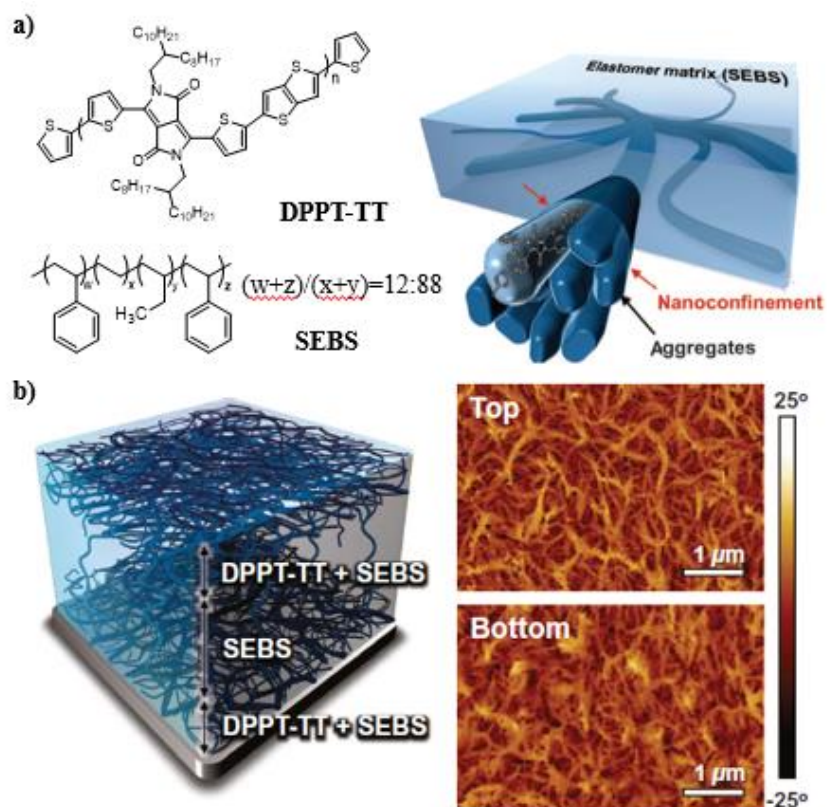


Figure 1. 15. **a)** Chemical structures of semiconducting polymer poly(2,5-bis(2-octyldodecyl)-3,6-di(thiophen-2-yl)diketopyrrolo[3,4-c]pyrrole-1,4-dione-alt-thieno[3,2-b]thiophen) (DPPT-TT) and SEBS elastomer. A 3D schematic of the desired morphology composed of embedded polymer nanofibrils in elastomer matrix to achieve nanoconfinement effect; **b)** A 3D illustration of the morphology of the polymer/elastomer blend; AFM phase images of the top and bottom interfaces of the blended film with 70 wt.% of SEBS. Adapted with permission from Ref. 110. Copyright 2017 The American Association for the Advancement of Science.

Reichmanis and coworkers showed a similar effect by blending poly-3-hexylthiophene (P3HT) with PDMS, resulting in highly stretchable devices.<sup>109,111,149</sup> These examples show the great potential of elastomeric additives to control and tune the solid-state morphology of

conjugated polymers. However, elastomer additives act as insulating materials which can potentially decrease the performance of large-scale fabricated devices. Therefore, various solvents and low molecular weight additives are used to enhance solid-state morphology and improve electronic properties.<sup>150</sup> One of the examples using solvent-additive was reported by Jeong *et al.* in 2018.<sup>97</sup> It was found that particular solvent blends increase intra- and interchain  $\pi$ - $\pi$  interactions that facilitate the self-assembly of P3HT polymer chains, enhancing charge transport properties. Different co-solvent systems such as dichlorobenzene (DCB, boiling point 180 °C) with chloroform (CHCl<sub>3</sub>, boiling point 61 °C) and acetonitrile (MeAN, boiling point 81 °C) with chloroform were used to promote the favourable self-assembly of  $\pi$ -conjugated polymer chains. The solvent blend system with P3HT polymer results in enhanced charge transport in P3HT organic OFET devices from 0.017 cm<sup>2</sup> V<sup>-1</sup> s<sup>-1</sup> to 0.082 cm<sup>2</sup> V<sup>-1</sup> s<sup>-1</sup> for DCB at 5 vol % and 0.044 cm<sup>2</sup> V<sup>-1</sup> s<sup>-1</sup> for acetonitrile (MeAN) at 2 vol % compared to the system without any solvent additive.

## 1.6. Scope of Thesis

There have been various DPP-based polymer blended systems reported in the literature using different solvent additives<sup>151,152</sup> and high molecular weight elastomeric materials<sup>111,112,114</sup> which showed impressive results, however, the incorporation of the large amount of insulating materials and additive can potentially influence the performance and stability of the fabricated OFET devices, especially in the large-scale production of the electronic devices.

Branched polyethylene (BPE) additive can be a promising candidate to enhance electronic and mechanical properties of semiconducting polymers due to its unique feature of being volatile

which allows a complete removal of the insulating material upon thermal annealing. The chemical structure of BPE is illustrated in Figure 1.16. Additionally, BPE additive was selected due to such factors as being non-toxic, low cost, low boiling point (135°C), molecular weight (500Da) and potential use for large-scale fabrication of OFETs. Most importantly, the aim is to strongly promote the phase separation and confinement of the semiconducting polymer to maintain stable charge transport mobility even at high amount of BPE added. Moreover, the effect of BPE additive on the mechanical properties of semiconducting polymers will also be investigated.

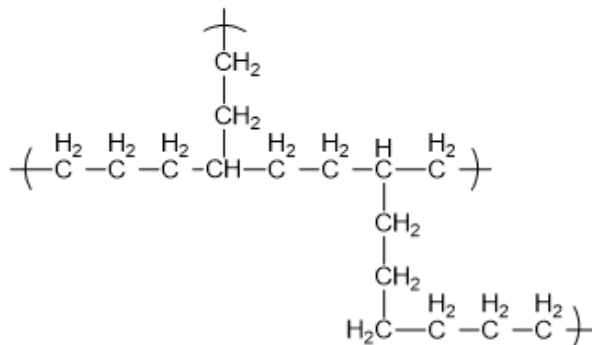


Figure 1. 16. Chemical structure of branched polyethylene

Our intended purpose is to design a novel blended system between high charge carrier mobility DPP-based conjugated polymer and BPE in order to probe the influence of BPE additive on the electronic and mechanical properties of semiconducting polymer. Over the course of this thesis, the effect of BPE additive on the electronic and mechanical properties of DPP-based conjugated polymer is investigated by various characterization techniques, including X-ray diffraction, UV-Vis spectroscopy and atomic force microscopy (AFM), Grazing-Incidence X-ray Diffraction (GIXRD) and OFET device fabrication

## REFERENCES

- (1) Yang, Y.; Gao, W. Wearable and Flexible Electronics for Continuous Molecular Monitoring. *Chem. Soc. Rev.* **2019**, *48*, 1465–1491.
- (2) Cicoira, F.; T, A. *Organic Electronics*; Cicoira, F., Santato, C., Eds.; Wiley-VCH Verlag GmbH & Co. KGaA: Weinheim, Germany, 2013.
- (3) Francisco, S.; States, U. Organic Electronics for a Better Tomorrow : Innovation , Accessibility , Sustainability. **2012**, 1–31.
- (4) Tok, B-H.J.; Bao, Z. Recent Advances in Flexible and Stretchable Electronics , Sensors and Power Sources. *Sci China Chem* **2012**, *55*, 718–725.
- (5) Braun, S. *Studies of Materials and Interfaces for Organic Electronics*; 2007.
- (6) Harris, K. D.; Elias, A. L.; Chung, H.-J. Flexible Electronics under Strain: A Review of Mechanical Characterization and Durability Enhancement Strategies. *J. Mater. Sci.* **2016**, *51*, 2771–2805.
- (7) Tuller, H. L. *Flexible Electronics : Materials and Applications Electronic Materials : Science and Technology*; 2009.
- (8) CRABB, R. L.; TREBLE, F. C. Thin Silicon Solar Cells for Large Flexible Arrays. *Nature* **1967**, *213*, 1223–1224.
- (9) Brody, T. P. The Thin Film Transistor—A Late Flowering Bloom. *IEEE Trans. Electron Devices* **2008**, *31*, 1614–1628.
- (10) Brody, T. P. The Birth and Early Childhood of Active Matrix — A Personal Memoir. *J. Soc. Inf. Disp.* **1996**, *4*, 113.
- (11) Derivatives, H.; Louis, J.; Macdiarmid, A. G. Synthesis of Electrically Conducting Organic Polymers : Halogen Derivatives of Polyacetylene, (CH)X. **1977**, No. 578, 578–580.

- (12) Arjmand, M.; Sadeghi, S. Nitrogen-Doped Carbon Nanotube/Polymer Nanocomposites Towards Thermoelectric Applications. In *Thermoelectrics for Power Generation - A Look at Trends in the Technology*; InTech, 2016; pp 324–342.
- (13) Li, T.; Suo, Z. Deformability of Thin Metal Films on Elastomer Substrates. *Int. J. Solids Struct.* **2006**, *43*, 2351–2363.
- (14) Sekitani, T.; Someya, T. Stretchable, Large-Area Organic Electronics. *Adv. Mater.* **2010**, *22*, 2228–2246.
- (15) Wang, Y.; Zhu, C.; Pfattner, R.; Yan, H.; Jin, L.; Chen, S.; Molina-Lopez, F.; Lissel, F.; Liu, J.; Rabiah, N. I.; Chen, Z.; Chung, J. W.; Linder, C.; Toney, M. F.; Murmann, B.; Bao, Z. A Highly Stretchable, Transparent, and Conductive Polymer. *Sci. Adv.* **2017**, *3*, e1602076.
- (16) Saion, E.; Harun, M. H.; Saion, E.; Kassim, A.; Yahya, N.; Mahmud, E. Conjugated Conducting Polymers : A Brief Conjugated Conducting Polymers : A Brief Overview. **1992**, No. January 2016.
- (17) Yao, Y.; Dong, H.; Hu, W. Charge Transport in Organic and Polymeric Semiconductors for Flexible and Stretchable Devices. **2016**, 4513–4523.
- (18) Sirringhaus, H. 25th Anniversary Article: Organic Field-Effect Transistors: The Path beyond Amorphous Silicon. *Adv. Mater.* **2014**, *26*, 1319–1335.
- (19) Liu, Y.; Pharr, M.; Salvatore, G. A. Lab-on-Skin: A Review of Flexible and Stretchable Electronics for Wearable Health Monitoring. **2017**, 9614–9635.
- (20) Tan, Y. J.; Wu, J.; Li, H.; Tee, B. C. K. Self-Healing Electronic Materials for a Smart and Sustainable Future. *ACS Appl. Mater. Interfaces* **2018**, *10*, 15331–15345.
- (21) Vannikov, A. V.; Saidov, A. C. Charge Carrier Transport in Conjugated Polymers. *Mol.*

- Cryst. Liq. Cryst. Sci. Technol. Sect. A. Mol. Cryst. Liq. Cryst.* **1993**, 228, 87–92.
- (22) Milián-Medina, B.; Gierschner, J.  $\pi$ -Conjugation. *Wiley Interdiscip. Rev. Comput. Mol. Sci.* **2012**, 2, 513–524.
- (23) Schmatz, B.; Pankow, R. M.; Thompson, B. C.; Reynolds, J. R. Perspective on the Advancements in Conjugated Polymer Synthesis, Design, and Functionality over the Past Ten Years. In *Conjugated Polymers*; CRC Press, 2019; pp 107–148.
- (24) Udaya, D.; John, A.; G., M.; V., A. Donor-Acceptor Conjugated Polymers and Their Nanocomposites for Photonic Applications. In *Nonlinear Optics*; InTech, 2012; pp 133–160.
- (25) Facchetti, A.  $\pi$ -Conjugated Polymers for Organic Electronics and Photovoltaic Cell Applications †. *Chem. Mater.* **2011**, 23, 733–758.
- (26) Zaki, T. *Short-Channel Organic Thin-Film Transistors*; Springer Theses; Springer International Publishing: Cham, 2015.
- (27) Rang, Z.; Haraldsson, A.; Kim, D. M.; Ruden, P. P.; Nathan, M. I.; Chesterfield, R. J.; Frisbie, C. D. Hydrostatic-Pressure Dependence of the Photoconductivity of Single-Crystal Pentacene and Tetracene. *Appl. Phys. Lett.* **2001**, 79, 2731–2733.
- (28) Tsumura, A.; Koezuka, H.; Ando, T. Macromolecular Electronic Device: Field-effect Transistor with a Polythiophene Thin Film. *Appl. Phys. Lett.* **1986**, 49, 1210–1212.
- (29) Assadi, A.; Svensson, C.; Willander, M.; Inganäs, O. Field-effect Mobility of Poly(3-hexylthiophene). *Appl. Phys. Lett.* **1988**, 53, 195–197.
- (30) Bertolazzi, S.; Wünsche, J.; Cicoira, F.; Santato, C. Tetracene Thin Film Transistors with Polymer Gate Dielectrics. *Appl. Phys. Lett.* **2011**, 99, 013301.
- (31) Facchetti, A.; Deng, Y.; Wang, A.; Koide, Y.; Sirringhaus, H.; Marks, T. J.; Friend, R. H.



- Tuning the Semiconducting Properties of Sexithiophene By  $\alpha,\omega$ -Substitution— $\alpha,\omega$ -Diperfluorohexylsexithiophene: The First n-Type Sexithiophene for Thin-Film Transistors. *Angew. Chemie* **2000**, *112*, 4721–4725.
- (32) Lei, T. *Design, Synthesis, and Structure-Property Relationship Study of Polymer Field-Effect Transistors*; Springer Theses; Springer Berlin Heidelberg: Berlin, Heidelberg, 2015.
- (33) Ebisawa, F.; Kurokawa, T.; Nara, S. Electrical Properties of Polyacetylene/Polysiloxane Interface. *J. Appl. Phys* **1983**, *54*, 3255–3259.
- (34) A. Tsumura, H. Koezuka, T. A. Polythiophene Field-Effect Transistor: Its Characteristics and Operation Mechanism. **1988**, *25*, 11–23.
- (35) Berrouard, P.; Najari, A.; Pron, A.; Gendron, D.; Morin, P.-O.; Pouliot, J.-R.; Veilleux, J.; Leclerc, M. Synthesis of 5-Alkyl[3,4-c]Thienopyrrole-4,6-Dione-Based Polymers by Direct Heteroarylation. *Angew. Chemie Int. Ed.* **2012**, *51*, 2068–2071.
- (36) Luo, C.; Kyaw, A. K. K.; Perez, L. A.; Patel, S.; Wang, M.; Grimm, B.; Bazan, G. C.; Kramer, E. J.; Heeger, A. J. General Strategy for Self-Assembly of Highly Oriented Nanocrystalline Semiconducting Polymers with High Mobility. *Nano Lett.* **2014**, *14*, 2764–2771.
- (37) Chang, M.; Lim, G.; Park, B.; Reichmanis, E. Control of Molecular Ordering, Alignment, and Charge Transport in Solution-Processed Conjugated Polymer Thin Films. *Polymers (Basel)*. **2017**, *9*, 212.
- (38) Kim, J.-S.; Kim, J.-H.; Lee, W.; Yu, H.; Kim, H. J.; Song, I.; Shin, M.; Oh, J. H.; Jeong, U.; Kim, T.-S.; Kim, B. J. Tuning Mechanical and Optoelectrical Properties of Poly(3-Hexylthiophene) through Systematic Regioregularity Control. *Macromolecules* **2015**, *48*, 4339–4346.

- (39) Son, S. Y.; Kim, Y.; Lee, J.; Lee, G.; Park, W.; Noh, Y.; Park, C. E.; Park, T. High-Field-Effect Mobility of Low-Crystallinity Conjugated Polymers with Localized Aggregates. *J. Am. Chem. Soc.* **2016**, *138*, 8096–8103.
- (40) Noriega, R.; Rivnay, J.; Vandewal, K.; Koch, F. P. V; Stingelin, N.; Smith, P.; Toney, M. F.; Salleo, A. A General Relationship between Disorder, Aggregation and Charge Transport in Conjugated Polymers. *Nat. Mater.* **2013**, *12*, 1038–1044.
- (41) Moliton, A.; Hiorns, R. C. Review of Electronic and Optical Properties of Semiconducting  $\pi$ -Conjugated Polymers: Applications in Optoelectronics. *Polym. Int.* **2004**, *53*, 1397–1412.
- (42) Tang, C. W. Two-layer Organic Photovoltaic Cell. *Appl. Phys. Lett.* **1986**, *48*, 183–185.
- (43) Houin, G.; Duez, F.; Garcia, L.; Cantatore, E.; Hirsch, L.; Belot, D.; Pellet, C.; Abbas, M. Device Engineering for High-Performance, Low-Voltage Operating Organic Field Effect Transistor on Plastic Substrate. *Flex. Print. Electron.* **2017**, *2*, 045004.
- (44) Khim, D.; Ryu, G.-S.; Park, W.-T.; Kim, H.; Lee, M.; Noh, Y.-Y. Precisely Controlled Ultrathin Conjugated Polymer Films for Large Area Transparent Transistors and Highly Sensitive Chemical Sensors. *Adv. Mater.* **2016**, *28*, 2752–2759.
- (45) Mas-Torrent, M.; Rovira, C. Novel Small Molecules for Organic Field-Effect Transistors: Towards Processability and High Performance. *Chem. Soc. Rev.* **2008**, *37*, 827.
- (46) Allard, N.; Leclerc, M. Conjugated Polymers for Organic Electronics. In *Functional Materials*; Leclerc, M., Gauvin, R., Eds.; DE GRUYTER: Berlin, München, Boston, 2014; pp 121–138.
- (47) Harris, L. A.; Wilson, R. H. Semiconductors for Photoelectrolysis. *Annu. Rev. Mater. Sci.* **1978**, *8*, 99–134.

- (48) Xu, Y.; Liu, C.; Khim, D.; Noh, Y.-Y. Development of High-Performance Printed Organic Field-Effect Transistors and Integrated Circuits. *Phys. Chem. Chem. Phys.* **2015**, *17*, 26553–26574.
- (49) Gholamrezaie, F.; Asadi, K.; Kicken, R. A. H. J.; Langeveld-Voss, B. M. W.; de Leeuw, D. M.; Blom, P. W. M. Controlling Charge Injection by Self-Assembled Monolayers in Bottom-Gate and Top-Gate Organic Field-Effect Transistors. *Synth. Met.* **2011**, *161*, 2226–2229.
- (50) Chen, Y.; Lee, B.; Yi, H. T.; Lee, S. S.; Payne, M. M.; Pola, S.; Kuo, C.-H.; Loo, Y.-L.; Anthony, J. E.; Tao, Y. T.; Podzorov, V. Dynamic Character of Charge Transport Parameters in Disordered Organic Semiconductor Field-Effect Transistors. *Phys. Chem. Chem. Phys.* **2012**, *14*, 14142.
- (51) Xu, Y. Characterization and Modeling of Static Properties and Low-Frequency Noise in Organic Field-Effect Transistors ( OFETs ) To Cite This Version : HAL Id : Tel-00747417  
Caractérisation et Modélisation Des Propretés Électriques et Du Bruit à Basse Fréquence D. **2012**.
- (52) Horowitz, G.; Hajlaoui, R.; Bouchriha, H.; Bourguiga, R.; Hajlaoui, M. Concept of 'threshold Voltage' in Organic Field-Effect Transistors. *Adv. Mater.* **1998**, *10*, 923–927.
- (53) Lüssem, B.; Tietze, M. L.; Kleemann, H.; Hoßbach, C.; Bartha, J. W.; Zakhidov, A.; Leo, K. Doped Organic Transistors Operating in the Inversion and Depletion Regime. *Nat. Commun.* **2013**, *4*, 2775.
- (54) Savagatrup, S.; Printz, A. D.; O'Connor, T. F.; Zaretski, A. V.; Lipomi, D. J. Molecularly Stretchable Electronics. *Chem. Mater.* **2014**, *26*, 3028–3041.
- (55) Date, P. Mechanical Properties of Semiconducting Polymers. *UC San Diego Electron.*

*Theses Diss.* **2018**, 280.

- (56) Shen, X.; Hu, W.; Russell, T. P. Measuring the Degree of Crystallinity in Semicrystalline Regioregular Poly(3-Hexylthiophene). *Macromolecules* **2016**, *49*, 4501–4509.
- (57) Scholes, D. T.; Yee, P. Y.; Lindemuth, J. R.; Kang, H.; Onorato, J.; Ghosh, R.; Luscombe, C. K.; Spano, F. C.; Tolbert, S. H.; Schwartz, B. J. The Effects of Crystallinity on Charge Transport and the Structure of Sequentially Processed F4 TCNQ-Doped Conjugated Polymer Films. *Adv. Funct. Mater.* **2017**, *27*, 1702654.
- (58) Wagner, S.; Bauer, S. Materials for Stretchable Electronics. *MRS Bull.* **2012**, *37*, 207–213.
- (59) Balar, N.; O'Connor, B. T. Correlating Crack Onset Strain and Cohesive Fracture Energy in Polymer Semiconductor Films. *Macromolecules* **2017**, *50*, 8611–8618.
- (60) Zhang, S.; Ocheje, M. U.; Luo, S.; Ehlenberg, D.; Appleby, B.; Weller, D.; Zhou, D.; Rondeau-Gagné, S.; Gu, X. Probing the Viscoelastic Property of Pseudo Free-Standing Conjugated Polymeric Thin Films. *Macromol. Rapid Commun.* **2018**, *39*, 1800092.
- (61) Rodriguez, D.; Kim, J.-H.; Root, S. E.; Fei, Z.; Boufflet, P.; Heeney, M.; Kim, T.-S.; Lipomi, D. J. Comparison of Methods for Determining the Mechanical Properties of Semiconducting Polymer Films for Stretchable Electronics. *ACS Appl. Mater. Interfaces* **2017**, *9*, 8855–8862.
- (62) Alkhadra, M. A.; Root, S. E.; Hilby, K. M.; Rodriguez, D.; Sugiyama, F.; Lipomi, D. J. Quantifying the Fracture Behavior of Brittle and Ductile Thin Films of Semiconducting Polymers. *Chem. Mater.* **2017**, *29*, 10139–10149.
- (63) Singh, J. P.; Verma, S. Raw Materials for Terry Fabrics. In *Woven Terry Fabrics*; Elsevier, 2017; pp 19–28.
- (64) Nolte, A. J.; Cohen, R. E.; Rubner, M. F. A Two-Plate Buckling Technique for Thin Film

- Modulus Measurements: Applications to Polyelectrolyte Multilayers. *Macromolecules* **2006**, *39*, 4841–4847.
- (65) Stafford, C. M.; Harrison, C.; Beers, K. L.; Karim, A.; Amis, E. J.; VanLandingham, M. R.; Kim, H.-C.; Volksen, W.; Miller, R. D.; Simonyi, E. E. A Buckling-Based Metrology for Measuring the Elastic Moduli of Polymeric Thin Films. *Nat. Mater.* **2004**, *3*, 545–550.
- (66) Tahk, D.; Lee, H. H.; Khang, D.-Y. Elastic Moduli of Organic Electronic Materials by the Buckling Method. *Macromolecules* **2009**, *42*, 7079–7083.
- (67) O'Connor, B.; Chan, E. P.; Chan, C.; Conrad, B. R.; Richter, L. J.; Kline, R. J.; Heeney, M.; McCulloch, I.; Soles, C. L.; DeLongchamp, D. M. Correlations between Mechanical and Electrical Properties of Polythiophenes. *ACS Nano* **2010**, *4*, 7538–7544.
- (68) Wilder, E. A.; Guo, S.; Lin-Gibson, S.; Fasolka, M. J.; Stafford, C. M. Measuring the Modulus of Soft Polymer Networks via a Buckling-Based Metrology. *Macromolecules* **2006**, *39*, 4138–4143.
- (69) Stafford, C. M.; Vogt, B. D.; Harrison, C.; Julthongpiput, D.; Huang, R. Elastic Moduli of Ultrathin Amorphous Polymer Films. *Macromolecules* **2006**, *39*, 5095–5099.
- (70) Chung, J. Y.; Nolte, A. J.; Stafford, C. M. Surface Wrinkling: A Versatile Platform for Measuring Thin-Film Properties. *Adv. Mater.* **2011**, *23*, 349–368.
- (71) Wang, D.; Russell, T. P. Advances in Atomic Force Microscopy for Probing Polymer Structure and Properties. *Macromolecules* **2018**, *51*, 3–24.
- (72) Hoffman, D.; Miskioglu, I.; Drelich, J.; Aifantis, K. Measuring the Elastic Modulus of Polymers by Nanoindentation with an Atomic Force Microscope. In *EPD Congress 2011*; John Wiley & Sons, Inc.: Hoboken, NJ, USA, 2012; pp 243–251.
- (73) Kontomaris, S. The Hertz Model in AFM Nanoindentation Experiments: Applications in

- Biological Samples and Biomaterials. *Micro Nanosyst.* **2018**, *10*, 11–22.
- (74) Notbohm, J.; Poon, B.; Ravichandran, G. Analysis of Nanoindentation of Soft Materials with an Atomic Force Microscope. *J. Mater. Res.* **2012**, *27*, 229–237.
- (75) Hertz, T. Determining the Elastic Modulus of Biological Samples Using Atomic Force Microscopy Using. 1–9.
- (76) Vinckier, A.; Semenza, G. Measuring Elasticity of Biological Materials by Atomic Force Microscopy. *FEBS Lett.* **1998**, *430*, 12–16.
- (77) Passeri, D.; Bettucci, A.; Biagioni, A.; Rossi, M.; Alippi, A.; Tamburri, E.; Lucci, M.; Davoli, I.; Berezina, S. Indentation Modulus and Hardness of Viscoelastic Thin Films by Atomic Force Microscopy: A Case Study. *Ultramicroscopy* **2009**, *109*, 1417–1427.
- (78) Kim, D.-H.; Liu, Z.; Kim, Y.-S.; Wu, J.; Song, J.; Kim, H.-S.; Huang, Y.; Hwang, K.; Zhang, Y.; Rogers, J. A. Optimized Structural Designs for Stretchable Silicon Integrated Circuits. *Small.* **2009**, *5*, 2841–2847.
- (79) Li, Y.; Tatum, W. K.; Onorato, J. W.; Barajas, S. D.; Yang, Y. Y.; Luscombe, C. K. An Indacenodithiophene-Based Semiconducting Polymer with High Ductility for Stretchable Organic Electronics. *Polym. Chem.* **2017**, *8*, 5185–5193.
- (80) Song, E.; Kang, B.; Choi, H. H.; Sin, D. H.; Lee, H.; Lee, W. H.; Cho, K. Stretchable and Transparent Organic Semiconducting Thin Film with Conjugated Polymer Nanowires Embedded in an Elastomeric Matrix. *Adv. Elect. Mater.* **2016**, 1–8.
- (81) Lee, Y.; Shin, M.; Thiyagarajan, K.; Jeong, U. Approaches to Stretchable Polymer Active Channels for Deformable Transistors. *Macromolecules* **2016**, *49*, 433–444.
- (82) Song, J.; Jiang, H.; Liu, Z. J.; Khang, D. Y.; Huang, Y.; Rogers, J. A.; Lu, C.; Koh, C. G. Buckling of a Stiff Thin Film on a Compliant Substrate in Large Deformation. *Int. J.*

- Solids Struct.* **2008**, *45*, 3107–3121.
- (83) Khang, D.-Y.; Rogers, J. A.; Lee, H. H. Mechanical Buckling: Mechanics, Metrology, and Stretchable Electronics. *Adv. Funct. Mater.* **2009**, *19*, 1526–1536.
- (84) Lipomi, D. J.; Tee, B. C.-K.; Vosgueritchian, M.; Bao, Z. Stretchable Organic Solar Cells. *Adv. Mater.* **2011**, *23*, 1771–1775.
- (85) Kaltenbrunner, M.; White, M. S.; Głowacki, E. D.; Sekitani, T.; Someya, T.; Sariciftci, N. S.; Bauer, S. Ultrathin and Lightweight Organic Solar Cells with High Flexibility Martin. **2012**.
- (86) Ocheje, M. U.; Charron, B. P.; Cheng, Y.-H.; Chuang, C.-H.; Soldera, A.; Chiu, Y.-C.; Rondeau-Gagné, S. Amide-Containing Alkyl Chains in Conjugated Polymers: Effect on Self-Assembly and Electronic Properties. *Macromolecules* **2018**, *51*, 1336–1344.
- (87) Li, Y.; Tatum, W. K.; Onorato, J. W.; Barajas, S. D.; Yang, Y. Y.; Luscombe, C. K. An Indacenodithiophene-Based Semiconducting Polymer with High Ductility for Stretchable Organic Electronics. **2017**, 5185–5193.
- (88) Müller, B. C.; Goffri, S.; Breiby, D. W.; Andreasen, J. W.; Chanzy, H. D.; Janssen, R. A. J.; Nielsen, M. M.; Radano, C. P.; Sirringhaus, H.; Smith, P.; Stingelin-stutzmann, N. Tough, Semiconducting Polyethylene-Poly(3-Hexylthiophene) Diblock Copolymers. **2007**, *Adv. Funct. Mater.* 2674–2679.
- (89) Peng, R.; Pang, B.; Hu, D.; Chen, M.; Zhang, G.; Wang, X.; Lu, H.; Cho, K.; Qiu, L. An ABA Triblock Copolymer Strategy for Intrinsically Stretchable Semiconductors. *J. Mater. Chem. C* **2015**, *3*, 3599–3606.
- (90) Oh, J. Y.; Rondeau-gagné, S.; Chiu, Y.; Chortos, A.; Lissel, F.; Wang, G. N.; Schroeder, B. C.; Kurosawa, T.; Lopez, J.; Katsumata, T.; et al. Intrinsically Stretchable and Healable

- Semiconducting Polymer for Organic Transistors. *Nat. Publ. Gr.* **2016**, 539, 411–415.
- (91) Mun, J.; Wang, G. N.; Oh, J. Y.; Katsumata, T.; Lee, F. L.; Kang, J.; Wu, H.; Lissel, F.; Rondeau-Gagné, S.; Tok, J. B.-H.; Bao, Z. Effect of Nonconjugated Spacers on Mechanical Properties of Semiconducting Polymers for Stretchable Transistors. *Adv. Funct. Mater.* **2018**, 28, 1804222.
- (92) Zhao, Y.; Zhao, X.; Zang, Y.; Di, C.; Diao, Y.; Mei, J. Conjugation-Break Spacers in Semiconducting Polymers: Impact on Polymer Processability and Charge Transport Properties. *Macromolecules* **2015**, 48, 2048–2053.
- (93) Printz, A. D.; Savagatrup, S.; Burke, D. J.; Purdy, T. N.; Lipomi, D. J. Increased Elasticity of a Low-Bandgap Conjugated Copolymer by Random Segmentation for Mechanically Robust Solar Cells. *RSC Adv.* **2014**, 4, 13635–13643.
- (94) Savagatrup, S.; Zhao, X.; Chan, E.; Mei, J.; Lipomi, D. J. Effect of Broken Conjugation on the Stretchability of Semiconducting Polymers. *Macromol. Rapid Commun.* **2016**, 37, 1623–1628.
- (95) Yu, H.; Park, K. H.; Song, I.; Kim, M.-J.; Kim, Y.-H.; Oh, J. H. Effect of the Alkyl Spacer Length on the Electrical Performance of Diketopyrrolopyrrole-Thiophene Vinylene Thiophene Polymer Semiconductors. *J. Mater. Chem. C* **2015**, 3, 11697–11704.
- (96) Lei, T.; Wang, J.; Pei, J. Roles of Flexible Chains in Organic Semiconducting Materials. *Chem. Mater.* **2014**, 26, 594–603.
- (97) Kang, I.; Yun, H.; Chung, D. S.; Kwon, S.; Kim, Y. Record High Hole Mobility in Polymer Semiconductors via Side-Chain Engineering. **2013**, No. c.
- (98) Xue, G.; Zhao, X.; Qu, G.; Xu, T.; Gumyusenge, A.; Zhang, Z.; Zhao, Y.; Diao, Y.; Li, H.; Mei, J. Symmetry Breaking in Side Chains Leading to Mixed Orientations and



- Improved Charge Transport in Isoindigo- Alt -Bithiophene Based Polymer Thin Films. *ACS Appl. Mater. Interfaces* **2017**, *9*, 25426–25433.
- (99) Zhang, F.; Hu, Y.; Schuettfort, T.; Di, C.; Gao, X.; McNeill, C. R.; Thomsen, L.; Mannsfeld, S. C. B.; Yuan, W.; Sirringhaus, H.; Zhu, D. Critical Role of Alkyl Chain Branching of Organic Semiconductors in Enabling Solution-Processed N-Channel Organic Thin-Film Transistors with Mobility of up to  $3.50 \text{ cm}^2 \text{ V}^{-1} \text{ s}^{-1}$ . *J. Am. Chem. Soc.* **2013**, *135*, 2338–2349.
- (100) Lei, T.; Dou, J.; Pei, J. Influence of Alkyl Chain Branching Positions on the Hole Mobilities of Polymer Thin-Film Transistors. *Adv. Mater.* **2012**, *24*, 6457–6461.
- (101) Wu, H.; Hung, C.; Hong, C.; Sun, H.; Wang, J.; Yamashita, G.; Higashihara, T.; Chen, W. Isoindigo-Based Semiconducting Polymers Using Carbosilane Side Chains for High Performance Stretchable Field-Effect Transistors. *Macromolecules* **2016**, *49*, 8540–8548.
- (102) Mei, J.; Kim, D. H.; Ayzner, A. L.; Toney, M. F.; Bao, Z. Siloxane-Terminated Solubilizing Side Chains: Bringing Conjugated Polymer Backbones Closer and Boosting Hole Mobilities in Thin-Film Transistors. *J. Am. Chem. Soc.* **2011**, *133*, 20130–20133.
- (103) Wen, H.; Wu, H.; Aimi, J.; Hung, C.; Chiang, Y.; Kuo, C.; Chen, W. Soft Poly(Butyl Acrylate) Side Chains toward Intrinsically Stretchable Polymeric Semiconductors for Field-Effect Transistor Applications. *Macromolecules* **2017**, *50*, 4982–4992.
- (104) Zhang, J.; Posselt, D.; Smilgies, D.; Perlich, J.; Kyriakos, K.; Jaksch, S.; Papadakis, C. M. Complex Macrophase-Separated Nanostructure Induced by Microphase Separation in Binary Blends of Lamellar Diblock Copolymer Thin Films. *Macromol. Rapid Commun.* **2014**, *35*, 1622–1629.
- (105) Spencer, R. K. W.; Matsen, M. W. Confinement Effects on the Miscibility of Block

- Copolymer Blends. *Eur. Phys. J. E* **2016**, *39*, 43.
- (106) He, Z.; Li, D.; Hensley, D. K.; Rondinone, A. J.; Chen, J. Switching Phase Separation Mode by Varying the Hydrophobicity of Polymer Additives in Solution-Processed Semiconducting Small-Molecule/Polymer Blends. *Appl. Phys. Lett.* **2013**, *103*, 113301.
- (107) Spencer, R. K. W.; Matsen, M. W. Confinement Effects on the Miscibility of Block Copolymer Blends. *Eur. Phys. J. E* **2016**, *39*, 43.
- (108) Shin, M.; Oh, J. Y.; Byun, K.; Lee, Y.; Kim, B.; Baik, H.; Park, J.; Jeong, U. Polythiophene Nanofibril Bundles Surface-Embedded in Elastomer: A Route to a Highly Stretchable Active Channel Layer. *Adv. Mater.* **2015**, *27*, 1255–1261.
- (109) Choi, D.; Kim, H.; Persson, N.; Chu, P. H.; Chang, M.; Kang, J. H.; Graham, S.; Reichmanis, E. Elastomer-Polymer Semiconductor Blends for High-Performance Stretchable Charge Transport Networks. *Chem. Mater.* **2016**, *28*, 1196–1204.
- (110) Xu, J.; Wang, S.; Wang, G.-J. N.; Zhu, C.; Luo, S.; Jin, L.; Gu, X.; Chen, S.; Feig, V. R.; To, J. W. F.; et al. Highly Stretchable Polymer Semiconductor Films through the Nanoconfinement Effect. *Science (80-. )*. **2017**, *355*, 59–64.
- (111) Zhang, G.; McBride, M.; Persson, N.; Lee, S.; Dunn, T. J.; Toney, M. F.; Yuan, Z.; Kwon, Y.; Chu, P.; Risteen, B.; Reichmanis, E. Versatile Interpenetrating Polymer Network Approach to Robust Stretchable Electronic Devices. *Chem. Mater.* **2017**, *29*, 7645–7652.
- (112) Kim, D. H.; Park, Y. D.; Jang, Y.; Kim, S.; Cho, K. Solvent Vapor-Induced Nanowire Formation in Poly(3-Hexylthiophene) Thin Films. *Macromol. Rapid Commun.* **2005**, *26*, 834–839.
- (113) Jo, S. B.; Lee, W. H.; Qiu, L.; Cho, K. Polymer Blends with Semiconducting Nanowires for Organic Electronics. *J. Mater. Chem.* **2012**, *22*, 4244.

- (114) Han, X.; Dai, Y.; Huang, Y.; Liu, H. Effect of Polymer-Substrate Interactions on the Surface Morphology of Polymer Blend Thin Films: Comparison between Simulation and Experiment. *J. Macromol. Sci. Part B* **2009**, *48*, 723–735.
- (115) Mannella, G. A.; Carfì Pavia, F.; La Carrubba, V.; Brucato, V. Phase Separation of Polymer Blends in Solution: A Case Study. *Eur. Polym. J.* **2016**, *79*, 176–186.
- (116) Thomas, K. R. Physical Phenomena of Thin Surface Layers. **2010**, No. July.
- (117) Dalxoki-veress, K. CONFINEMENT EFFECTS ON. **1998**.
- (118) Coveney, S. Fundamentals of Phase Separation in Polymer Blend Thin Films. **2014**, 1–26.
- (119) Mokarian-Tabari, P.; Geoghegan, M.; Howse, J. R.; Heriot, S. Y.; Thompson, R. L.; Jones, R. A. L. Quantitative Evaluation of Evaporation Rate during Spin-Coating of Polymer Blend Films: Control of Film Structure through Defined-Atmosphere Solvent-Casting. *Eur. Phys. J. E* **2010**, *33*, 283–289.
- (120) Heriot, S. Y.; Jones, R. A. L. An Interfacial Instability in a Transient Wetting Layer Leads to Lateral Phase Separation in Thin Spin-Cast Polymer-Blend Films. *Nat. Mater.* **2005**, *4*, 782–786.
- (121) Coveney, S.; Clarke, N. Pattern Formation in Polymer Blend Thin Films: Surface Roughening Couples to Phase Separation. *Phys. Rev. Lett.* **2014**, *113*, 218301.
- (122) Lee, C.; Kim, J. Enhanced Light Out-Coupling of OLEDs with Low Haze by Inserting Randomly Dispersed Nanopillar Arrays Formed by Lateral Phase Separation of Polymer Blends. **2013**, 1–6.
- (123) Ebbens, S.; Hodgkinson, R.; Parnell, A. J.; Dunbar, A.; Martin, S. J.; Topham, P. D.; Clarke, N.; Howse, J. R. In Situ Imaging and Height Reconstruction of Phase Separation Processes in Polymer Blends during Spin Coating. *ACS Nano* **2011**, *5*, 5124–5131.

- (124) Chien, S.-C.; Yang, H.-C.; Chen, F.-C. Highly-Stable and Efficient Polymer Solar Cells Incorporating Nanoscale Buffer Layers Induced by Spontaneous Vertical Phase Separation. In *2010 35th IEEE Photovoltaic Specialists Conference*; IEEE, 2010; pp 001073–001078.
- (125) Goffri, S.; Müller, C.; Stingelin-Stutzmann, N.; Breiby, D. W.; Radano, C. P.; Andreasen, J. W.; Thompson, R.; Janssen, R. A. J.; Nielsen, M. M.; Smith, P.; Sirringhaus, H. Multicomponent Semiconducting Polymer Systems with Low Crystallization-Induced Percolation Threshold. *Nat. Mater.* **2006**, *5*, 950–956.
- (126) Arias, A. C.; Endicott, F.; Street, R. A. Surface-Induced Self-Encapsulation of Polymer Thin-Film Transistors. *Adv. Mater.* **2006**, *18*, 2900–2904.
- (127) Qiu, L.; Lim, J. A.; Wang, X.; Lee, W. H.; Hwang, M.; Cho, K. Versatile Use of Vertical-Phase-Separation-Induced Bilayer Structures in Organic Thin-Film Transistors. *Adv. Mater.* **2008**, *20*, 1141–1145.
- (128) Lee, W. H.; Lim, J. A.; Kwak, D.; Cho, J. H.; Lee, H. S.; Choi, H. H.; Cho, K. Semiconductor-Dielectric Blends: A Facile All Solution Route to Flexible All-Organic Transistors. *Adv. Mater.* **2009**, *21*, 4243–4248.
- (129) Zhao, K.; Wodo, O.; Ren, D.; Khan, H. U.; Niazi, M. R.; Hu, H.; Abdelsamie, M.; Li, R.; Li, E. Q.; Yu, L.; Yan, B.; Payne, M. M.; Smith, J.; Anthony, J. E.; Anthopoulos, T. D.; Thoroddsen, S. T.; Ganapathysubramanian, B.; Amassian, A. Vertical Phase Separation in Small Molecule:Polymer Blend Organic Thin Film Transistors Can Be Dynamically Controlled. *Adv. Funct. Mater.* **2016**, *26*, 1737–1746.
- (130) Shin, N.; Kang, J.; Richter, L. J.; Prabhu, V. M.; Kline, R. J.; Fischer, D. A.; DeLongchamp, D. M.; Toney, M. F.; Satija, S. K.; Gundlach, D. J.; Purushothaman, B.;

- Anthony, J. E.; Yoon, D. Y. Vertically Segregated Structure and Properties of Small Molecule-Polymer Blend Semiconductors for Organic Thin-Film Transistors. *Adv. Funct. Mater.* **2013**, *23*, 366–376.
- (131) Zhang, L.; Xing, X.; Zheng, L.; Chen, Z.; Xiao, L.; Qu, B.; Gong, Q. Vertical Phase Separation in Bulk Heterojunction Solar Cells Formed by in Situ Polymerization of Fulleride. *Sci. Rep.* **2015**, *4*, 5071.
- (132) Claudia Arias, A. Vertically Segregated Polymer Blends: Their Use in Organic Electronics. *J. Macromol. Sci. Part C Polym. Rev.* **2006**, *46*, 103–125.
- (133) Chen, L.-M.; Hong, Z.; Li, G.; Yang, Y. Recent Progress in Polymer Solar Cells: Manipulation of Polymer:Fullerene Morphology and the Formation of Efficient Inverted Polymer Solar Cells. *Adv. Mater.* **2009**, *21*, 1434–1449.
- (134) Kim, M.; Lee, J.; Jo, S. B.; Sin, D. H.; Ko, H.; Lee, H.; Lee, S. G.; Cho, K. Critical Factors Governing Vertical Phase Separation in Polymer–PCBM Blend Films for Organic Solar Cells. *J. Mater. Chem. A* **2016**, *4*, 15522–15535.
- (135) Li, H.; Tang, H.; Li, L.; Xu, W.; Zhao, X.; Yang, X. Solvent-Soaking Treatment Induced Morphology Evolution in P3HT/PCBM Composite Films. *J. Mater. Chem.* **2011**, *21*, 6563.
- (136) Yang, Q.; Wang, J.; Zhang, X.; Zhang, J.; Fu, Y.; Xie, Z. Constructing Vertical Phase Separation of Polymer Blends via Mixed Solvents to Enhance Their Photovoltaic Performance. *Sci. China Chem.* **2015**, *58*, 309–316.
- (137) Cheun, H.; Berrigan, J. D.; Zhou, Y.; Fenoll, M.; Shim, J.; Fuentes-Hernandez, C.; Sandhage, K. H.; Kippelen, B. Roles of Thermally-Induced Vertical Phase Segregation and Crystallization on the Photovoltaic Performance of Bulk Heterojunction Inverted

- Polymer Solar Cells. *Energy Environ. Sci.* **2011**, *4*, 3456.
- (138) Jouane, Y.; Colis, S.; Schmerber, G.; Leuvrey, C.; Dinia, A.; Lévêque, P.; Heiser, T.; Chapuis, Y.-A. Annealing Treatment for Restoring and Controlling the Interface Morphology of Organic Photovoltaic Cells with Interfacial Sputtered ZnO Films on P3HT:PCBM Active Layers. *J. Mater. Chem.* **2012**, *22*, 1606–1612.
- (139) Xue, B.; Vaughan, B.; Poh, C.; Burke, K. B.; Thomsen, L.; Stapleton, A.; Zhou, X.; Bryant, G. W.; Belcher, W.; Dastoor, P. C. Vertical Stratification and Interfacial Structure in P3HT:PCBM Organic Solar Cells. *J. Phys. Chem. C* **2010**, *114*, 15797–15805.
- (140) Wei, H. X.; Li, J.; Xu, Z. Q.; Cai, Y.; Tang, J. X.; Li, Y. Q. Thermal Annealing-Induced Vertical Phase Separation of Copper Phthalocyanine: Fullerene Bulk Heterojunction in Organic Photovoltaic Cells. *Appl. Phys. Lett.* **2010**, *97*, 083302.
- (141) Chen, D.; Liu, F.; Wang, C.; Nakahara, A.; Russell, T. P. Bulk Heterojunction Photovoltaic Active Layers via Bilayer Interdiffusion. *Nano Lett.* **2011**, *11*, 2071–2078.
- (142) Kokubu, R.; Yang, Y. Vertical Phase Separation of Conjugated Polymer and Fullerene Bulk Heterojunction Films Induced by High Pressure Carbon Dioxide Treatment at Ambient Temperature. *Phys. Chem. Chem. Phys.* **2012**, *14*, 8313.
- (143) Ruderer, M. A.; Guo, S.; Meier, R.; Chiang, H.; Körstgens, V.; Wiedersich, J.; Perlich, J.; Roth, S. V; Müller-Buschbaum, P. Solvent-Induced Morphology in Polymer-Based Systems for Organic Photovoltaics. *Adv. Funct. Mater.* **2011**, *21*, 3382–3391.
- (144) Chen, F. Spontaneous Phase Separation for Efficient Polymer Solar Cells. *SPIE Newsroom* **2008**, 8–10.
- (145) Joshua, I. S. Characterization of Mechanical and Electrical Properties of Polymer Semiconductor Blend Films. **2015**, 1–34.

- (146) Ford, M. J.; Wang, M.; Patel, S. N.; Phan, H.; Segalman, R. A.; Nguyen, T.; Bazan, G. C. High Mobility Organic Field-Effect Transistors from Majority Insulator Blends. *Chem. Mater.* **2016**, *28*, 1256–1260.
- (147) Kwak, D.; Choi, H. H.; Kang, B.; Kim, D. H.; Lee, W. H.; Cho, K. Liquid-Crystalline Semiconductors: Tailoring Morphology and Structure of Inkjet-Printed Liquid-Crystalline Semiconductor/Insulating Polymer Blends for High-Stability Organic Transistors (Adv. Funct. Mater. 18/2016). *Adv. Funct. Mater.* **2016**, *26*, 3180–3180.
- (148) Lei, Y.; Deng, P.; Li, J.; Lin, M.; Zhu, F.; Ng, T.; Lee, C.; Ong, B. S. Solution-Processed Donor-Acceptor Polymer Nanowire Network Semiconductors For High-Performance Field-Effect Transistors. *Sci. Rep.* **2016**, *6*, 24476.
- (149) McBride, M.; Persson, N.; Keane, D.; Bacardi, G.; Reichmanis, E.; Grover, M. A. A Polymer Blend Approach for Creation of Effective Conjugated Polymer Charge Transport Pathways. *ACS Appl. Mater. Interfaces* **2018**, *10*, 36464–36474.
- (150) Scaccabarozzi, A. D.; Stingelin, N. Semiconducting:Insulating Polymer Blends for Optoelectronic Applications—a Review of Recent Advances. *J. Mater. Chem. A* **2014**, *2*, 10818–10824.
- (151) Kyaw, A. K. K.; Wang, D. H.; Luo, C.; Cao, Y.; Nguyen, T.; Bazan, G. C.; Heeger, A. J. Effects of Solvent Additives on Morphology, Charge Generation, Transport, and Recombination in Solution-Processed Small-Molecule Solar Cells. *Adv. Energy Mater.* **2014**, *4*, 1301469.
- (152) Jeong, J. W.; Jo, G.; Choi, S.; Kim, Y. A.; Yoon, H.; Ryu, S.; Jung, J.; Chang, M. Solvent Additive-Assisted Anisotropic Assembly and Enhanced Charge Transport of  $\pi$ -Conjugated Polymer Thin Films. *ACS Appl. Mater. Interfaces* **2018**, *10*, 18131–18140.

## CHAPTER II. EXPERIMENTAL PROCEDURE AND CHARACTERIZATION METHODS

### 2.1. Materials

Commercial reactants were used without further purification unless stated otherwise. All the solvents used in these reactions were distilled prior to use. Low molecular-weight branched polyethylene (BPE, ~ 500 Da) was purchased from PolyAnalytik (London, Ontario) and used as it is. Tris(dibenzylideneacetone)dipalladium(0)-chloroform adduct ( $\text{Pd}_2(\text{dba})_3 \cdot \text{CHCl}_3$ ) was purchased from Sigma Aldrich and recrystallized following a reported procedure<sup>1</sup>. (*E*)-1,2-bis(5-(trimethylstannyl)thiophen-2-yl)ethene (TVT), 3,6-bis(5-bromothiophen-2-yl)-2,5-bis(2-decyltetradecyl)-2,5-dihydropyrrolo[3,4-*c*]pyrrole-1,4-dione were synthesized according to literature<sup>2</sup>.

### 2.2. Experimental Procedure

The preparation of the DPP-based conjugated polymer has been performed using previously reported procedure (Figure 2.1.).<sup>3</sup> Briefly, a decyltetradecyl-branched diketopyrrolopyrrole monomer was copolymerized with bis(trimethyltin)thienovinylthiophene *via* Stille polymerization<sup>4</sup>. The resulting polymer was precipitated with methanol, and purified by Soxhlet extraction with methanol, acetone and hexane, and was collected, precipitated in methanol and dried under vacuum.



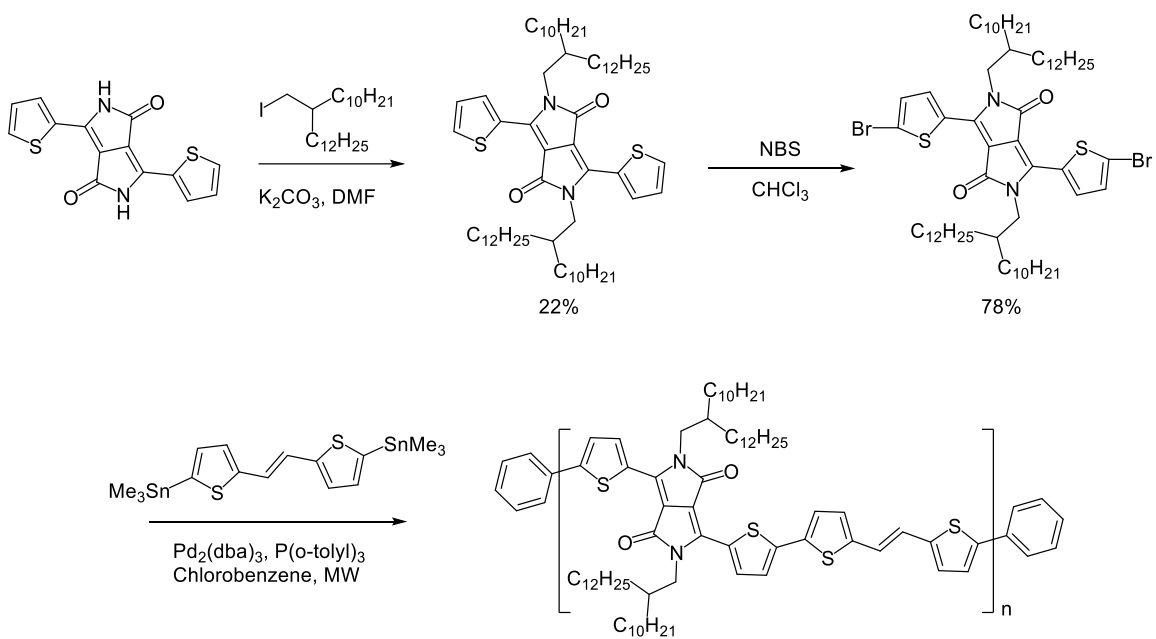


Figure 2.1. Synthetic pathway towards P(DPPTVT) polymer.

### General procedure for Stille polymerization of P(DPPTVT)

A microwave vessel equipped with a stir bar was charged with *E*-1,2-bis(5-(trimethylstannyl)thiophen-2-yl)ethene (45.78 mg, 0.088 mmol), 3,6-bis(5-bromothiophen-2-yl)-2,5-bis(2-decyltetradecyl)-2,5-dihydropyrrolo[3,4-*c*]pyrrole-1,4-dione (100 mg, 0.088 mmol), degassed chlorobenzene (3.5 mL), Pd<sub>2</sub>(dba)<sub>3</sub> (1.6 mg, 0.0017 mmol), and P(*o*-tolyl)<sub>3</sub> (2.4 mg, 0.0078 mmol). The vessel was then immediately sealed with a snap cap and microwave irradiated under the following conditions with ramping temperature (Microwave Setup: Biotage Microwave Reactor; Power, 300 W; Temperature and Time, 2 minutes at 100°C, 2 minutes at 120°C, 5 minutes at 140°C, 5 minutes at 160°C, and 40 minutes at 180°C; Pressure, 17 bar; Stirring, 720). After completion, the polymer was end-capped with trimethyltin phenyl (21.2 mg, 0.088 mmol) and bromobenzene (13.8 mg, 0.088 mmol), successively. The reaction was then cooled to room temperature and dissolved in TCE. This solution was then precipitated in methanol and the solid

was collected by filtration into a glass thimble. The contents of the thimble were then extracted in a Soxhlet extractor with methanol, acetone, hexane and finally chlorobenzene. The chlorobenzene fraction was concentrated and reprecipitated in methanol, followed by filtration and drying under vacuum. Molecular weight estimated from high temperature GPC:  $M_n = 41.9$  kDa,  $M_w = 138.1$  kDa, PDI = 3.2.

### **2.3. Sample Preparation**

The various polymer blends (3 mg/mL) were prepared by dissolving the conjugated polymer and branched polyethylene with selected weight ratios in chlorobenzene, at 80°C overnight. The stock solution of branched polyethylene (75 mg) was first prepared in 10 mL of diethyl ether. According to the selected weight% of BPE required (from 0 to 98 wt. %), a certain amount of BPE (stock solution) was transferred in a scintillation vial and evaporated. Then, a specific amount of conjugated polymer was added to the system and stirred overnight in chlorobenzene at 80°C. The obtained solutions were directly spin-coated onto the SiO<sub>2</sub> for further characterization.

### **2.4. Measurements and Characterization**

Nuclear magnetic resonance (NMR) spectra were recorded on a Bruker 300 MHz spectrometer. The spectra for all polymers were obtained in deuterated 1,1,2,2-tetrachloroethane (TCE-d<sub>2</sub>) at 120 °C. Chemical shifts are given in parts per million (ppm) (Figure A1). Number average molecular weight ( $M_n$ ), weight average molecular weight ( $M_w$ ), and polydispersity index (PDI) were evaluated by high temperature size exclusion chromatography (SEC) using 1,2,4-

trichlorobenzene and performed on a EcoSEC HLC-8321GPC/HT (Tosoh Bioscience, PolyAnalytik) equipped with a single TSKgel GPC column (GMH<sub>HR</sub>-H; 300 mm × 7.8 mm) calibrated with monodisperse polystyrene standards. UV Visible spectroscopy was performed on a Varian UV/Visible Cary 50 spectrophotometer. The surface structure of polymer film was obtained using a Multimode atomic force microscope (AFM, Digital Instruments) operated in the tapping mode at room temperature. Images were collected using Nanoscope 6 software and processed using WSxM 5.0 Develop 8.0 software. Grazing incidence X-ray diffraction (GIXRD) was performed at the Canadian Light source at beamline HXMA. The X-ray wavelength was 0.9758 Å or a beam energy of 12.7 keV. The incidence angle of X-ray was set at 0.12. The sample to detector distance is about 150 mm. Numerical integration of the diffraction peak areas was performed using the software fit2d. All measurements were conducted using a Keithley 4200 semiconductor parameter analyzer (Keithley Instruments Inc.) under dry N<sub>2</sub> (glovebox) and ambient atmosphere at room temperature. X-Ray diffraction was performed on a Proto AXRD Benchtop Powder Diffractometer with a Cu source ( $\lambda = 1.5406 \text{ \AA}$ ). The chemical topographies of the polymer films were mapped using a Bruker Anasys nanoIR3 equipped with a Daylight Solutions MIRcat-QT IR laser and Anasys PR-EX-TnIR-A cantilever tip. A wavelength of 1664 cm<sup>-1</sup> was used to measure relative wavelength absorption of the DPP domains and 5 μm<sup>2</sup> images were collected using Analysis Studio software at a scan rate of 0.5 Hz using a 512 x 512 points raster resolution.

#### **2.4.1. FET Device Fabrication and Characterization**

FET devices were fabricated on highly doped n-type Si(100) wafer with a 300 nm thick SiO<sub>2</sub> functionalized with an n-octadecyltrimethoxysilane (OTS) self-assembled monolayer,

according to the reported method<sup>5</sup>. Before spin-coating the active layers, the OTS-treated substrate was washed with toluene, acetone and isopropyl alcohol, and then dried with nitrogen before use. The organic semiconductor thin films were spin-cast on the OTS-treated substrates and controlled the thickness at ~40 nm from prepared polymer solutions in chlorobenzene (3 mg mL<sup>-1</sup>). The thermal annealing process was carried out inside a N<sub>2</sub>-filled glove box. For thermal annealing at 100°C and 170°C, films were directly heated on a hot plate for 1 hour. For the as-prepared films, samples were left to dry at ambient temperature after spincoating before being introduced and tested in a N<sub>2</sub>-filled glove box. A top-contact gold electrode (70 nm) was subsequently deposited by evaporation through a shadow mask with a channel length (L) and width (W) defined as 50 and 1000 μm, respectively. All the measurements of the transistor memories were conducted using a Keithley 4200-SCS semiconductor parameter analyzer (Keithley Instruments Inc., Cleveland, OH, USA) in an N<sub>2</sub>- filled glove box at room temperature.

#### **2.4.2. Film-on-water (FOW) procedure**

To perform the stretching tests for P(DPPTVT)/BPE blend, the blend solutions with certain weight percentage of BPE were spin-coated onto the polystyrene sulfonate (PSS) glass slide. The concentration of PSS solution is 50mg in 1ml of DH<sub>2</sub>O. Poly(dimethylsiloxane) (PDMS) was chosen as the elastomer substrate for all FOW experiments. The PDMS was mixed at a base to crosslinker ratio of 20:1 and allowed to cure in the oven at 60<sup>0</sup>C for 24 h before use in any experiment. After curing the PDMS was cut into rectangular strips ( $l = 3$  cm,  $w = 0.5$  cm,  $h = 0.1$  cm) and place onto the spin-coated P(DPPTVT)/BPE blend on the PSS glass slide. By floating the specimen on the water surface led to the penetration of water into the PSS layer. Consequently,

the PSS layer was dissolved and the active layer was delaminated from the glass substrate, attached to the PDMS-slide (Figure 2.2.)<sup>6</sup>. The obtained polymer thin blends were stretched to a certain percent strain and transferred back on silicon wafer for further characterization.

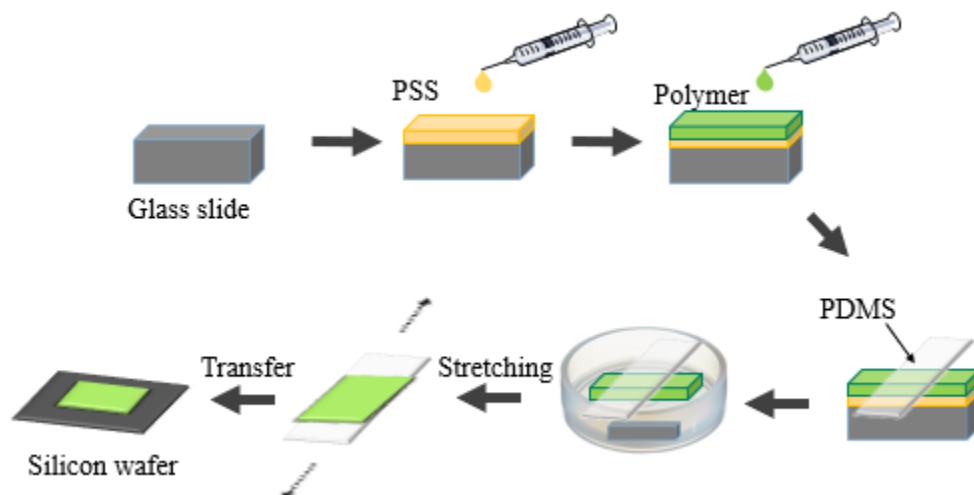


Figure 2.2. A schematic illustration of preparing a DPP-based polymer/BPE thin film under strain through film-on-water (FOW) method.

### 2.4.3. Atomic Force Microscopy (AFM)

AFM has become an essential tool in various areas of interest in materials chemistry. It is mainly used to look at the topography of materials with a high resolution down to nanometer scale.<sup>7</sup> AFM operates by using a probe, which consists of a cantilever and tip, to scan the surface of the sample. The sharp tip, attached to the end of the cantilever, is brought into close contact with a surface and scanned line-by-line over a sample (Figure 2.3.).<sup>8,9</sup> The motion of the tip as it scans along the surface is monitored *via* a laser beam reflected off the cantilever, which records the deflection of the cantilever. Depending on the nature of the tip's motion, AFM can operate in contact, non-contact, and tapping modes.<sup>10</sup> Moreover, AFM also permits the determination of the

root mean square roughness ( $R_q$  or RMS) of the surface. It provides the mean squared absolute values of the surface roughness profile which is more sensitive to peaks and valleys than the average roughness ( $R_a$ ).<sup>11</sup>

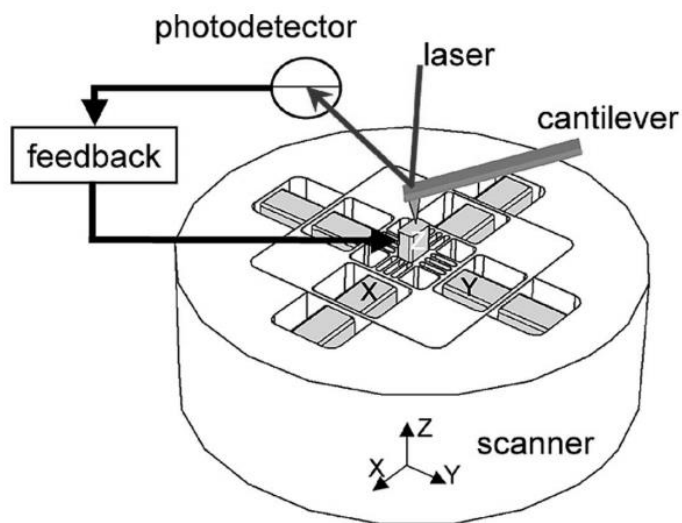


Figure 2.3. Schematic illustration of a typical AFM set up.<sup>11</sup>

#### 2.4.4. Grazing Incidence X-Ray Diffraction (GIXRD)

GIXRD is a powerful surface sensitive technique which can be used to study semiconducting polymer thin films. The incident X-ray beam strikes a sample at a small angle (less than a specific critical angle) in order to undergo a total reflection which avoids scattering from the substrate.<sup>12</sup> The reflected beam is detected by a 2-dimensional (2D) detector to determine the backbone orientation in thin films. There are two main types of semiconducting polymer orientations: edge-on and face-on which are illustrated in Figure 2.4a using P3HT polymer as an example. The edge-on orientation involves the lamellar side-chains wetting the interfaces, which means the lamellar stacking is vertical ((100) diffraction peak along  $q_z$  axis), and  $\pi$ - $\pi$ -stacking is

then in-plane which gives a rise in (010) diffraction peak along the  $q_{xy}$  axis (Figure 2.4b). The face-on orientation involves the aromatic rings facing the substrate, which means the  $\pi$ - $\pi$ -stacking is in the vertical direction and a (101) diffraction peak appears along  $q_z$ , while the lamellar stacking is in-plane ((100) peak along  $q_{xy}$ ) (Figure 2.4c).<sup>13</sup>

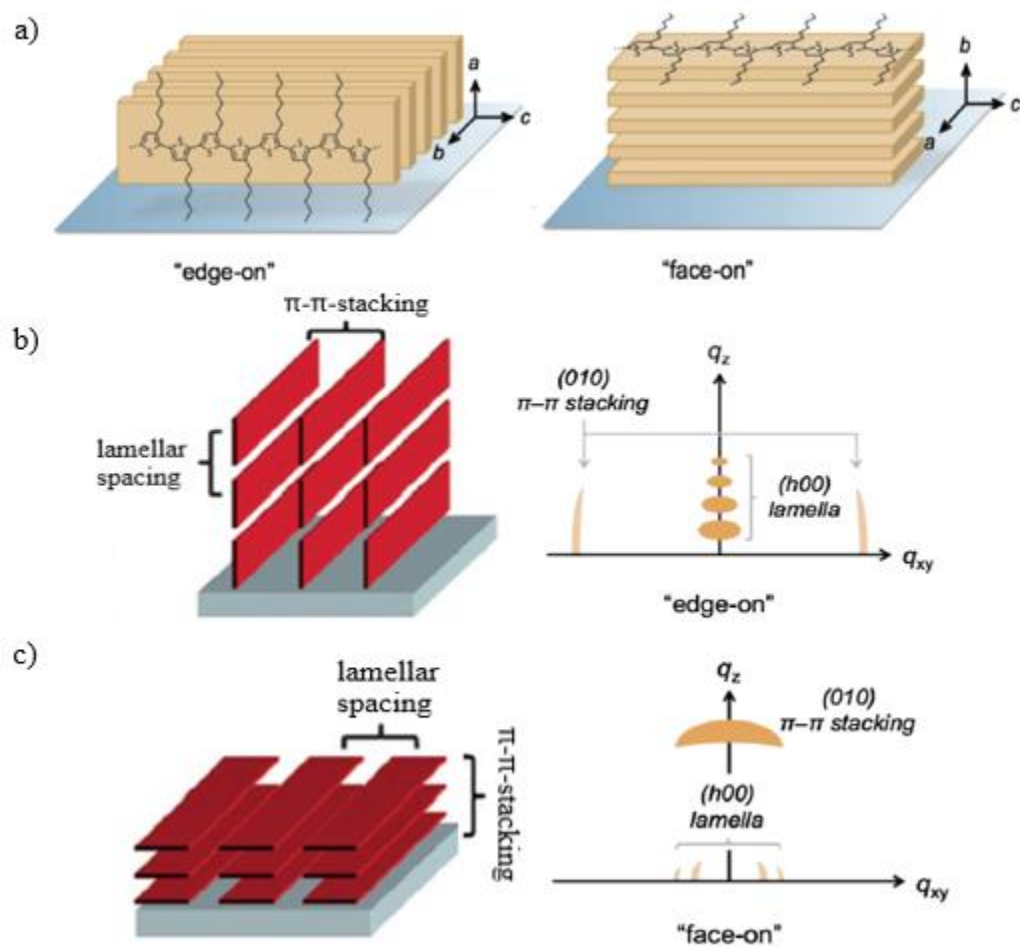


Figure 2.4. a) Representation of edge-on and face-on orientations of the P3HT backbone semiconducting polymer with respect to the substrate surface; schematic illustration of the typical 2D GIXRD pattern which corresponds to b) edge-on orientation and c) face-on orientation. Adapted with permission from Ref. 13. Copyright 2015 Elsevier.

#### 2.4.5. Dichroic Ratio Measurements

The influence of BPE on mechanical properties of DPP-based polymer has been investigated using the UV-vis spectroscopy with a polarizer in parallel and perpendicular directions to the strain. Dichroic ratio is used to get an insight on the chain alignment, induced by strain, of polymer chains at different weight percentage of BPE. Schematic diagram of polarized UV-vis characterization on stretched polymer blend films is illustrated in Figure 2.5. A dichroic ratio equals to around 1 at 0% strain meaning that the degree of alignment is nearly isotropic. The value of dichroic ratio is expected to steadily increase upon strain before cracks are formed.

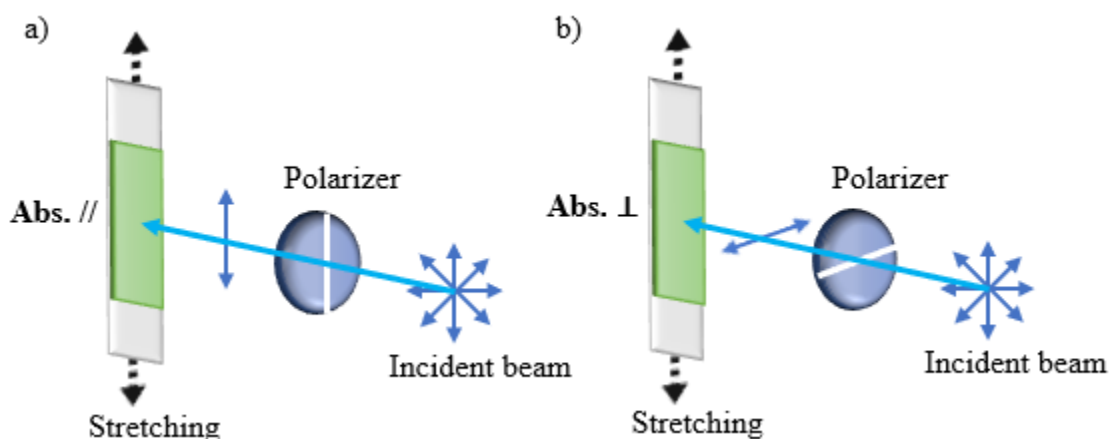


Figure 2.5. Schematic diagram of polarized UV-vis characterization on stretched polymer blend films with the polarization direction of light a) parallel and b) perpendicular to the stretching direction.

#### 2.4.6. Crack onset strain

Crack on-set strain was measured using active polymer blend thin films on PDMS stripes obtained from FOW method. Each film, with a specific weight ratio of BPE additive, was stretched



to a certain percent strain increasing it by 5% each time before cracks start to propagate. Stretching the polymer thin films on PDMS substrate is followed by transferring them onto the SiO<sub>2</sub>-wafers to monitor the formation of cracks by the optical microscope.

#### **2.4.7. Film-on-Water (FOW) Tensile Pull Test**

The BPE/ P(DPPTVT) polymer blends (3 mg/mL) were prepared and spin-casted on prime Si wafers pre-coated with poly(sodium 4-styrenesulfonate) (PSS) as a sacrificial layer. The samples were then tightly bonded to PDMS pads through van der Waals forces. The samples were immersed in a water bath to dissolve the PSS layer and float the film. The floated thin films were directly used for tensile pull test at a strain rate of  $2 \times 10^{-4} \text{ sec}^{-1}$  to obtain stress-strain curves. The elastic modulus of a film (E) is calculated as a slope of the curve in the linear, elastic zone. The detailed tensile stage set-up can be found in previous reports.<sup>6,7</sup>

## REFERENCES

- (1) Zaleskiy, S. S.; Ananikov, V. P. Pd 2 (Dba) 3 as a Precursor of Soluble Metal Complexes and Nanoparticles: Determination of Palladium Active Species for Catalysis and Synthesis. *Organometallics* **2012**, *31*, 2302–2309.
- (2) Yu, H.; Park, K. H.; Song, I.; Kim, M.-J.; Kim, Y.-H.; Oh, J. H. Effect of the Alkyl Spacer Length on the Electrical Performance of Diketopyrrolopyrrole-Thiophene Vinylene Thiophene Polymer Semiconductors. *J. Mater. Chem. C* **2015**, *3*, 11697–11704.
- (3) Ocheje, M. U.; Charron, B. P.; Cheng, Y.-H.; Chuang, C.-H.; Soldera, A.; Chiu, Y.-C.; Rondeau-Gagné, S. Amide-Containing Alkyl Chains in Conjugated Polymers: Effect on Self-Assembly and Electronic Properties. *Macromolecules* **2018**, *51*, 1336–1344.
- (4) Yu, H.; Park, K. H.; Song, I.; Kim, M.-J.; Kim, Y.-H.; Oh, J. H. Effect of the Alkyl Spacer Length on the Electrical Performance of Diketopyrrolopyrrole-Thiophene Vinylene Thiophene Polymer Semiconductors. *J. Mater. Chem. C* **2015**, *3*, 11697–11704.
- (5) Zheng, Y.-Q.; Wang, Z.; Dou, J.-H.; Zhang, S.-D.; Luo, X.-Y.; Yao, Z.-F.; Wang, J.-Y.; Pei, J. Effect of Halogenation in Isoindigo-Based Polymers on the Phase Separation and Molecular Orientation of Bulk Heterojunction Solar Cells. *Macromolecules* **2015**, *48*, 5570–5577.
- (6) Rodriguez, D.; Kim, J.-H.; Root, S. E.; Fei, Z.; Boufflet, P.; Heeney, M.; Kim, T.-S.; Lipomi, D. J. Comparison of Methods for Determining the Mechanical Properties of Semiconducting Polymer Films for Stretchable Electronics. *ACS Appl. Mater. Interfaces* **2017**, *9*, 8855–8862.
- (7) Ferencz, R.; Sanchez, J.; Blümich, B.; Herrmann, W. AFM Nanoindentation to Determine Young's Modulus for Different EPDM Elastomers. *Polym. Test.* **2012**, *31*, 425–432.

- (8) Vinckier, A.; Semenza, G. Measuring Elasticity of Biological Materials by Atomic Force Microscopy. *FEBS Lett.* **1998**, *430*, 12–16.
- (9) Zhang, S.; Ocheje, M. U.; Luo, S.; Ehlenberg, D.; Appleby, B.; Weller, D.; Zhou, D.; Rondeau-Gagné, S.; Gu, X. Probing the Viscoelastic Property of Pseudo Free-Standing Conjugated Polymeric Thin Films. *Macromol. Rapid Commun.* **2018**, *39*, 1800092.
- (10) Wang, D.; Russell, T. P. Advances in Atomic Force Microscopy for Probing Polymer Structure and Properties. *Macromolecules* **2018**, *51*, 3–24.
- (11) Oliveira, R. R. L. De; Albuquerque, D. A. C.; Cruz, T. G. S. Measurement of the Nanoscale Roughness by Atomic Force Microscopy : Basic Principles and Applications. **2012**, 150–174.
- (12) Dutta, P. Grazing Incidence X-Ray Diffraction. *Current Science.* **2000**, *78*, 1–21.
- (13) Osaka, I.; Takimiya, K. Backbone Orientation in Semiconducting Polymers. *Polymer (Guildf)*. **2015**, *59*, A1–A15.

## CHAPTER III. MORPHOLOGY AND ELECTRONIC PROPERTIES OF SEMICONDUCTING POLYMER AND BRANCHED POLYETHYLENE BLENDS

### 3.1. Introduction

Organic semiconductors, particularly  $\pi$ -conjugated polymers, are a class of materials widely utilized for the development of new organic electronic devices, especially promising for the fabrication of the next generation of flexible, and stretchable devices.<sup>1-5</sup> In fact, since the discovery by MacDiarmid, Shirakawa and Heeger, conjugated polymers have shown great promise in organic electronics as semiconducting materials in organic field-effect transistors (OFETs), and as light absorbing materials in organic photovoltaics (OPVs) mainly due to their good electronic properties, easy processing *via* solution-based methods, synthetic versatility, and potential for large-scale production.<sup>6-9</sup> Since the last decade, research on new  $\pi$ -conjugated materials with constantly improved properties has intensified leading to new materials with carrier mobility of  $>10 \text{ cm}^2\text{V}^{-1}\text{s}^{-1}$ , and OPV devices with power conversions exceeding 10%.<sup>10-12</sup> Many novel chemical designs have been developed to enhance the electronic and mechanical properties of conjugated polymers.<sup>13,14</sup> Among others, backbone rational design and side-chain engineering have showed great promise for tuning various properties, including backbone planarity, bandgap, and crystallinity, which have a direct influence on the resulting properties of  $\pi$ -conjugated materials.<sup>15-18</sup> Despite these major advancements, rational control on the polymer morphology in the solid-state is a parameter still difficult to predict and significantly impairs electronic and mechanical properties.

Recently, various solvent additives have been shown to improve domain purity and enhance the morphology on conjugated polymers in the solid-state.<sup>19,20</sup> Among these, diiodoctane

(DIO) is one of the most used additives, leading to a drastic improvement in efficiency by promoting an increased aggregation and improving charge transport.<sup>21</sup> In OFETs, different materials and additives have also been developed and used to control the solid-state morphology.<sup>22,23</sup> Pioneered by Reichmanis and coworkers, the blending of conjugated polymers with high molecular weight elastomeric materials, often based on poly(dimethylsiloxane) (PDMS) or poly(styrene) (PS), have showed impressive results for the enhancement of both charge transport and mechanical compliance through the confinement of the conjugated polymer chains.<sup>24,25</sup> This innovative approach was shown to be particularly effective for the design of highly stretchable and deformable devices and also demonstrated the great potential of solvent and elastomeric additives for the control and tuning of the solid-state morphology of conjugated polymers.<sup>26–28</sup> However, the large incorporation of insulating materials and additives can potentially decrease the overall efficiency of the devices and long-term stability. The impossibility of removing those additives completely after thermal treatment can also be a major issue during fabrication.<sup>29</sup> Moreover, several challenges remain to be addressed in order to expand the utilization of conjugated polymers for large-scale production of electronics and develop more efficient functional devices.<sup>30,31</sup> Among others, the amount of active materials needed and their cost, combined with the important quantity of chlorinated solvent often used in large-scale deposition are limitations that need to be considered and improved.<sup>32,33</sup> Therefore, many new techniques have been developed to reduce the production costs of organic electronics while maintaining the performance of electronic devices.<sup>34</sup>

Herein, we report the blending of a low molecular weight branched polyethylene (BPE) with a high charge carrier mobility DPP-based conjugated polymer for the fine tuning of the morphology in the solid-state (Figure 3.1).

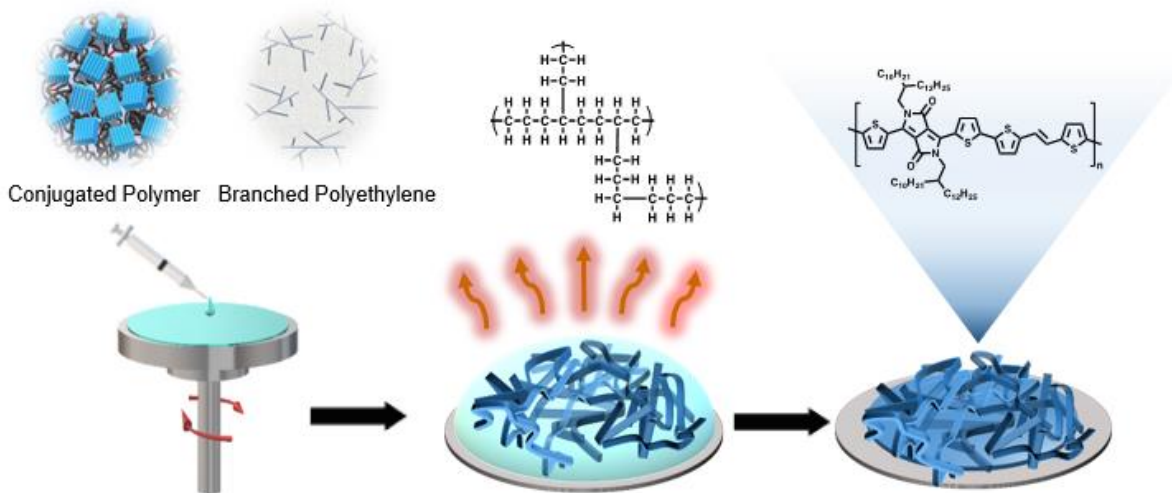


Figure 3.1. Blending of low molecular weight branched polyethylene (BPE) with a DPP-based polymer for fine-tuning of the solid-state morphology.

The high charge carrier mobility polymer was blended with different weight ratios of BPE additive, from 0 to 90 wt.%. The resulting thin films were characterized by various techniques, including UV-Vis spectroscopy, atomic force microscopy (AFM), and X-ray diffraction (XRD) in order to probe the influence of the BPE on the nanoscale morphology before and after removal of the additive. Interestingly, the new BPE additive promoted aggregation of the  $\pi$ -conjugated polymer in thin films, while also being volatile due to its low molecular weight. This unique feature allowed for a complete removal of the additives upon thermal annealing without drastically affecting the aggregation promoted by the physical blending. Moreover, the new blended systems were utilized for the fabrication of OFET devices. The resulting devices were shown not to be significantly affected by the addition of the insulating additive before and after its removal by thermal annealing. Interestingly, the devices without annealing showed a decent average mobility of around  $0.3 \text{ cm}^2\text{V}^{-1}\text{s}^{-1}$ , even when 90% of the blend was prepared with BPE. This new strategy

is particularly promising for the large-scale fabrication of OFETs with minimal utilization of semiconducting polymers, and for the control of the solid-state morphology with non-toxic materials and additives.

### 3.2. Results and Discussion

To investigate the blending of conjugated polymers with the BPE additive, a poly-diketopyrrolopyrrole-co-thienovinythiophene (DPPTVT) copolymer was selected as semiconducting material since this conjugated polymer previously showed good charge mobility in OFETs and good mechanical compliance.<sup>10,35</sup> The preparation of the DPP-based conjugated polymer has been performed using a previously reported procedure.<sup>17</sup> Briefly, a decyltetradecyl-branched diketopyrrolopyrrole monomer was copolymerized with bis(trimethyltin)thienovinythiophene *via* Stille polymerization.<sup>36</sup> The resulting polymer was precipitated with methanol, and purified by Soxhlet extraction with methanol, acetone and hexane, and was collected, precipitated in methanol and dried under vacuum.

In order to promote aggregation and fine-tuning of the morphology in the solid state, the polyethylene-based additive was selected due to many factors. First, the preparation of polyethylene is well-established and can be performed in large scale, and low costs.<sup>37</sup> Since the thermal removal of the additive can be a potential issue for the final stability and performance of the resulting materials, the branched PE derivative was designed to minimize the boiling point and to maximize phase separation (confinement of the semiconducting polymer) in the solid-state. In comparison to its linear counterpart, a branched polyethylene with a more important hydrodynamic volume can allow for a phase separation when blended to a conjugated polymer, while maintaining

a low boiling point and good solubility. Moreover, BPE has been shown to be non-toxic, which represents an important advantage over current additives used to fine-tune the morphology of conjugated polymers in the solid state, and solvents used to process those materials in large scale.<sup>38,39</sup> Therefore, a branched polyethylene derivative with a molecular weight of 500 Da and a boiling point of 135°C was used (Figure A2). Interestingly, the materials showed a low viscosity, facilitating the processing and blending with the DPP-based conjugated polymer. The structure of the selected DPP-based polymers and branched PE additive are shown on Figure 3.2.a-b.

To investigate the influence of BPE on the electronic and physical properties of P(DPPTVT) in thin films, materials were mixed in various ratios, ranging from 0 to 90 wt.% of BPE and P(DPPTVT). The resulting BPE/DPP-based polymer blends were first characterized by UV-Vis spectroscopy to get insight on the aggregation behavior and optical properties, and the results are summarized on Figure 3.2.c-d and A3. As expected, the different blends exhibited two distinct absorption bands in thin films, with an absorption band at 450 nm, attributed to the  $\pi$ - $\pi^*$  transition. This transition was not impacted by the addition of BPE. Furthermore, for all polymer blends, a broad band centered at 700 nm was observed, attributed to the intramolecular donor-acceptor charge transfer of the conjugated polymers, and showed two vibrational peaks (0-0 and 0-1).<sup>40</sup>

Interestingly, the intensity of the 0-0 peak gradually increased upon the addition of BPE. Previously observed for other  $\pi$ -conjugated polymer blend systems, this finding indicates that an increased incorporation of BPE forces the conjugated polymer chains to aggregate strongly, potentially due to phase separation.<sup>20,41</sup> Since BPE is volatile and can be removed by a mild thermal annealing (170°C), the UV-Vis spectra of the different blends were also recorded after removal of the additive (Figure 3.2.d and A3).



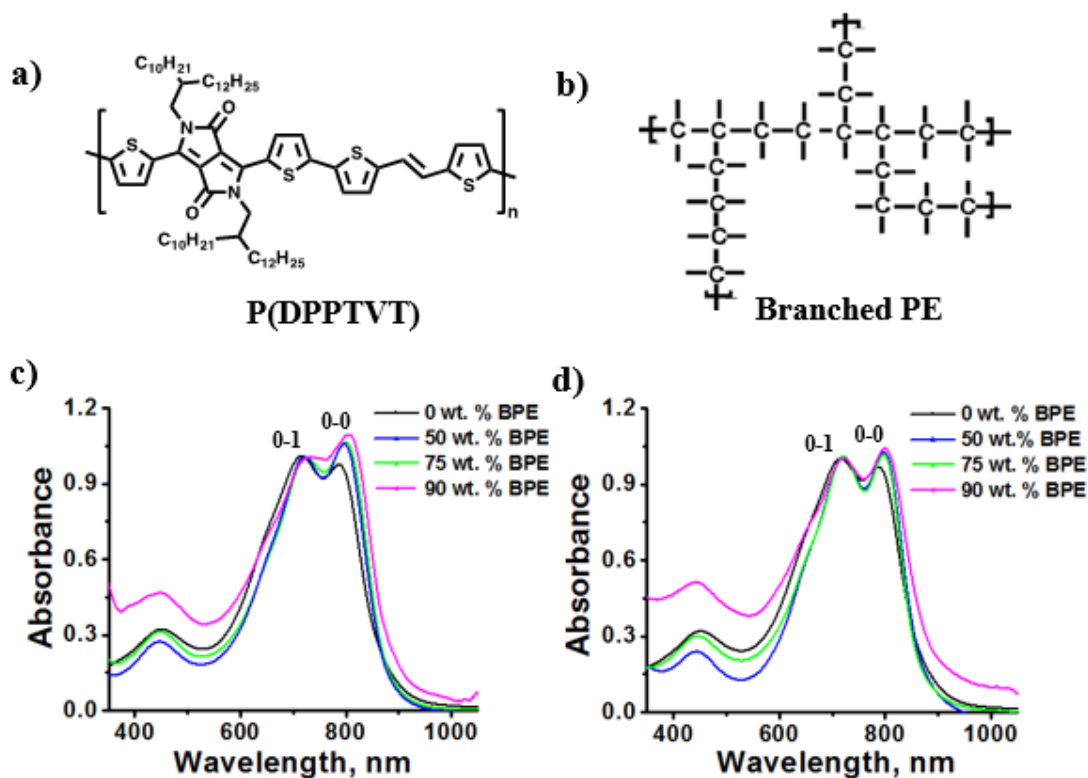


Figure 3.2. a) Chemical structure of P(DPPTVT) conjugated polymer; b) chemical structure of branched polyethylene (BPE) utilized in polymer blends; c) UV-Vis spectra of P(DPPTVT) blended with 0 wt.% to 90 wt.% BPE (thin films) before thermal annealing, and d) UV-Vis spectra of P(DPPTVT) blended with 0 wt.% to 90 wt.% BPE (thin films) after thermal annealing.

Interestingly, despite reducing the aggregation after removal, the conjugated polymers initially blended with higher amount of BPE still showed an increased intensity of the 0-0 peak. This observation indicates the conjugated polymers chains are aggregated even after removal of the BPE. In order to get insight on the importance of the branched architecture on the molecular aggregation, a control experiment was performed by UV-Vis spectroscopy using a commercially available linear polyethylene additive (LPE,  $M_n = 1700$  Da) blended with P(DPPTVT). As observed with BPE, the addition of LPE caused a small change in the 0-0 peak, attributed to the aggregation of the semiconducting polymer, which progressively increased from 0 to 90 wt.% LPE

(Figure 3.3.). This result was attributed, similar to the blending of conjugated polymer with BPE, to the molecular aggregation indicated by phase separation.

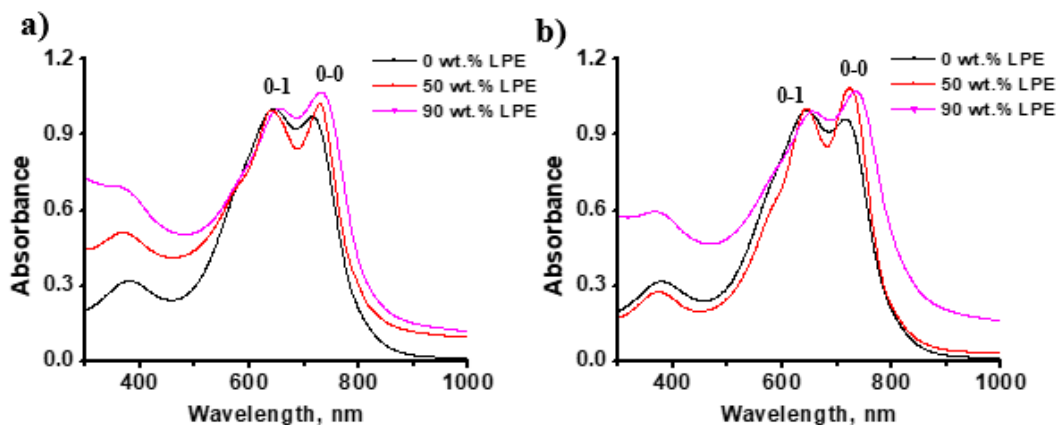


Figure 3.3. UV-Vis spectra of P(DPPTVT) blended with 0 wt.% to 90 wt.% LPE (thin films) a) before thermal annealing, and b) after thermal annealing at 170°C.

As shown on Figure 3.4., molecular aggregation was not significantly affected by a thermal annealing treatment, which indicated that, in contrast to the BPE additive, LPE that cannot be removed thermally. It is important to note that the LPE additive used was shown to have a melting point of 92°C. Upon heating to 200°C, no evaporation of the solid was observed and further heating led to polymer decomposition.

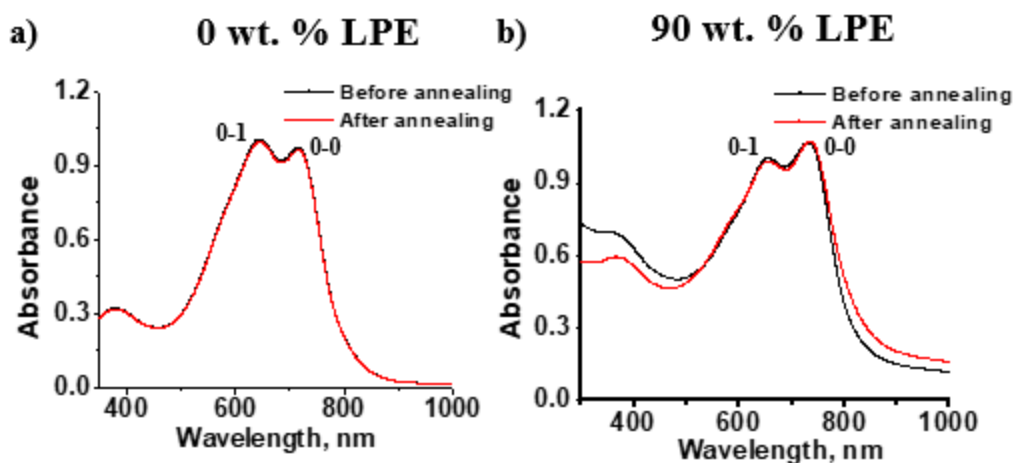


Figure 3.4. UV-Vis spectra of conjugated polymer blended with a) 0 wt% LPE and b) 90 wt.% LPE before and after thermal annealing at 170°C.

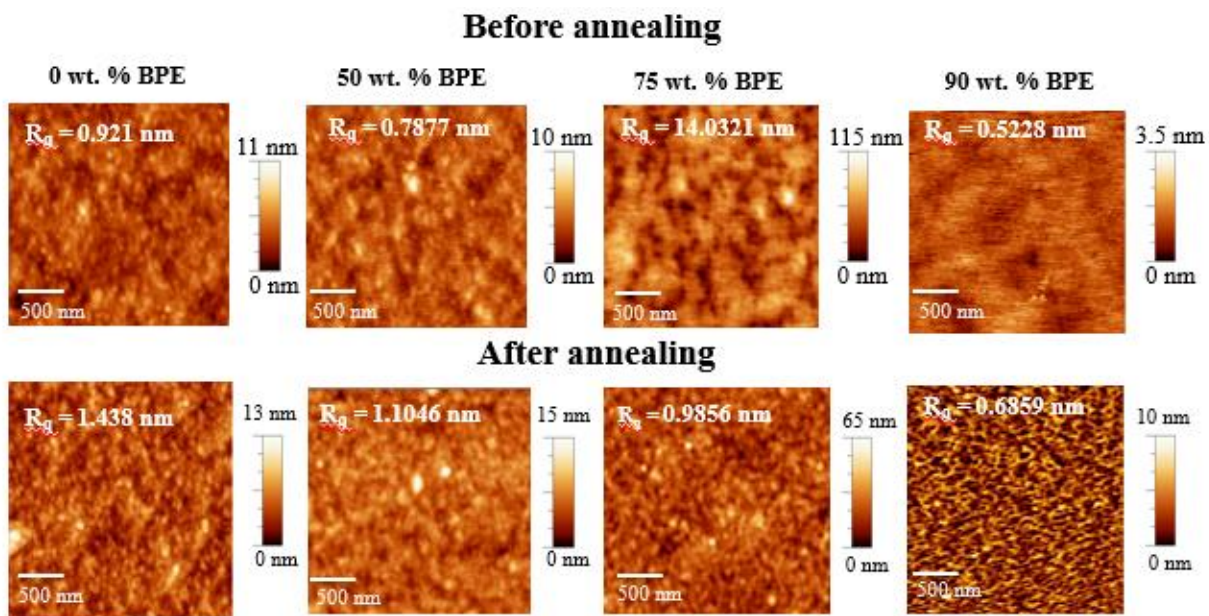


Figure 3.5. Atomic force microscopy images (height) of 0, 50, 75 and 90 wt. BPE/P(DPPTVT) blends, before and after thermal annealing (170°C). Scale bar is 500 nm.

To further characterize the morphology of the different BPE/conjugated polymer blends in the solid-state, atomic force microscopy (AFM) was utilized, and the results are summarized in Figure 3.5 and A4. Before annealing, all the blends showed a relatively smooth surface. However, upon addition of 50 wt.% of BPE, the formation of nanodomains began to be observed. Upon increasing the amount of BPE to 75 and 90 wt.%, these phase-separated nanodomains progressively increased in size, which can be directly related to the increase in aggregation, as observed by UV-Vis spectroscopy. The surface roughness of the different thin films before annealing progressively increased upon addition of BPE, which demonstrates an increase in the aggregation and phase separation in the blends. As shown in Figure A5, both top and bottom interfaces of the 75 wt.% BPE/conjugated polymer blends were also imaged by AFM to get insight on the vertical phase separation. This specific ratio was selected due to the obvious phase separation observed. Interestingly, a significant difference in nanoscale morphology and phase separation was observed as the top interface showed aggregated domains, while the bottom interface, i.e. the one in contact with the silicon substrate, showed a much more uniform morphology with smaller aggregated. This result potentially indicates that phase separation between the conjugated polymer and the polyethylene derivative phase does not occur uniformly over the entire thin films, which can potentially be attributed to interfacial effects or a lower affinity of the BPE for chlorinated solvents. In order to characterize the system after removal of the BPE, the samples were then subjected to a thermal annealing at 170°C. Interestingly, as observed by AFM, the large nanodomains resulting from phase separation, observed before annealing completely disappeared after annealing, indicating a complete or partial removal of the BPE additive. Furthermore, similar to the trend observed in UV-Vis, the conjugated polymers initially blended with higher amount of BPE shows an increased surface roughness, which

confirms that even after removal of the additive, the polymer chains are strongly aggregated and possess a different surface morphology than the non-blended P(DPPTVT).

In order to confirm the influence of the BPE additive on the solid-state morphology, AFM was also performed on a reference system prepared from pure conjugated polymer diluted in chlorobenzene, and the results are showed in Figures A6 and A7. In contrast to the BPE/DPP-based polymer blends, chlorobenzene did not influence the morphology of the polymer film, which showed a relatively uniform roughness when diluted. The same trend was also observed after thermal annealing (removal of the solvent), thus confirming the phase-separation promoted by the addition of the BPE. In addition, AFM was also performed on LPE/conjugated polymer blends in order to probe for phase separation at the nanoscale. Results are showed in Figure A8. Interestingly, the addition of LPE caused a significant change in the solid-state morphology of the thin films, which went from a smooth surface for the pure conjugated polymer to a fiber-like morphology upon adding 50 and 90 wt.% of LPE. This phenomenon can be attributed to the phase separation caused by the addition of LPE, which was also observed with BPE/conjugated polymer blends to a lesser extent probably due to the difference in molecular weight between BPE and LPE additives. Interestingly, the morphology remained fairly similar upon thermal annealing, which confirms that the LPE additive is not removed, in contrast to the BPE additive.

As shown on Figure 3.6., X-ray diffraction (XRD) was used to investigate the solid-state packing of the blends before and after annealing. To avoid any influence of the quantity of conjugated polymer on the intensity of scattering, the amount of conjugated polymer remained constant upon adding more BPE additive.

Similar to previous reports, the as-spun film of P(DPPTVT) showed a clear diffraction peak at  $2\theta = \sim 4.2^\circ$ , which can be attributed to the interlamellar packing of the conjugated polymer

chains ( $d$ -spacing of 21 Å).<sup>42,43</sup> Upon addition of BPE, this peak gradually decreased, thus indicating a progressive reduction in crystallinity (Figure 3.6.a). This result indicates that, despite favoring aggregation between the polymer chains, BPE act as a plasticizer, thus disrupting the solid-state morphology and preventing the formation of large crystalline phases.

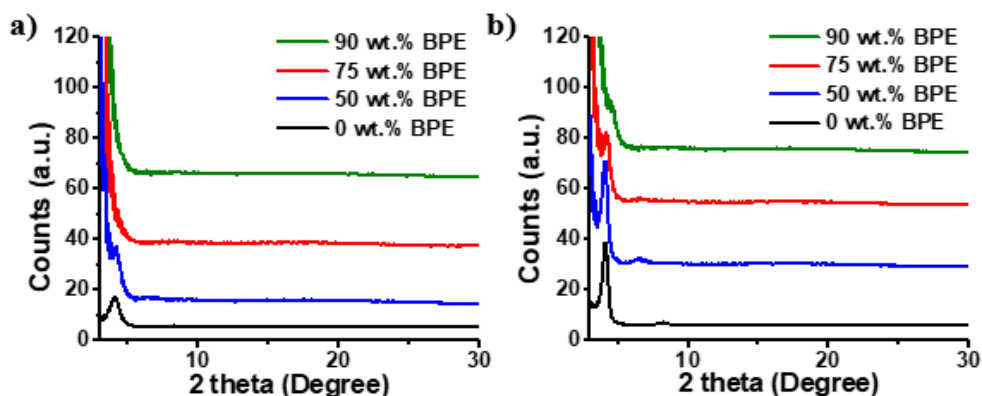


Figure 3.6. X-ray diffraction spectra (reflectance mode) of P(DPPTVT) blended with 0 to 90 wt.% BPE a) before thermal annealing and b) after thermal annealing at 170°C. The concentration of conjugated polymer was kept constant (1.5 mg/mL).

Interestingly, upon removal of the BPE *via* thermal annealing, the different blends showed a significant enhancement of their crystallinity, confirmed by the apparition of an intense peak related to the interlamellar packing (Figure 3.6.b). However, the conjugated polymers initially blended with more important ratios of BPE (75 and 90 wt.% BPE) still showed a drastically reduced crystallinity in comparison to the sample initially blended with 0 to 50 wt.% BPE. Finally, it is important to mention that the absence of diffraction corresponding to  $\pi$ - $\pi$  distance on thin films indicates that the polymer chains are potentially adopting an edge-on morphology, independent of the presence of BPE, which can be ideal for charge-transport in OFET devices.<sup>44,45</sup> In order to confirm the orientation in the solid-state, grazing incidence X-Ray scattering (GIXRD) experiments were performed on 0, 50 and 90 wt.% polymer blends. Results are summarized in

Figures 3.7. and A9. Interestingly, independent of the ratio of conjugated polymer and BPE, the materials showed diffraction patterns typical of an edge-on orientation. This result is in good agreement with the observations from X-ray diffractometry, and indicates that BPE, despite reducing the film crystallinity, does not impact the molecular orientation in the solid-state, thus maintaining a good morphology for the charge to percolate in OFETs. It is important to mention that, the 50% polymer blend showed the most ordered conformation in the thin films, confirmed by a narrowing of the diffraction peaks (Figure 3.7.). This result is particularly promising for the large- scale coating of functional substrates with conjugated materials.

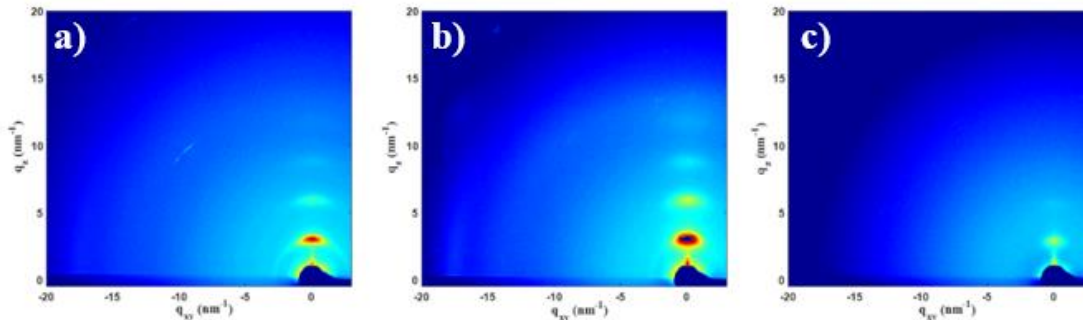


Figure 3.7. Wide-angle grazing incident X-Ray diffractogram (GIXRD) of a) P(DPPTVT), b) P(DPPTVT) + 50 wt.% BPE, and c) P(DPPTVT) + 90 wt.% BPE.

To assess the semiconducting performance of the P(DPPTVT)/BPE blends and to determine the influence of the additive on the charge carrier mobility, bottom-gate top-contact organic field-effect transistors (OFETs) were fabricated on highly doped *n*-type Si(100) with a 300 nm layer of SiO<sub>2</sub> functionalized with *n*-octadecyltrimethoxysilane (OTS).<sup>46</sup> The results are summarized in Table 1, and the detailed fabrication procedure and device characteristics are detailed in supporting information (Figures A10 and A11). First, considering the relatively low boiling point of the BPE and its ability to promote aggregation of the conjugated polymer chains, the semiconducting performance of the different polymer blends were investigated in OFETs

before thermal annealing. Interestingly, the incorporation of BPE did not affect the charge mobility, which remained relatively stable from 0 to 90 wt.% BPE. Independently of the amount of BPE added to the conjugated polymer, which was shown to cause a reduction in crystallinity and promotion of chain aggregation, the charge mobility remained around  $0.3 \text{ cm}^2\text{V}^{-1}\text{s}^{-1}$ , which represents a decent value for non-annealed devices, and confirms that addition of BPE can be an interesting alternative for the large-scale fabrication of OFETs with non-toxic additives. This result also indicates that the formation of aggregated phases in the BPE/conjugated polymer blends is enough to allow for the charges to efficiently percolate, which is in good agreement with previous reports that concluded that amorphous semiconducting materials can still possess a good charge mobility as the conformational order in aggregates can be enough to allow for charge percolation.<sup>47-49</sup>

Table 3.1. Average and maximum hole mobility ( $\mu_{\text{h}}^{\text{ave}}$ ,  $\mu_{\text{h}}^{\text{max}}$ ), threshold voltages ( $V_{\text{th}}$ ),  $I_{\text{on}}/I_{\text{off}}$ , and ratios for OFETs fabricated from polymer blends of 0 wt.% to 90 wt.% BPE before and after thermal annealing. The device performances were averaged from 12 devices, from three different batches. Thickness was evaluated by profilometry.

Sample	Annealing Temperature [°C]	W/L	Thickness (nm)	$\mu_{\text{h}}^{\text{ave}} / \mu_{\text{h}}^{\text{max}}$ [ $\text{cm}^2\text{V}^{-1}\text{s}^{-1}$ ]	$I_{\text{ON}}/I_{\text{OFF}}^{\text{ave}}$	$V_{\text{th}}^{\text{ave}}$ [V]
0 wt.% BPE	as cast	20	25.8	$0.27 \pm 0.04 / 0.50$	$10^6$	$-0.1 \pm 4.90$
	170		30.8	$0.75 \pm 0.16 / 0.97$	$10^6$	$-9.8 \pm 4.04$
50 wt.% BPE	as cast	20	34.1	$0.33 \pm 0.09 / 0.52$	$10^5$	$-1.9 \pm 4.82$
	170		29.6	$0.64 \pm 0.09 / 0.89$	$10^6$	$-3.5 \pm 6.87$
75 wt.% BPE	as cast	20	33.1	$0.32 \pm 0.08 / 0.47$	$10^6$	$-1.8 \pm 4.10$
	170		30.7	$0.79 \pm 0.09 / 1.04$	$10^6$	$-2.6 \pm 5.24$
90 wt.% BPE	as cast	20	29.5	$0.29 \pm 0.10 / 0.46$	$10^5$	$-5.8 \pm 2.52$
	170		33.2	$0.53 \pm 0.10 / 0.84$	$10^6$	$-2.6 \pm 4.41$



It is also important to mention that all samples had a similar thickness around 30 nm. Interestingly, all threshold voltages were shown to be below -5.0 V, except for the 0 wt.% BPE/PDPPTVT sample annealed at 170 °C, which showed a threshold voltage of -9.8 V. This slightly increased value was attributed to the higher crystallinity of the sample after thermal annealing, potentially increasing grain boundaries and resulting in an increased threshold voltage. Similar to the trend observed with the threshold voltages, film thickness did not have a significant effect on on/off currents ( $10^5$ - $10^6$ ).

Following the investigation of the semiconducting performance of the different blends before annealing, the thin films were thermally annealed at 170°C for 30 min. to remove the BPE additive. As a result, the charge carrier mobility increased for all blends upon thermal annealing, going from  $0.3 \text{ cm}^2\text{V}^{-1}\text{s}^{-1}$  to as high as  $1.0 \text{ cm}^2\text{V}^{-1}\text{s}^{-1}$  (75 wt.% BPE/DPP-based polymer). This phenomenon indicates that the removal of the BPE additive, combined with a thermal annealing, induces an increase in crystallinity, thus promoting charge transport in OFETs. This is also in good agreement with the results obtained by AFM and PXRD, which clearly showed an increase in crystallinity upon thermal annealing of the different polymer blends. However, it is important to mention that despite having an increased crystallinity, the blends are still much less crystalline than the pure conjugated polymer system, which showed an average charge carrier mobility of  $0.75 \text{ cm}^2\text{V}^{-1}\text{s}^{-1}$  after thermal annealing. Semiconducting performance of P(DPPTVT)/LPE blends were also evaluated as reference, and results are summarized in Figures A12. In contrast to the trend observed for the incorporation of BPE, the addition of a linear polyethylene derivative significantly affected the charge mobility, which gradually decreased upon addition of 50 to 98 wt.% LPE. This result can be attributed to the addition of insulating materials in the active layer, which prevent charge to percolate. In contrast to BPE, the thermal annealing treatment is not

enough to entirely remove the LPE additive, thus preventing the charge mobility to remain stable upon adding more LPE.

Previously observed by AFM, XRD and UV-Vis spectroscopy, the BPE additive allows for an improved aggregation in the solid-state despite decreasing the overall crystallinity of the conjugated polymer. As observed for other ratios of BPE/conjugated polymers, the aggregation of the conjugated polymer (evaluated by the intensity of the 0-0 absorption bands centered at around 720 nm) upon addition of 98 wt.% was shown to be increased (Figure 3.8.a). Upon thermal removal of the BPE, the aggregation was reduced in the system, as also observed with other ratios of BPE (Figures 3.8.b and A3). This result is another evidence that the formation of aggregated phases in the BPE/conjugated polymer blends is enough to allow for the charges to efficiently percolate.

Table 3.2. Average and maximum hole mobility ( $\mu_h^{\text{ave}}$ ,  $\mu_h^{\text{max}}$ ), threshold voltages ( $V_{\text{th}}$ ),  $I_{\text{on}}/I_{\text{off}}$ , and ratios for OFETs fabricated from diluted solution of various conjugated polymers blended with 98 wt.% BPE before and after thermal annealing. The device performances were averaged from 12 devices, from three different batches. Thickness was evaluated by profilometry.

Sample	Annealing Temperature [°C]	W/L	Thickness (nm)	$\mu_h^{\text{ave}} / \mu_h^{\text{max}}$ [ $\text{cm}^2 \text{V}^{-1} \text{s}^{-1}$ ]	$I_{\text{ON}}/I_{\text{OFF}}$	$V_{\text{th}}^{\text{ave}}$ [V]
<b>Diluted P(DPPTVT) in chlorobenzene</b>	as cast	20	10	0.0047±0.0001/0.0056	$10^3$	-3.7
	170					
<b>98 wt.% BPE/P(DPPTVT)</b>	as cast	20	33.9	0.047±0.021/0.054	$10^5$	-3.0
	170		23.6	0.038±0.006/0.044	$10^5$	-3.1
	100		34.5	0.087±0.051/0.110	$10^5$	-2.7

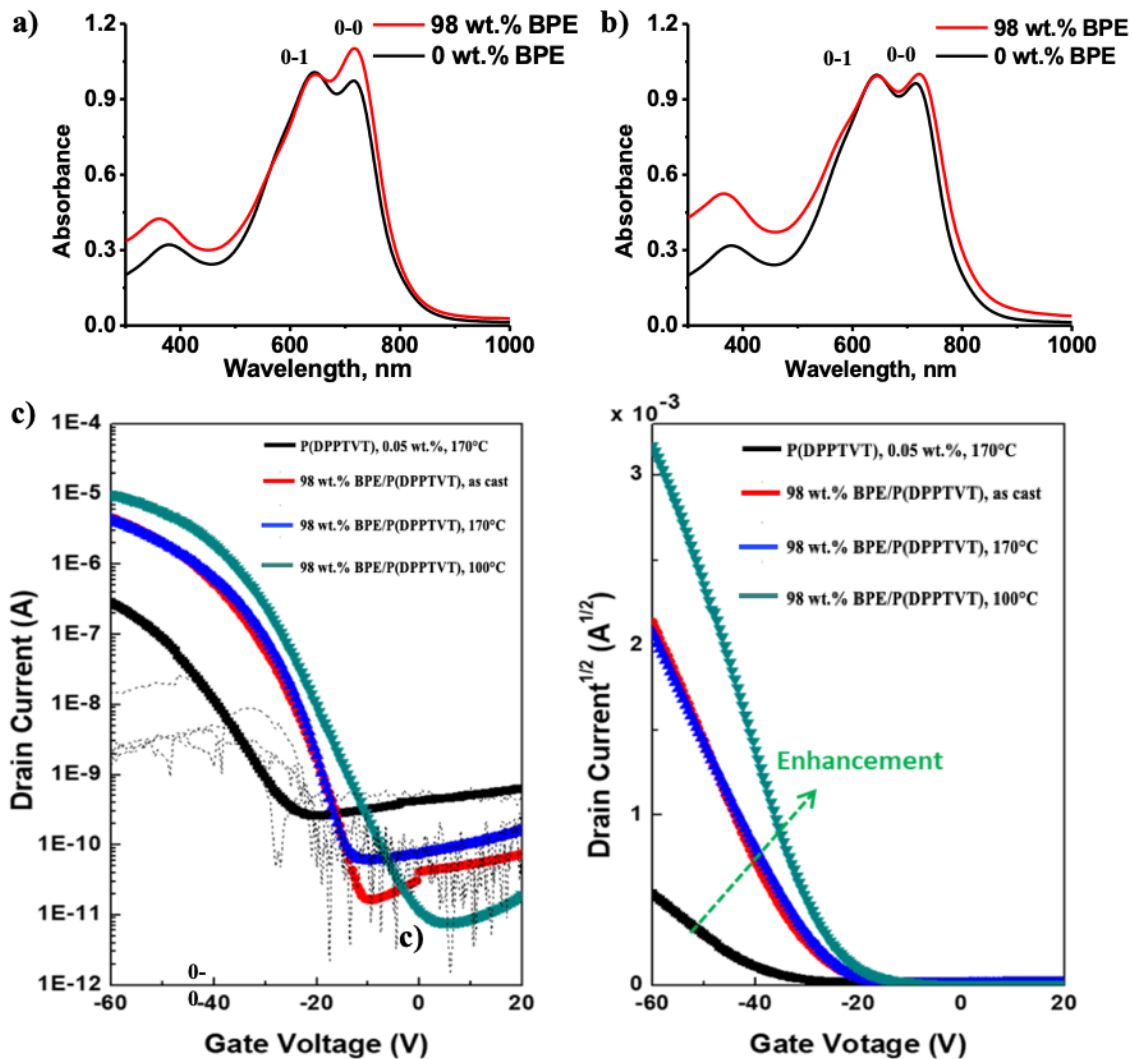


Figure 3.8. UV-Vis spectra of P(DPPTVT) blended with 0 wt.% to 98 wt.% BPE (thin films) a) before and b) after thermal annealing; c) transfer curves for OFET devices built from P(DPPTVT) 0.05 wt.% in chlorobenzene and 98 wt.% BPE/P(DPPTVT).

Since the BPE additive can help to achieve a better thin film morphology in the solid-state and can contribute to getting smoother films at lower amount of conjugated polymer, OFETs were also fabricated with a highly diluted solution of DPP-based polymer with or without BPE additive, and the results are summarized in Table 3.2, Figure 3.8.c and Figure A13. First, a solution of highly diluted conjugated polymer was prepared in chlorobenzene (0.05 wt.%) and was used as reference.

As expected, by using this diluted solution, it was very difficult to achieve a smooth and uniform thin film, thus leading to very low values of mobility in devices after thermal annealing ( $\mu_n^{\text{ave}} = 0.0047 \text{ cm}^2\text{V}^{-1}\text{s}^{-1}$ ). Interestingly, no working device was measured without annealing, which can be attributed to poor film quality.

To verify the influence of BPE on the performance of OFETs fabricated out of very diluted solution of conjugated polymer, a solution of DPP-based polymer blended with 98 wt.% BPE was prepared and investigated. Overall, all OFETs prepared from this solution showed enhanced performance in terms of charge transport. To our surprise, devices prepared from non-annealed film showed decent average mobility of  $0.054 \text{ cm}^2\text{V}^{-1}\text{s}^{-1}$ , which confirms the significant influence of BPE on thin film morphology and charge transport. More importantly, the devices prepared from annealed films at  $170 \text{ }^\circ\text{C}$  and  $100 \text{ }^\circ\text{C}$  showed respectively an average charge mobility of  $0.038$  and  $0.087 \text{ cm}^2\text{V}^{-1}\text{s}^{-1}$ , which is one order of magnitude higher than the diluted solution of pure DPP-based polymer. It is important to mention that the maximum mobility determined for some devices annealed at  $100 \text{ }^\circ\text{C}$  can reach over  $0.1 \text{ cm}^2\text{V}^{-1}\text{s}^{-1}$ , which is not only almost two order of magnitude higher than the diluted solution of pure DPP-based polymer, but also in the same order of value than devices prepared from pure DPP-based polymer at higher concentration (see Table 1). As shown in Table A1 and Figure A14 and S15, similar results were obtained upon blending the BPE additive with polyisoindigo-*co*-thienovinythiophene (P(iITVT)), another commonly used semiconducting polymer in organic electronics.<sup>18,50</sup> Analogous to the results obtained with BPE/DPP-based polymer blends, the blending of BPE with P(iITVT) was shown to help maintaining a good charge mobility despite a significant reduction of the quantity of conjugated polymers used as semiconducting layer in OFETs.

To gain insight into the morphology of the highly diluted blends (98 wt.%), further analysis was performed by GIXRD (Figures 3.9.a-c). Compared to thin film cast from higher concentration of DPP-based polymer (Figure 3.7.a), the intensity of the diffraction peaks of the thin film prepared from the highly-diluted conjugated polymer solution (0.05 wt.% in chlorobenzene) decreased significantly, which can explain the poor performance in terms of charge transport. As observed with concentrated samples, all conjugated polymer blended with BPE showed an amorphous morphology with a drastically decreased crystallinity. To gain insight into the solid-state morphology, AFM analysis was also performed for 0.05 wt.% conjugated polymer and 98 wt.% BPE/conjugated polymer in thin films.

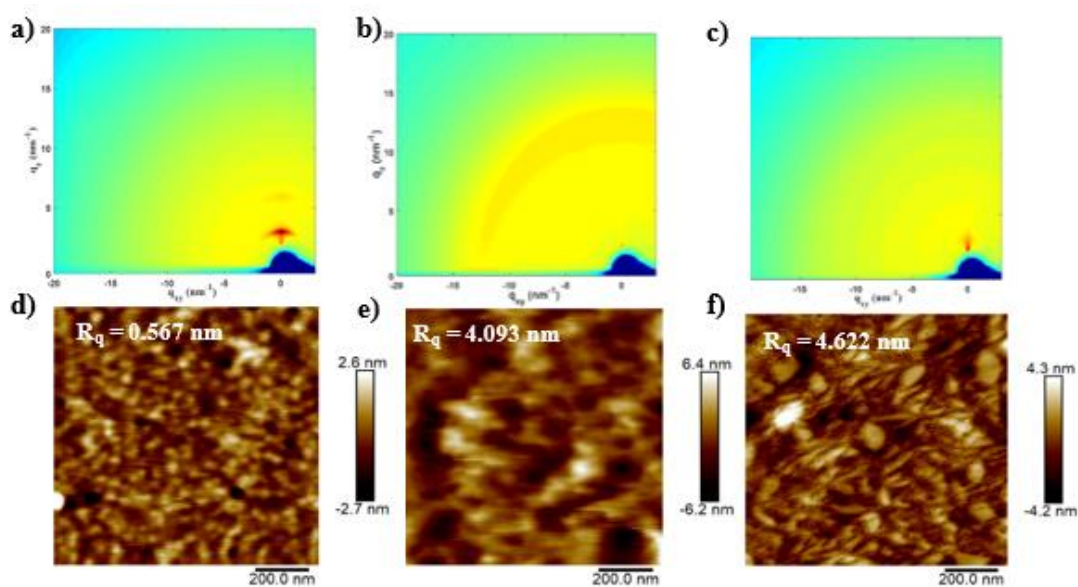


Figure 3.9. Wide-angle grazing incident X-Ray diffractogram (GIXRD) of a) P(DPPTVT) solution (0.05 wt.% in chlorobenzene) annealed at 170<sup>0</sup>C, b) P(DPPTVT) blended with 98 wt.% BPE after thermal annealing at 170 °C, and c) P(DPPTVT) blended with 98 wt.% BPE without thermal annealing; Atomic force microscopy (AFM) height images of thin films of d) P(DPPTVT) 0.05 wt.% in chlorobenzene, annealed at 170 °C; e) P(DPPTVT) blended with 98 wt.% BPE without thermal annealing; f) P(DPPTVT) blended with 98 wt.% BPE after annealing at 170<sup>0</sup>C. Scale bar is 200 nm.

As shown in Figures 3.9.d-f and A16-A17, the sample prepared from diluted P(DPPTVT) after annealing showed a sphere-like structure in a uniform thin film. The addition of BPE additive at 98 wt.% clearly induced an important aggregation through phase separation. Interestingly, the dense fibrillar structure formed upon the addition of BPE progressively decreased upon increasing the annealing temperature (Figures 3.9.e-f), which can indicate the removal of the BPE additive. This observation confirms the significant influence of the BPE additive on the solid-state morphology of conjugated polymers and can have a significant potential for the fabrication of OFET devices by helping to reduce the amount of conjugated polymer required. Moreover, since the additive is non-toxic and low-boiling point, those results also highlight the potential of this technique for advanced manufacturing of organic electronics at large-scale.

### **3.3. Conclusion**

In conclusion, this work successfully demonstrated the potential to control and fine-tune the solid-state morphology of conjugated polymers through the addition of a branched polyethylene additive. This non-toxic additive, when blended to a diketopyrrolopyrrole-based conjugated polymer at different ratios (from 0 to 90 wt.%) was shown to promote aggregation, decrease crystallinity and induce phase separation, as investigated by various characterization technique. Interestingly, the BPE additive possesses a low boiling point (around 80°C), which allows for its complete removal by thermal annealing. The resulting thin films of conjugated polymer were shown to still possess a similar morphology as the non-annealed film, thus confirming the influence of the BPE on the solid-state morphology, even after its removal. To verify the potential of this new approach for the fine-tuning of conjugated polymer morphology,

the resulting polymer blends were directly used to fabricate bottom-gate top-contact organic field-effect transistors (OFETs). Interestingly, the devices were shown to have a relatively good charge mobility before thermal annealing. Independently of the amount of BPE added to the conjugated polymer, no decrease in charge mobility was observed. More importantly, devices fabricated from a highly diluted solution of conjugated polymer with BPE (98 wt.%) were shown to maintain good charge transport properties, in contrast to a diluted solution of pure conjugated polymer. This result confirmed that BPE is a promising candidate for fine-tuning the solid-state morphology without sacrificing performance in organic electronics and can have an important impact for the fabrication of OFETs with lower amounts of conjugated polymer and without the use of toxic additives.

With the rise of flexible and printed electronics, the development of new non-toxic additives and plasticizers to control the physical and solid-state properties of semiconductors is particularly desirable. Furthermore, the easy removal of BPE without harsh conditions and its influence on aggregation and polymer crystallinity, make this additive an interesting candidate for the large-scale processing of organic semiconductors. The influence of BPE on other properties of organic semiconductors, such as mechanical compliance, stretchability, and printability will be further discussed below.

## REFERENCES

- (1) O'Connor, T. F.; Rajan, K. M.; Printz, A. D.; Lipomi, D. J. Toward Organic Electronics with Properties Inspired by Biological Tissue. *J. Mater. Chem. B* **2015**, *3*, 4947–4952.
- (2) Savagatrup, S.; Printz, A. D.; O'Connor, T. F.; Zaretski, A. V.; Lipomi, D. J. Molecularly Stretchable Electronics. *Chem. Mater.* **2014**, *26*, 3028–3041.
- (3) Ocheje, M. U.; Charron, B. P.; Nyayachavadi, A.; Rondeau-Gagné, S. Stretchable Electronics: Recent Progress in the Preparation of Stretchable and Self-Healing Semiconducting Conjugated Polymers. *Flex. Print. Electron.* **2017**, *2*, 043002.
- (4) Onorato, J.; Pakhnyuk, V.; Luscombe, C. K. Structure and Design of Polymers for Durable, Stretchable Organic Electronics. *Polym. J.* **2017**, *49*, 41–60.
- (5) Wang, G.-J. N.; Gasperini, A.; Bao, Z. Stretchable Polymer Semiconductors for Plastic Electronics. *Adv. Electron. Mater.* **2018**, 1700429.
- (6) Guo, X.; Baumgarten, M.; Müllen, K. Designing  $\pi$ -Conjugated Polymers for Organic Electronics. *Prog. Polym. Sci.* **2013**, *38*, 1832–1908.
- (7) Cheng, Y.-J.; Yang, S.-H.; Hsu, C.-S. Synthesis of Conjugated Polymers for Organic Solar Cell Applications. *Chem. Rev.* **2009**, *109*, 5868–5923.
- (8) Gsänger, M.; Bialas, D.; Huang, L.; Stolte, M.; Würthner, F. Organic Semiconductors Based on Dyes and Color Pigments. *Adv. Mater.* **2016**, 3615–3645.
- (9) Nie, Z.; Kumacheva, E. Patterning Surfaces with Functional Polymers. *Nat. Mater.* **2008**, *7*, 277–290.
- (10) Kang, I. I.; Yun, H.-J.; Chung, D. S.; Kwon, S.-K.; Kim, Y.-H. Record High Hole Mobility in Polymer Semiconductors via Side-Chain Engineering. *J. Am. Chem. Soc.* **2013**, *135*, 14896–14899.



- (11) Yao, J.; Yu, C.; Liu, Z.; Luo, H.; Yang, Y.; Zhang, G.; Zhang, D. Significant Improvement of Semiconducting Performance of the Diketopyrrolopyrrole-Quaterthiophene Conjugated Polymer through Side-Chain Engineering via Hydrogen-Bonding. *J. Am. Chem. Soc.* **2016**, *138*, 173–185.
- (12) Meng, L.; Zhang, Y.; Wan, X.; Li, C.; Zhang, X.; Wang, Y.; Ke, X.; Xiao, Z.; Ding, L.; Xia, R.; Yip, H.; Cao, Y.; Chen, Y. Organic and Solution-Processed Tandem Solar Cells with 17.3% Efficiency. *Science* **2018**, *2612*, 1–10.
- (13) Roth, B.; Savagatrup, S.; De Los Santos, N. V.; Hagemann, O.; Carle, J. E.; Helgesen, M.; Livi, F.; Bundgaard, E.; Sondergaard, R. R.; Krebs, F. C.; Lipomi, D. J. Mechanical Properties of a Library of Low-Band-Gap Polymers. *Chem. Mater.* **2016**, *28*, 2363–2373.
- (14) Root, S. E.; Savagatrup, S.; Printz, A. D.; Rodrigues, D.; Lipomi, D. J. Mechanical Properties of Organic Semiconductors for Stretchable, Highly Flexible, and Mechanically Robust Electronics. *Chem. Rev.* **2017**, *117*, 6467–6499.
- (15) Lei, T.; Wang, J. Y.; Pei, J. Roles of Flexible Chains in Organic Semiconducting Materials. *Chem. Mater.* **2014**, *26*, 594–603.
- (16) Cai, Z.; Guo, Y.; Yang, S.; Peng, Q.; Luo, H.; Liu, Z.; Zhang, G.; Liu, Y.; Zhang, D. New Donor-Acceptor-Donor Molecules with Pechmann Dye as the Core Moiety for Solution-Processed Good-Performance Organic Field-Effect Transistors. *Chem. Mater.* **2013**, *25*, 471–478.
- (17) Ocheje, M. U.; Charron, B. P.; Cheng, Y.-H.; Chuang, C.-H.; Soldera, A.; Chiu, Y.-C.; Rondeau-Gagné, S. Amide-Containing Alkyl Chains in Conjugated Polymers: Effect on Self-Assembly and Electronic Properties. *Macromolecules* **2018**, *51*, 1336–1344.
- (18) Mei, J.; Kim, D. H.; Ayzner, A. L.; Toney, M. F.; Bao, Z. Siloxane-Terminated Solubilizing

- Side Chains: Bringing Conjugated Polymer Backbones Closer and Boosting Hole Mobilities in Thin-Film Transistors. *J. Am. Chem. Soc.* **2011**, *133*, 20130–20133.
- (19) Liao, H. C.; Ho, C. C.; Chang, C. Y.; Jao, M. H.; Darling, S. B.; Su, W. F. Additives for Morphology Control in High-Efficiency Organic Solar Cells. *Mater. Today* **2013**, *16*, 326–336.
- (20) Kyaw, A. K. K.; Wang, D. H.; Luo, C.; Cao, Y.; Nguyen, T. Q.; Bazan, G. C.; Heeger, A. J. Effects of Solvent Additives on Morphology, Charge Generation, Transport, and Recombination in Solution-Processed Small-Molecule Solar Cells. *Adv. Energy Mater.* **2014**, *4*, 1–9.
- (21) Lee, J. K.; Ma, W. L.; Brabec, C. J.; Yuen, J.; Moon, J. S.; Kim, J. Y.; Lee, K.; Bazan, G. C.; Heeger, A. J. Processing Additives for Improved Efficiency from Bulk Heterojunction Solar Cells. *J. Am. Chem. Soc.* **2008**, *130*, 3619–3623.
- (22) Chae, G. J.; Jeong, S.-H.; Baek, J. H.; Walker, B.; Song, C. K.; Seo, J. H. Improved Performance in TIPS-Pentacene Field Effect Transistors Using Solvent Additives. *J. Mater. Chem. C* **2013**, *1*, 4216–4221.
- (23) Jeong, J. W.; Jo, G.; Choi, S.; Kim, Y. A.; Yoon, H.; Ryu, S. W.; Jung, J.; Chang, M. Solvent Additive-Assisted Anisotropic Assembly and Enhanced Charge Transport of  $\pi$ -Conjugated Polymer Thin Films. *ACS Appl. Mater. Interfaces* **2018**, *10*, 18131–18140.
- (24) McBride, M.; Persson, N. E.; Keane, D.; Bacardi, E.; Reichmanis, E.; Grover, M. A. A Polymer Blend Approach for Creation of Effective Conjugated Polymer Charge Transport Pathways. *ACS Appl. Mater. Interfaces* **2018**, *10*, 36464–36474.
- (25) Choi, D.; Kim, H.; Persson, N.; Chu, P. H.; Chang, M.; Kang, J. H.; Graham, S.; Reichmanis, E. Elastomer-Polymer Semiconductor Blends for High-Performance

- Stretchable Charge Transport Networks. *Chem. Mater.* **2016**, *28*, 1196–1204.
- (26) Choi, D.; Kim, H.; Persson, N.; Chu, P. H.; Chang, M.; Kang, J. H.; Graham, S.; Reichmanis, E. Elastomer-Polymer Semiconductor Blends for High-Performance Stretchable Charge Transport Networks. *Chem. Mater.* **2016**, *28*, 1196–1204.
- (27) Zhang, G.; McBride, M.; Persson, N.; Lee, S.; Dunn, T. J.; Toney, M. F.; Yuan, Z.; Kwon, Y. H.; Chu, P. H.; Risteen, B.; Reichmanis, E. Versatile Interpenetrating Polymer Network Approach to Robust Stretchable Electronic Devices. *Chem. Mater.* **2017**, *29*, 7645–7652.
- (28) Ford, M. J.; Wang, M.; Patel, S. N.; Phan, H.; Segalman, R. A.; Nguyen, T. Q.; Bazan, G. C. High Mobility Organic Field-Effect Transistors from Majority Insulator Blends. *Chem. Mater.* **2016**, *28*, 1256–1260.
- (29) Tremolet De Villers, B. J.; O'Hara, K. A.; Ostrowski, D. P.; Biddle, P. H.; Shaheen, S. E.; Chabinyk, M. L.; Olson, D. C.; Kopidakis, N. Removal of Residual Diiodooctane Improves Photostability of High-Performance Organic Solar Cell Polymers. *Chem. Mater.* **2016**, *28*, 876–884.
- (30) Dimitrakopoulos, C.; Dimitrakopoulos, B. C. D.; Malenfant, P. R. L. Organic Thin Film Transistors for Large Area Electronics Organic Thin Film Transistors for Large Area Electronics. *Adv. Mater.* **2002**, *14*, 99–117.
- (31) Xu, Y.; Zhang, F.; Feng, X. Patterning of Conjugated Polymers for Organic Optoelectronic Devices. *Small* **2011**, *7*, 1338–1360.
- (32) Vohra, V.; Mróz, W.; Inaba, S.; Porzio, W.; Giovanella, U.; Galeotti, F. Low-Cost and Green Fabrication of Polymer Electronic Devices by Push-Coating of the Polymer Active Layers. *ACS Appl. Mater. Interfaces* **2017**, *9*, 25434–25444.
- (33) Le, T. H.; Kim, Y.; Yoon, H. Electrical and Electrochemical Properties of Conducting

- Polymers. *Polymers (Basel)*. **2017**, *9*.
- (34) Chang, M.; Lim, G. T.; Park, B.; Reichmanis, E. Control of Molecular Ordering, Alignment, and Charge Transport in Solution-Processed Conjugated Polymer Thin Films. *Polymers (Basel)*. **2017**, *9*, 23–31.
- (35) Chen, H.; Guo, Y.; Yu, G.; Zhao, Y.; Zhang, J.; Gao, D.; Liu, H.; Liu, Y. Highly ??-Extended Copolymers with Diketopyrrolopyrrole Moieties for High-Performance Field-Effect Transistors. *Adv. Mater.* **2012**, *24*, 4618–4622.
- (36) Yu, H.; Park, K. H.; Song, I.; Kim, M.-J.; Kim, Y.-H.; Oh, J. H. Effect of the Alkyl Spacer Length on the Electrical Performance of Diketopyrrolopyrrole-Thiophene Vinylene Thiophene Polymer Semiconductors. *J. Mater. Chem. C* **2015**, *3*, 11697–11704.
- (37) Aggarwal, S. L.; Sweeting, O. J. Polyethylene: Preparation, Structure, and Properties. *Chem. Rev.* **1957**, *57*, 665–742.
- (38) Mozumder, M. S.; Mairpady, A.; Mourad, A. H. I. Polymeric Nanobiocomposites for Biomedical Applications. *J. Biomed. Mater. Res. - Part B Appl. Biomater.* **2017**, *105*, 1241–1259.
- (39) Chen, Y.; Wang, L.; Yu, H.; Zhao, Y.; Sun, R.; Jing, G.; Huang, J.; Khalid, H.; Abbasi, N. M.; Akram, M. Synthesis and Application of Polyethylene-Based Functionalized Hyperbranched Polymers. *Prog. Polym. Sci.* **2015**, *45*, 23–43.
- (40) Schroeder, B. C.; Chiu, Y.-C.; Gu, X.; Zhou, Y.; Xu, J.; Lopez, J.; Lu, C.; Toney, M. F.; Bao, Z. Non-Conjugated Flexible Linkers in Semiconducting Polymers: A Pathway to Improved Processability without Compromising Device Performance. *Adv. Electron. Mater.* **2016**, *2*, 1600104.
- (41) Yu, X.; Xiao, K.; Chen, J.; Lavrik, N. V.; Hong, K.; Sumpter, B. G.; Geohegan, D. B. High-

- Performance Field-Effect Transistors Based on Polystyrene-*b*-Poly(3-Hexylthiophene) Diblock Copolymers. *ACS Nano* **2011**, *5*, 3559–3567.
- (42) Wessendorf, C. D.; Schulz, G. L.; Mishra, A.; Kar, P.; Ata, I.; Weidener, M.; Urdanpilleta, M.; Hanisch, J.; Mena-Osteritz, E.; Lindén, M.; Ahlswede, E.; Bäuerle, P. Efficiency Improvement of Solution-Processed Dithienopyrrole-Based A-D-A Oligothiophene Bulk-Heterojunction Solar Cells by Solvent Vapor Annealing. *Adv. Energy Mater.* **2014**, 1–10.
- (43) Biniek, L.; Pouget, S.; Djurado, D.; Gonthier, E.; Tremel, K.; Kayunkid, N.; Zaborova, E.; Crespo-Monteiro, N.; Boyron, O.; Leclerc, N.; Ludwigs, S.; Brinkmann, M. High-Temperature Rubbing: A Versatile Method to Align  $\pi$ -Conjugated Polymers without Alignment Substrate. *Macromolecules* **2014**, *47*, 3871–3879.
- (44) Sun, B.; Hong, W.; Aziz, H.; Li, Y. Diketopyrrolopyrrole-Based Semiconducting Polymer Bearing Thermocleavable Side Chains. *J. Mater. Chem.* **2012**, *22*, 18950.
- (45) He, Y.; Hong, W.; Li, Y. New Building Blocks for *p*-Conjugated Polymer Semiconductors for Organic Thin Film Transistors and Photovoltaics. *J. Mater. Chem. C* **2014**, *2*, 8651–8661.
- (46) Ito, Y.; Virkar, A. a; Mannsfeld, S.; Oh, J. H.; Toney, M. Crystalline Ultra Smooth Self-Assembled Monolayers of Alkylsilanes for Organic Field-Effect Transistors. *J. Am. Chem. Soc.* **2009**, *131*, 9396–9404.
- (47) Noriega, R.; Rivnay, J.; Vandewal, K.; Koch, F. P. V; Stingelin, N.; Smith, P.; Toney, M. F.; Salleo, A. A General Relationship between Disorder, Aggregation and Charge Transport in Conjugated Polymers. *Nat. Mater.* **2013**, *12*, 1038–1044.
- (48) Cheng, Y.; Qi, Y.; Tang, Y.; Zheng, C.; Wan, Y.; Huang, W.; Chen, R.; Jackson, N. E.; Kohlstedt, K. L.; Savoie, B. M.; Olvera De La Cruz, M.; Schatz, G. C.; Chen, L. X.; Ratner,

- M. A. Conformational Order in Aggregates of Conjugated Polymers. *J. Am. Chem. Soc.* **2015**, *137*, 6254–6262.
- (49) Wang, S.; Fabiano, S.; Himmelberger, S.; Puzinas, S.; Crispin, X.; Salleo, A.; Berggren, M. Experimental Evidence That Short-Range Intermolecular Aggregation Is Sufficient for Efficient Charge Transport in Conjugated Polymers. *Proc. Natl. Acad. Sci.* **2015**, *112*, 10599–10604.
- (50) Charron, B. P.; Ocheje, M. U.; Selivanova, M.; Hendsbee, A.; Li, Y.; Rondeau-Gagné, S. Electronic Properties of Isoindigo-Based Conjugated Polymers Bearing Urea-Containing and Linear Alkyl Side Chains. *J. Mater. Chem. C* **2018**, *6*, 12070.
- (51) Zalesskiy, S. S.; Ananikov, V. P. Pd<sub>2</sub>(dba)<sub>3</sub> as a Precursor of Soluble Metal Complexes and Nanoparticles: Determination of Palladium Active Species for Catalysis and Synthesis. *Organometallics* **2012**, *31*, 2302–2309.

## CHAPTER IV. BRANCHED POLYETHYLENE AS A PLASTICIZING ADDITIVE TO MODULATE THE MECHANICAL PROPERTIES OF MORPHOLOGY AND ELECTRONIC PROPERTIES OF $\pi$ -CONJUGATED POLYMERS

### 4.1. Introduction

The expanding field of flexible and stretchable organic electronics has driven the development of soft and stretchable electronic materials with better performance and enhanced thermophysical properties.<sup>1-3</sup> One of the biggest challenges for the design and preparation of flexible and stretchable electronics is to maintain their good performance while applying physical and mechanical stimuli as both properties are in competition.<sup>4,5</sup> To address this challenge, organic electronics are particularly promising as their fabrication involves materials that possess both good electronic and mechanical properties, particularly desirable for the production of new stretchable electronics.<sup>6-9</sup> Particularly, semiconducting  $\pi$ -conjugated polymers are remarkable candidates to develop stretchable organic electronics.<sup>7,10</sup> More specifically, conjugated polymers possess the advantages of being potentially low-cost, light weight, and easily processable through large-scale solution deposition, thus providing an interesting route to stretchable electronics.<sup>11,12</sup> As a result, an important scope of research has been focused on the development of novel strategies to enhance mechanical properties of conjugated polymers while maintaining their good electronic properties upon stretching.<sup>13-15</sup>

One common approach to achieve mechanically robust and stretchable conjugated polymers is through physical blending of the rigid-rod materials with soft elastomeric materials.<sup>16-18</sup> Polydimethylsiloxane (PDMS) has become one of the most commonly used elastomers for fabricating stretchable devices, being used either as a substrate, dielectric material,

or as a component of a semiconducting polymer/elastomer blends.<sup>19</sup> In recent years, Reichmanis *et al.* pioneered the utilization of PDMS with conjugated polymers, reporting an improvement of both electronic and mechanical properties of the semiconductor.<sup>20–22</sup> Interestingly, organic field-effect transistor (OFET) devices, using PDMS and Poly(3-hexylthiophene, P3HT) blends as a semiconducting materials, were fabricated and showed good electronic properties under strain.<sup>21</sup> In addition to PDMS, other soft polymers such as poly(styrene) (PS) and polystyrene-*block*-poly(ethylene-co-butylene)-*block*-polystyrene (SEBS) were used to improve charge transport and mechanical compliance of conjugated polymers.<sup>23–25</sup> Despite promising results, the impossibility of removing the soft polymer from the semiconducting layer upon thermal annealing can potentially have an effect on the overall performance as a significant amount of insulating material has to be used. Therefore, additives that can be removed during device fabrication have been developed recently, and have been shown to enhance the charge transport of conjugated polymers by promoting aggregation between polymer chains.<sup>26,27</sup> Recently reported by Jeong *et al.*, the utilization of dichlorobenzene (DCB) as a solvent additive in the processing of P3HT for thin film transistor was shown to be particularly interesting.<sup>28</sup> As a result, the charge transport mobility in OFETs was enhanced from  $0.017 \text{ cm}^2\text{V}^{-1}\text{s}^{-1}$  for pure conjugated polymer to  $0.082 \text{ cm}^2\text{V}^{-1}\text{s}^{-1}$  with solvent additive, which was attributed to the influence of the additive on the solid-state morphology of the conjugated polymer. Despite the promises for control and fine-tuning of thin film morphology, and potential positive impact on the electronic properties of  $\pi$ -conjugated materials, the effect of low boiling point additives on the mechanical properties of conjugated polymers has not been fully evaluated.



Recently our group reported the blending of a low molecular weight branched polyethylene (BPE) with a high charge carrier mobility poly(diketopyrrolopyrrole-*co*-thienovinylthiophene) P(DPPTVT) conjugated polymer for controlling the morphology in the solid state.<sup>29</sup> The new branched polyethylene/conjugated polymer blends were found to increase aggregation, decrease crystallinity and maintain good charge transport (hole mobility of  $0.3 \text{ cm}^2\text{V}^{-1}\text{s}^{-1}$  in top-contact bottom-gate OFETs) even though the amount of polymer was reduced to 0.05 wt.%. This result is especially promising for the large-scale fabrication of organic semiconductors *via* solution deposition.

Herein, we report the effect of BPE on the mechanical properties of conjugated polymers in thin films and its impact on the solid-state morphology of the conjugated polymer. The resulting thin films were characterized by various techniques, including UV-Vis spectroscopy, atomic force microscopy (AFM), and X-ray diffraction (XRD) in order to probe the influence of the BPE on the nanoscale morphology before and after removal of the additive. Based on the obtained results, BPE was found to act as a plasticizer (Figure 4.1), making the polymer thin films more amorphous, which is beneficial for mechanical properties. More specifically, the addition of BPE to a rigid conjugated polymer showed a reduction in crack propagation and crack width upon strain, and a moderate decrease in Young's modulus was also observed. The influence of this new additive on the thermomechanical properties can be attributed to a nanophase separation in the polymer blend, which helps to reduce the Young's modulus and crack on-set strain. The BPE additive is, therefore, particularly promising for the design of stretchable electronic devices and the development of innovative technologies based on organic polymer blends.

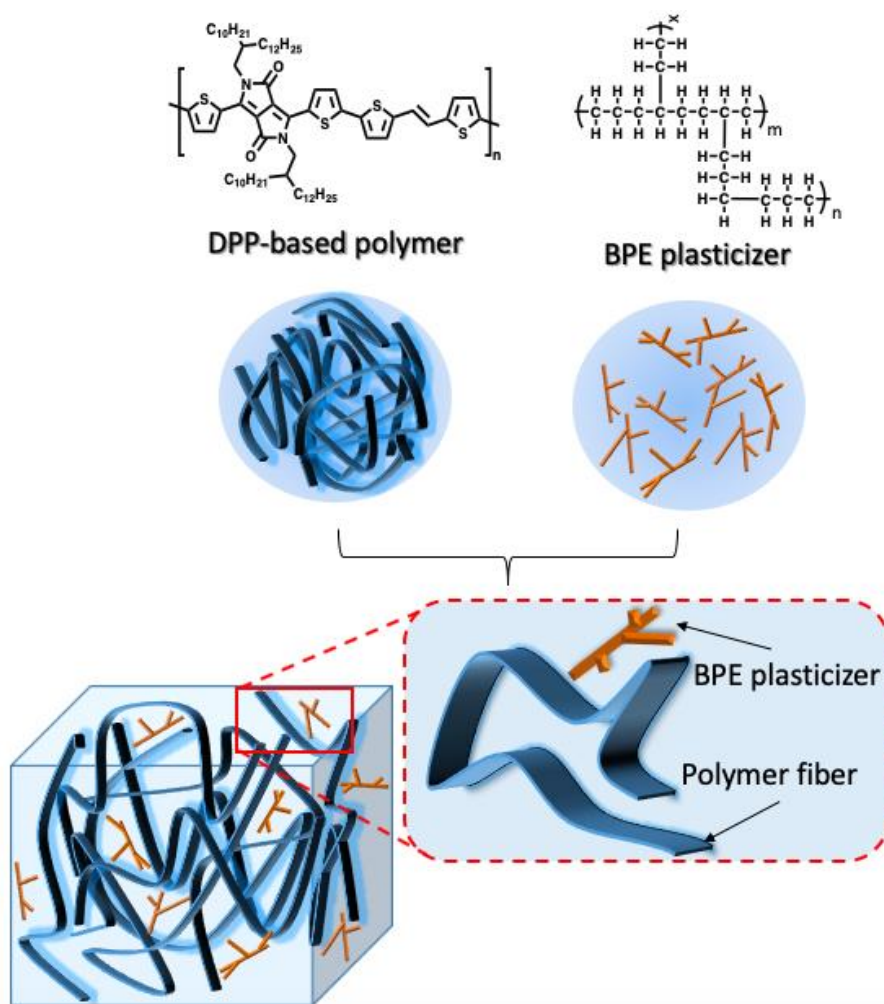


Figure 4.1. Blending of low molecular weight branched polyethylene (BPE) with a DPP-based polymer for modulation of the mechanical properties.

## 4.2. Results and Discussion

To investigate the influence of BPE on the mechanical compliance of conjugated polymers, a diketopyrrolopyrrole-based (DPP) polymer was directly blended with different weight ratios of BPE. The preparation of the DPP-based conjugated polymer was performed using a previously reported procedure.<sup>32</sup> Known to typically lead to good charge transport mobility, a DPP-based

monomer was copolymerized with bis(trimethyltin)thienovinylthiophene (TVT) *via* Stille polymerization.<sup>33</sup> The resulting polymer was precipitated in methanol, and purified by Soxhlet extraction with methanol, acetone and hexane, and was collected in chlorobenzene, followed by precipitation in methanol and vacuum filtration. Among other additives, BPE was selected due to unique features, which include non-toxicity, low viscosity, and most interestingly, low boiling point (135 °C) and low molecular weight (500 Da), which allows for the additive to be removed after thermal annealing. Due to its hyperbranched structure, BPE also strongly promotes molecular aggregation of the conjugated polymer and phase segregated solid-state morphology. Previously reported results of organic field-effect transistor characterization of non-annealed BPE/polymer blends are summarized in Table B1 showing a relatively stable charge transport mobility (average mobility around  $0.3 \text{ cm}^2\text{V}^{-1}\text{s}^{-1}$ ) independent of the amount of BPE added.<sup>29</sup> After annealing, the annealed devices showed increased charge carrier mobility, going from  $0.3 \text{ cm}^2\text{V}^{-1}\text{s}^{-1}$  to as high as  $1.0 \text{ cm}^2\text{V}^{-1}\text{s}^{-1}$  (75 wt.% BPE/DPP-based polymer).<sup>29</sup> The OFETs were also fabricated with a highly diluted solution of DPP-based polymer with or without the BPE additive; interestingly, no working devices were obtained without annealing for a highly diluted solution of conjugated polymer (0.05 wt.%) in chlorobenzene which can be attributed to poor film quality. A solution of DPP-based polymer blended with 98 wt.% BPE showed enhanced performance before thermal annealing, reaching a charge transport mobility of  $0.054 \text{ cm}^2\text{V}^{-1}\text{s}^{-1}$ .

In order to investigate the plasticizing effect of BPE, blending with the conjugated polymer at different weight ratios of BPE additive (0-90 wt.%) was performed. The effect of BPE on the mechanical properties of conjugated polymers was investigated by lamination of soft substrates.<sup>15,34</sup> Briefly, the blended solutions were spin-coated on top of a glass slide pre-coated with polystyrene sulfonate (PSS). Then, a PDMS slab was placed on top of the blended materials.

By dissolving the PSS sacrificial layer with water, the blended film was transferred on PDMS and the resulting transferred films were directly stretched on PDMS at certain pre-determined strain. Finally, to help with materials characterization and device fabrication, the stretched thin films were transferred back onto silicon wafer, functionalized with a monolayer of octadecyltrichlorosilane (OTS). The complete procedure of lamination of soft substrates is detailed in Supporting Information (Figure B1).

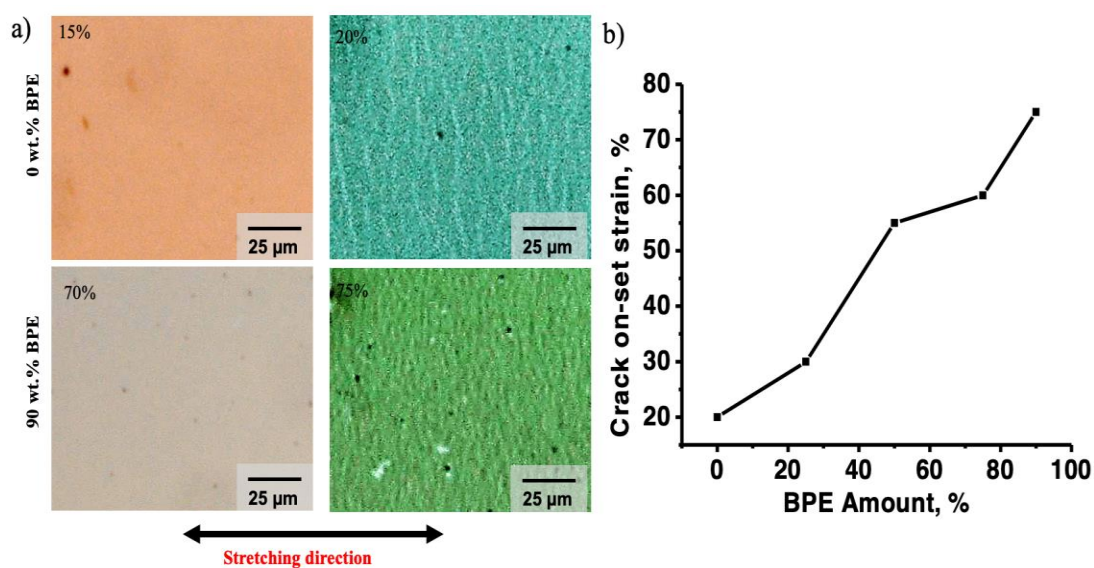


Figure 4.2. a) Crack on-set strain of P(DPPTVT)/BPE blends containing 0 wt.% and 90 wt.% of BPE before (left) and after (right) the formation of cracks, as observed by optical microscopy. Scale bars are 25μm; b) Crack onset strain versus the amount of BPE as determined by optical microscopy before thermal annealing.

To investigate the influence of BPE on the mechanical properties of P(DPPTVT) at the micron scale, the crack onset strain before thermal annealing of BPE/polymer blends containing 0-90 wt.% of BPE was measured by optical microscopy. Crack on-set strain is defined as the minimum strain at which cracks start to propagate at the microscale. As shown in Figure 4.2.a, for

the blended system containing 0 wt.% BPE micron-scaled cracks are observed at 20% strain, while incorporation of 90 wt.% BPE to the conjugated polymer led to an increase in crack onset strain, reaching a maximum of 75% strain, as shown in Figure 4.2.b. Upon progressive addition of BPE to the conjugated polymer, its tolerance to mechanical stress and crack onset strain at the micron scale is significantly increased, which can be directly attributed to the effect of BPE on the solid-state morphology and softness of the blend (Figure B2).

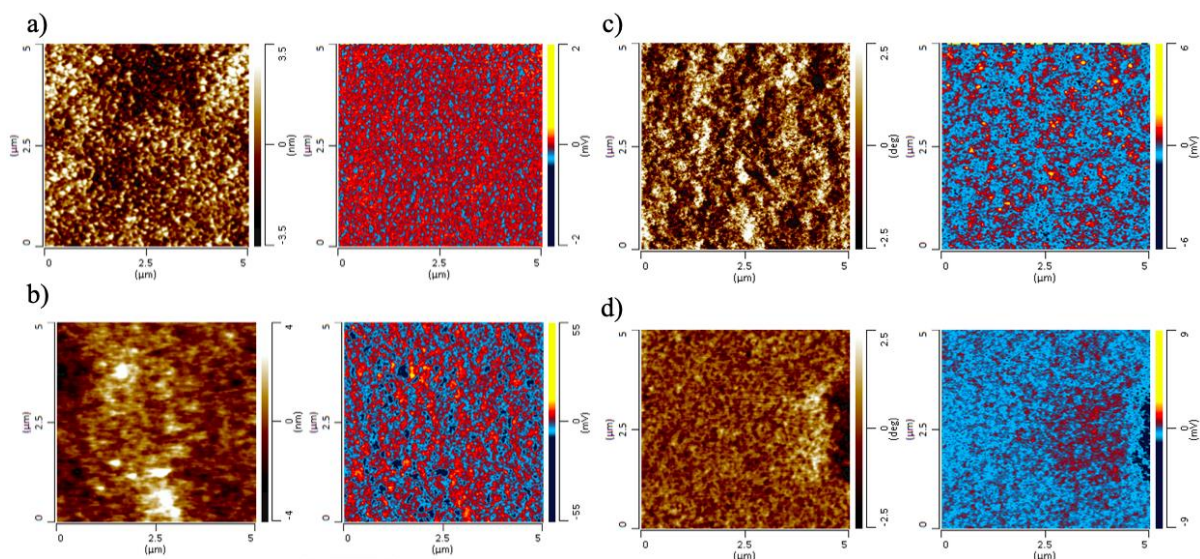


Figure 4.3. Atomic force microscopy – Fourier-transform infrared spectroscopy analysis of polymer blends prepared with a) 25 wt.%, b) 50 wt.%, c) 75 wt.%, and d) 90 wt.% of BPE. DPP-based polymer is depicted in red/yellow and BPE is depicted in blue.

Since phase separation is a key parameter for promoting stretchability in conjugated polymer blends, atomic force microscopy coupled with Fourier-transform infrared spectroscopy was performed to probe the nanoscale morphology of the blends.<sup>35</sup> Samples composed of branched polyethylene (BPE) and the DPP-based conjugated polymer were measured as a function of DPP-based polymer content. The results are summarized in Figure 4.3, and the parameters used for the experiment are listed in Table B2. All images were measured on a 5x5 μm scale. As one would

predict, as the BPE concentration increases in the blends (going from 25 wt.% to 90 wt.%), the area occupied by the DPP-based polymer (coloured in yellow-red) phase decreases significantly, and an increase in blue domains, associated to BPE-rich domains, can be observed. This observation confirms that the addition of BPE causes a phase separation, which ultimately can impact the mechanical properties of the polymer blends.

In order to fully elucidate the plasticizing effect of BPE before thermal annealing at the nanoscale, the characterization of BPE/P(DPPTVT) blends containing 0-90 wt.% of BPE under strain was performed using atomic force microscopy (AFM). Based on the obtained results, upon incorporation of BPE to the conjugated polymer, the number of cracks and their width has been drastically decreased. As shown in Figure 4.4, at 0 wt.% BPE (pure conjugated polymer), the thin film mostly consists of long, large nanoscale cracks. Upon addition of BPE, the nanoscale cracks significantly decrease in width, independent of the strain applied to the materials. The important influence of BPE on crack width and propagation indicates that the additive can act as a plasticizer, improving the mechanical properties of conjugated polymers by reducing their ductility and helping in stress dissipation. The detailed AFM analysis with height profiles is summarized in Supporting Information (Figure B3-B7).

Interestingly, at 90 wt.% of BPE, no nanoscale crack was observed at 10% strain. This finding is also supported by optical microscope observations, resulting in the highest crack onset strain for 90 wt.% of BPE compared to the other ratios. Moreover, for 90 wt.% BPE/DPP-based polymer blends stretched at 100% strain elongation, the number of cracks is decreased by approximately a factor of 10 when compared to the pure P(DPPTVT), as shown in Figure 4.4.c. Since the BPE additive is easily removed upon thermal treatment, the AFM images of P(DPPTVT)/BPE blends containing 0 wt.%, 50 wt.% and 90 wt.% at 50% strain were recorded

after annealing (Figure B8). Based on the observed AFM images, the same trend of increased stretchability was observed even without the presence of BPE in the final thin film. Finally, independent of the strain or blending ratio, the addition of BPE promotes a uniform distribution of smaller cracks as oppose to the native conjugated polymer which showed localized larger cracks.

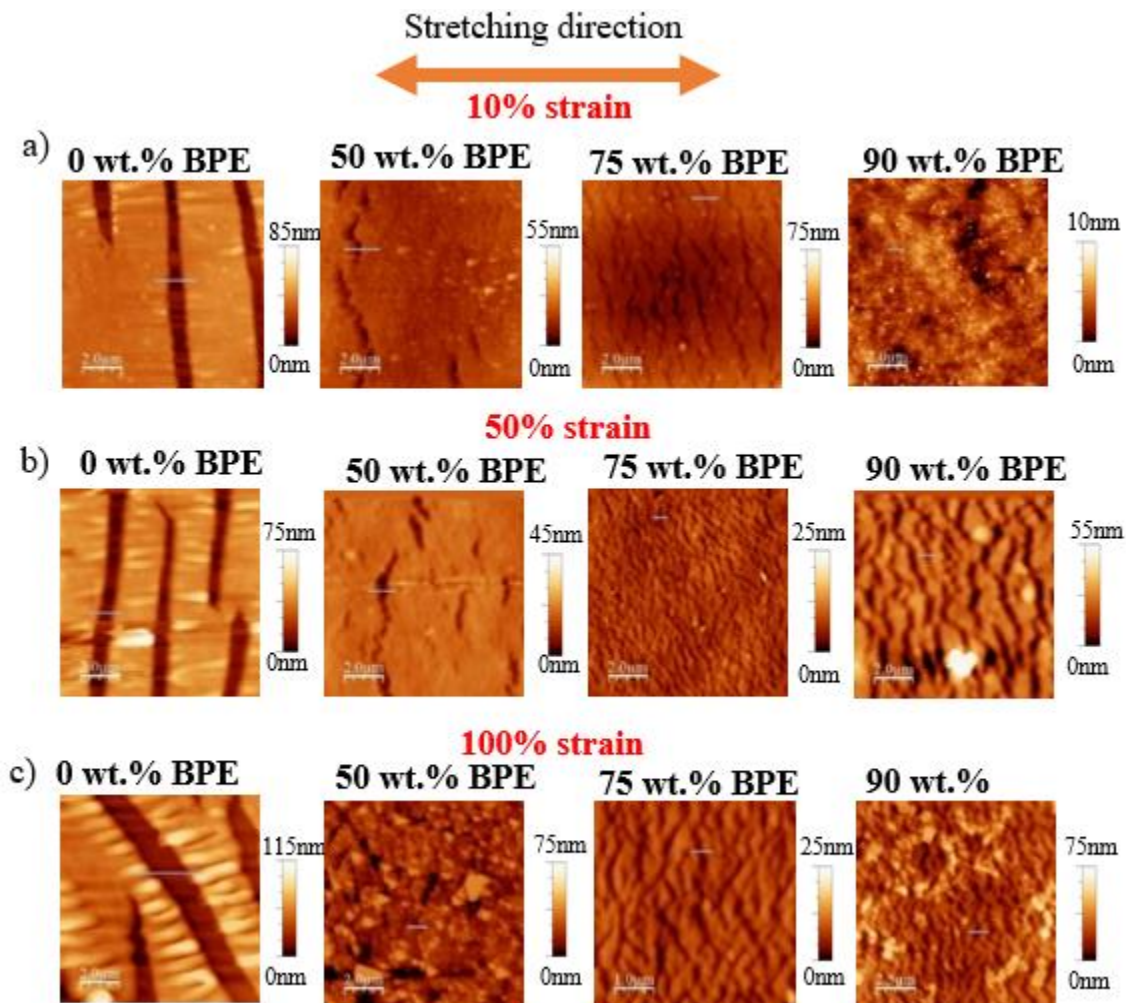


Figure 4.4. Atomic force microscopy images (height) of BPE/P(DPPTVT) blends containing 0 to 90 wt.% BPE at a) 10, b) 50 and c) 100% strain before thermal annealing.

Crack width analysis at the nanoscale for different blended systems under strain are summarized in Figure 4.5. At 25% strain, the crack width was reduced from 1500 nm for P(DPPTVT) to 300 nm for the 90 wt.% BPE/polymer blended system. Moreover, a thin film of P(DPPTVT), without introducing any amount of BPE additive, reached a crack width of 3100 nm at 100% strain, followed by an abrupt decrease to 500 nm upon incorporation of 90 wt.% BPE to the system. The same trend is observed for BPE/polymer thin film blends at 50% strain. Interestingly, the blending of the conjugated polymer with various ratios of BPE tends to prevent crack propagation, as observed in Figure 4.5. In all cases, the crack width remains fairly stable upon various strains in contrast to the pure conjugated polymer, which undergoes significant crack propagation and increased nanoscale cracks width.

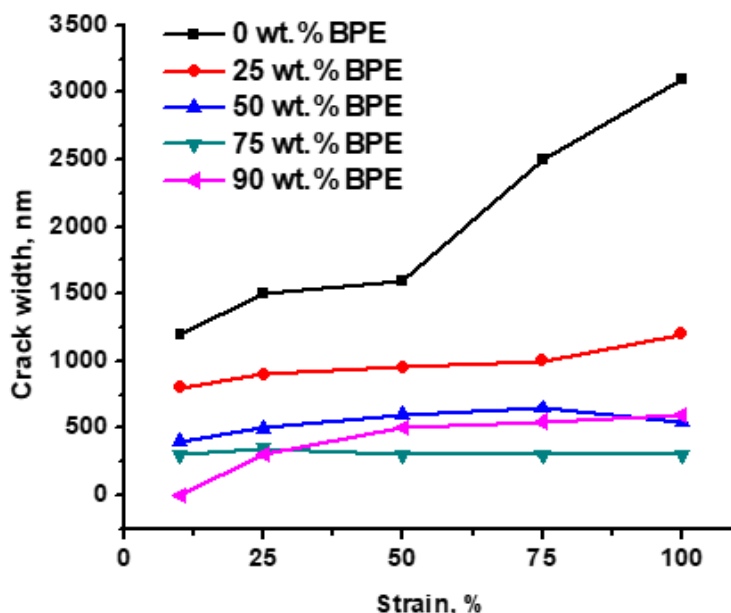


Figure 4.5. Thin film crack width versus the amount of BPE additive for a) 25 %; b) 50%; c) 75%, and d) 100% strain elongation as determined by atomic force microscopy (AFM).

As demonstrated by AFM analysis and crack on-set results, the BPE additive acts as a plasticizer and is responsible for the enhancement of the mechanical compliance of conjugated



polymers. In order to gain insight into the influence of BPE on the stretchability of conjugated polymers, the degree of polymer chain alignment under strain was measured using polarized UV-Vis spectroscopy by determining the dichroic ratio. The dichroic ratio is defined as  $\alpha_{//} / \alpha_{\perp}$ , where  $\alpha_{//}$  and  $\alpha_{\perp}$  are the absorption of light polarized parallel and perpendicular to the stretching direction, respectively. A schematic diagram of polarized UV-vis characterization on stretched polymer blend films is illustrated in Figure B9. The measurements were performed with all the BPE/P(DPP-TVTVT) blending systems at different weight percentages of BPE (from 0 wt.% to 90 wt.%) to demonstrate the influence of BPE on the chain alignment of conjugated polymers which is critical for its mechanical properties (Figures B10 to B14). The value of the dichroic ratio is expected to steadily increase upon chain alignment.<sup>36,37</sup> Once cracks are formed, the dichroic ratio becomes smaller meaning that the chain alignment is disrupted.

For the pure conjugated polymer (0 wt.% BPE), the dichroic ratio increased to 1.9 upon 25% strain, indicating a certain chain alignment (Figure B15.a). However, upon further stress the dichroic ratio was shown to decrease to 1.3 at 100% strain, which means that the polymer chains can no longer align past 25% strain. This observation is consistent with the results obtained from AFM (Figure B5). In comparison, the dichroic ratio of BPE/P(DPPTVTVT) blends containing 50 wt.% linearly increased up to 2.5 at 100% strain whereas BPE/P(DPPTVTVT) blended systems containing 25 wt.% linearly increased to 1.6 as the strain increased to 100% starting to reach a plateau. (Figure B15.b-c). The best linear trend of dichroic ratio in function of strain was observed in the blended system of conjugated polymer and 75 wt.% BPE as shown in Figure 10d. Similarly, the blending system with 90 wt.% BPE showed polymer chain alignment up to 100% strain, reaching a value of 3. (Figure B15.e). These findings indicate that the conjugated polymer can withstand 100% strain with aligned chains upon incorporation of BPE to the system.

As previously reported for polymer blends, the incorporation of the soft component to the conjugated polymers strongly influence their elasticity.<sup>24,25</sup> The effect of the BPE additive on the elastic modulus of conjugated polymers was studied using a *pseudo* freestanding thin film tensile test.<sup>38,39</sup>

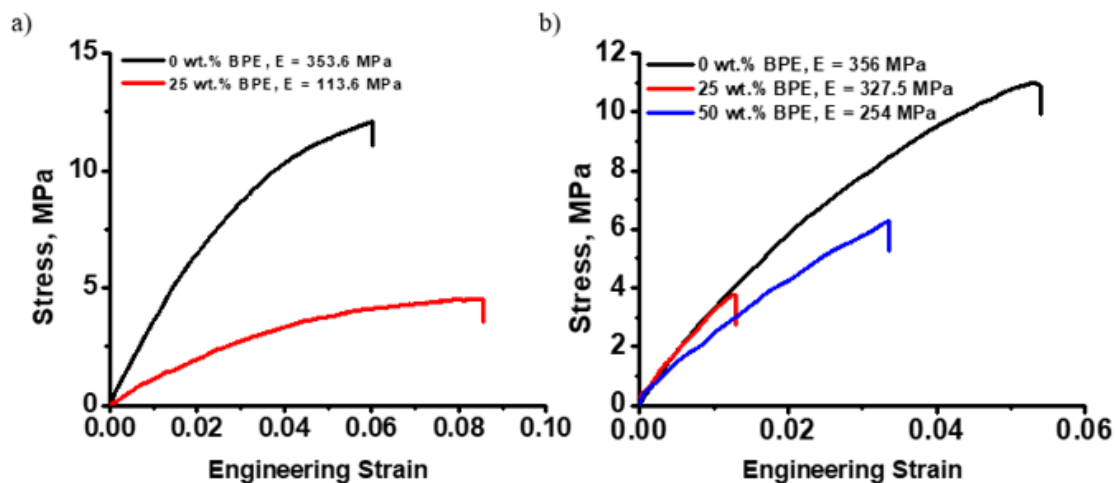


Figure 4.6. Elastic modulus of polymer blends with different weight ratios of BPE additive, determined by Film-On-Water tensile pull test a) before thermal annealing and b) after thermal annealing.

The Young's modulus was first measured for the BPE/polymer blends before thermal annealing to gain insight into the effect of BPE on the elastic modulus of the conjugated polymer before it has been removed. The Young's modulus of the 25 wt.% BPE/P(DPPTVT) blend was found to be 113.6 MPa, which is three times lower than the elastic modulus of 353.6 MPa for the pure conjugated polymer before thermal annealing (Figure 4.6.a) It is important to mention that it was impossible to measure the elastic modulus for the blended system above 25 wt.% BPE in the conjugated polymer due to the fact that the freestanding thin films are fragile as shown in Figure B16. The elastic modulus of BPE/conjugated polymer blends was also measured after thermal annealing. The Young's modulus of the pure conjugated polymer was found to be 356

MPa, while the elastic modulus of blended system containing 25 wt.% and 50 wt.% of BPE decreased to 327.5 MPa and 254 MPa, respectively (Figure 4.6.b). The Young's modulus was not measured at 90 wt.% of BPE even after thermal annealing again due to the brittleness of the freestanding thin films. Interestingly, the Young's modulus of thin film at 25 w.% of BPE is almost 3 times lower before thermal annealing (112 MPa) comparing to the thermally annealed film (327.5 MPa), which is another indirect proof of BPE additive removal, and increased crystallinity. This result indicates that the incorporation of BPE to the blended system reduced the Young's modulus of the conjugated polymer even after its removal, which in a good agreement with a decrease in the crystallinity of BPE/polymer blends.

To further investigate the solid-state morphology of BPE/polymer blends and gain insight into the thin-films' crystallinity, grazing incidence wide angle x-ray scattering (GIWAXS) experiments were performed on 0, 50 and 90 wt.% polymer blends. The results indicate that the BPE additive is disrupting the solid-state morphology and preventing the formation of large crystalline phases. The intensities of the diffraction peaks are progressively reduced upon incorporation of 90 wt.% BPE to the conjugated polymer as shown in Figure B17. Interestingly, BPE additive, despite reducing the film crystallinity, does not impact the molecular orientation in the solid-state, thus potentially adopting an edge-on morphology even at 50 wt.% BPE added (Figure B17.b). This observation confirms the significant influence of the BPE additive on the morphology of P(DPPTVT) conjugated polymer as well as its potential for the fabrication of flexible and stretchable OFET devices by acting as a plasticizer to improve mechanical properties of conjugated polymer. Moreover, since the additive is non-toxic and has a low-boiling point, those results also highlight the potential of this technique for advanced manufacturing of organic electronics at large-scale.

### 4.3. Conclusion

In conclusion, this study demonstrates a useful way to improve the mechanical properties of conjugated polymers *via* physical blending with a branched polyethylene additive. Incorporation of BPE additive at different ratios was shown to drastically decrease the crystallinity of a DPP-based conjugated polymer which is beneficial for flexible and stretchable electronic devices. At the micron scale, the BPE additive acts as plasticizer and significantly reduces the Young's modulus of the conjugated polymer (112 MPa at 25 wt.% BPE before thermal annealing) and largely increases the crack on-set strain, reaching a maximum of 75% strain elongation when blended with 90 wt.% BPE. The stretchability of BPE/P(DPPTVT) thin films is significantly improved upon introducing more BPE additive to the system. At the nanoscale, cracks can be observed at various strains, but the crack width was reduced from 3100 nm to 600 nm at 0 wt.% and 90 wt.% of BPE, respectively, under 100% strain. The addition of BPE promotes a uniform distribution of numerous smaller cracks across the thin film compared to the pure conjugated polymer thin film which showed few localized larger cracks. Interestingly, following the removal of blended BPE, the thin films showed the same trend with improved stretchability. Additionally, the BPE additive influence the chain alignment of conjugated polymers, showing chain alignment of polymer chains even above 100% strain at 90 wt.% BPE while the pure conjugated polymer stops aligning at 25% strain. With the growth of flexible and stretchable electronics, BPE additive is a promising candidate to enhance the mechanical properties of conjugated polymers. We believe that this work will advance the research and development of new flexible and stretchable electronic devices.

## REFERENCES

- (1) Harris, K. D.; Elias, A. L.; Chung, H.-J. Flexible Electronics under Strain: A Review of Mechanical Characterization and Durability Enhancement Strategies. *J. Mater. Sci.* **2016**, *51*, 2771–2805.
- (2) Hammock, M. L.; Chortos, A.; Tee, B. C.-K.; Tok, J. B.-H.; Bao, Z. 25th Anniversary Article: The Evolution of Electronic Skin (e-Skin): A Brief History, Design Considerations, and Recent Progress. *Adv. Mater.* **2013**, *25*, 5997–6038.
- (3) Rim, Y. S.; Bae, S. H.; Chen, H.; De Marco, N.; Yang, Y. Recent Progress in Materials and Devices toward Printable and Flexible Sensors. *Adv. Mater.* **2016**, *28*, 4415–4440.
- (4) Printz, A. D.; Lipomi, D. J. Competition between Deformability and Charge Transport in Semiconducting Polymers for Flexible and Stretchable Electronics. *Appl. Phys. Rev.* **2016**, *3*, 021302.
- (5) O'Connor, B.; Chan, E. P.; Chan, C.; Conrad, B. R.; Richter, L. J.; Kline, R. J.; Heeney, M.; McCulloch, I.; Soles, C. L.; DeLongchamp, D. M. Correlations between Mechanical and Electrical Properties of Polythiophenes. *ACS Nano* **2010**, *4*, 7538–7544.
- (6) Benight, S. J.; Wang, C.; Tok, J. B. H.; Bao, Z. Stretchable and Self-Healing Polymers and Devices for Electronic Skin. *Prog. Polym. Sci.* **2013**, *38*, 1961–1977.
- (7) Ocheje, M. U.; Charron, B. P.; Nyayachavadi, A.; Rondeau-Gagné, S. Stretchable Electronics: Recent Progress in the Preparation of Stretchable and Self-Healing Semiconducting Conjugated Polymers. *Flex. Print. Electron.* **2017**, *2*, 043002.
- (8) Mechael, S. S.; Wu, Y.; Schlingman, K.; Carmichael, T. B. Stretchable Metal Films. *Flex. Print. Electron.* **2018**, *3*, 043001.
- (9) Rogers, J. A.; Someya, T.; Huang, Y. Materials and Mechanics for Stretchable

- Electronics. *Science* **2010**, 327, 1603–1608.
- (10) Nelson, T. L.; Young, T. M.; Liu, J.; Mishra, S. P.; Belot, J. a.; Balliet, C. L.; Javier, A. E.; Kowalewski, T.; McCullough, R. D. Transistor Paint: High Mobilities in Small Bandgap Polymer Semiconductor Based on the Strong Acceptor, Diketopyrrolopyrrole and Strong Donor, Dithienopyrrole. *Adv. Mater.* **2010**, 22, 4617–4621.
- (11) Lee, S.; Kim, J.; Jang, H.; Yoon, S. C.; Lee, C.; Hong, B. H.; Rogers, J. A.; Cho, J. H.; Ahn, J. Stretchable Graphene Transistors with Printed Dielectrics and Gate Electrodes. *Nano Lett.* **2011**, 4642–4646.
- (12) Sirringhaus, H. 25th Anniversary Article : Organic Field-Effect Transistors : The Path Beyond Amorphous Silicon. *Adv. Mater.* **2014**, 26, 1319–1335.
- (13) Noriega, R.; Rivnay, J.; Vandewal, K.; Koch, F. P. V; Stingelin, N.; Smith, P.; Toney, M. F.; Salleo, A. A General Relationship between Disorder, Aggregation and Charge Transport in Conjugated Polymers. *Nat. Mater.* **2013**, 12, 1038–1044.
- (14) O ’connor, T. F.; Rajan, K. M.; Printz, A. D.; Lipomi, D. J. Toward Organic Electronics with Properties Inspired by Biological Tissue. *J. Mater. Chem. B* **2015**, 3, 4947–4952.
- (15) Wu, H.-C.; Hung, C.-C.; Hong, C.-W.; Sun, H.-S.; Wang, J.-T.; Yamashita, G.; Higashihara, T.; Chen, W.-C. Isoindigo-Based Semiconducting Polymers Using Carbosilane Side Chains for High Performance Stretchable Field-Effect Transistors. *Macromolecules* **2016**, 49, 8540–8548.
- (16) Ahn, J.-H.; Je, J. H. Stretchable Electronics: Materials, Architectures and Integrations. *J. Phys. D. Appl. Phys.* **2012**, 45, 103001.
- (17) Wang, G.-J. N.; Gasperini, A.; Bao, Z. Stretchable Polymer Semiconductors for Plastic Electronics. *Adv. Electron. Mater.* **2018**, 1700429.

- (18) Riera-Galindo, S.; Leonardi, F.; Pfattner, R.; Mas-Torrent, M. Organic Semiconductor/Polymer Blend Films for Organic Field-Effect Transistors. *Adv. Mater. Technol.* **2019**, 1900104.
- (19) Johnston, I. D.; McCluskey, D. K.; Tan, C. K. L.; Tracey, M. C. Mechanical Characterization of Bulk Sylgard 184 for Microfluidics and Microengineering. *J. Micromech. Microeng.* **2014**, *24*, 035017.
- (20) Choi, D.; Kim, H.; Persson, N.; Chu, P. H.; Chang, M.; Kang, J. H.; Graham, S.; Reichmanis, E. Elastomer-Polymer Semiconductor Blends for High-Performance Stretchable Charge Transport Networks. *Chem. Mater.* **2016**, *28*, 1196–1204.
- (21) Zhang, G.; McBride, M.; Persson, N.; Lee, S.; Dunn, T. J.; Toney, M. F.; Yuan, Z.; Kwon, Y. H.; Chu, P. H.; Risteen, B.; Reichmanis, E. Versatile Interpenetrating Polymer Network Approach to Robust Stretchable Electronic Devices. *Chem. Mater.* **2017**, *29*, 7645–7652.
- (22) McBride, M.; Persson, N. E.; Keane, D.; Bacardi, E.; Reichmanis, E.; Grover, M. A. A Polymer Blend Approach for Creation of Effective Conjugated Polymer Charge Transport Pathways. *ACS Appl. Mater. Interfaces* **2018**, *10*, 36464–36474.
- (23) Yu, X.; Xiao, K.; Chen, J.; Lavrik, N. V; Hong, K.; Sumpter, B. G.; Geohegan, D. B. High-Performance Field-Effect Transistors Based on Polystyrene-*b*-Poly(3-Hexylthiophene) Diblock Copolymers. *ACS Nano* **2011**, *5*, 3559–3567.
- (24) Shin, M.; Oh, J. Y.; Byun, K.-E.; Lee, Y.-J.; Kim, B.; Baik, H.-K.; Park, J.-J.; Jeong, U. Polythiophene Nanofibril Bundles Surface-Embedded in Elastomer: A Route to a Highly Stretchable Active Channel Layer. *Adv. Mater.* **2015**, 1255–1261.
- (25) Xu, J.; Wang, S.; Wang, G. N.; Zhu, C.; Luo, S.; Jin, L.; Gu, X.; Chen, S.; Feig, V. R.; To,

- J. W. F.; et al. Highly Stretchable Polymer Semiconductor Films through the Nanoconfinement Effect. *Science* **2017**, *355*, 1–6.
- (26) Kyaw, A. K. K.; Wang, D. H.; Luo, C.; Cao, Y.; Nguyen, T. Q.; Bazan, G. C.; Heeger, A. J. Effects of Solvent Additives on Morphology, Charge Generation, Transport, and Recombination in Solution-Processed Small-Molecule Solar Cells. *Adv. Energy Mater.* **2014**, *4*, 1–9.
- (27) Chae, G. J.; Jeong, S.-H.; Baek, J. H.; Walker, B.; Song, C. K.; Seo, J. H. Improved Performance in TIPS-Pentacene Field Effect Transistors Using Solvent Additives. *J. Mater. Chem. C* **2013**, *1*, 4216–4221.
- (28) Jeong, J. W.; Jo, G.; Choi, S.; Kim, Y. A.; Yoon, H.; Ryu, S. W.; Jung, J.; Chang, M. Solvent Additive-Assisted Anisotropic Assembly and Enhanced Charge Transport of  $\pi$ -Conjugated Polymer Thin Films. *ACS Appl. Mater. Interfaces* **2018**, *10*, 18131–18140.
- (29) Selivanova, M.; Chuang, C.-H.; Billet, B.; Malik, A.; Xiang, P.; Landry, E.; Chiu, Y.-C.; Rondeau-Gagné, S. Morphology and Electronic Properties of Semiconducting Polymer and Branched Polyethylene Blends. *ACS Appl. Mater. Interfaces* **2019**.
- (30) Zalesskiy, S. S.; Ananikov, V. P.  $\text{Pd}_2(\text{dba})_3$  as a Precursor of Soluble Metal Complexes and Nanoparticles: Determination of Palladium Active Species for Catalysis and Synthesis. *Organometallics* **2012**, *31*, 2302–2309.
- (31) Ito, Y.; Virkar, A. A.; Mannsfeld, S.; Oh, J. H.; Toney, M.; Locklin, J.; Bao, Z. Crystalline Ultrasoother Self-Assembled Monolayers of Alkylsilanes for Organic Field-Effect Transistors. *J. Am. Chem. Soc.* **2009**, *131*, 9396–9404.
- (32) Ocheje, M. U.; Charron, B. P.; Cheng, Y.-H.; Chuang, C.-H.; Soldera, A.; Chiu, Y.-C.; Rondeau-Gagné, S. Amide-Containing Alkyl Chains in Conjugated Polymers: Effect on



- Self-Assembly and Electronic Properties. *Macromolecules* **2018**, *51*, 1336–1344.
- (33) Chen, H.; Guo, Y.; Yu, G.; Zhao, Y.; Zhang, J.; Gao, D.; Liu, H.; Liu, Y. Highly ??-Extended Copolymers with Diketopyrrolopyrrole Moieties for High-Performance Field-Effect Transistors. *Adv. Mater.* **2012**, *24*, 4618–4622.
- (34) Wu, H. C.; Benight, S. J.; Chortos, A.; Lee, W. Y.; Mei, J.; To, J. W. F.; Lu, C.; He, M.; Tok, J. B. H.; Chen, W. C.; Bao, Z. A Rapid and Facile Soft Contact Lamination Method: Evaluation of Polymer Semiconductors for Stretchable Transistors. *Chem. Mater.* **2014**, *26*, 4544–4551.
- (35) Gu, K. L.; Zhou, Y.; Morrison, W. A.; Park, K.; Park, S.; Bao, Z. Nanoscale Domain Imaging of All-Polymer Organic Solar Cells by Photo-Induced Force Microscopy. *ACS Nano* **2018**, *12*, 1473–1481.
- (36) Qu, G.; Zhao, X.; Newbloom, G. M.; Zhang, F.; Mohammadi, E.; Strzalka, J. W.; Pozzo, L. D.; Mei, J.; Diao, Y. Understanding Interfacial Alignment in Solution Coated Conjugated Polymer Thin Films. *ACS Appl. Mater. Interfaces* **2017**, *9*, 27863–27874.
- (37) O'Connor, B.; Kline, R. J.; Conrad, B. R.; Richter, L. J.; Gundlach, D.; Toney, M. F.; DeLongchamp, D. M. Anisotropic Structure and Charge Transport in Highly Strain-Aligned Regioregular Poly(3-Hexylthiophene). *Adv. Funct. Mater.* **2011**, *21*, 3697–3705.
- (38) Alkhadra, M. A.; Root, S. E.; Hilby, K. M.; Rodriguez, D.; Sugiyama, F.; Lipomi, D. J. Quantifying the Fracture Behavior of Brittle and Ductile Thin Films of Semiconducting Polymers. *Chem. Mater.* **2017**, *29*, 10139–10149.
- (39) Zhang, S.; Ocheje, M. U.; Luo, S.; Appleby, B.; Weller, D.; Rondeau-Gagné, S.; Gu, X. Probing the Viscoelastic Property of Pseudo Free-Standing Conjugated Polymeric Thin Films Conjugated Polymeric Thin Films. *Macromol. Rapid Commun.* **2018**, 1800092.

## CHAPTER V

### 5.1. Conclusion

In summary, DPP-based semiconducting polymer was successfully synthesized and blended with different weight ratios of low molecular weight BPE additive. BPE additive was selected due to such factors as being non-toxic, low cost, low boiling point (135°C) and low molecular weight (500Da). Most importantly, its unique feature of being volatile allows a complete removal of the insulating material upon thermal annealing which makes it a promising candidate for large-scale fabrication of OFETs. The incorporation of large amount of BPE additive to the conjugated polymer strongly promoted molecular aggregation, reduction in crystallinity and a good charge transport mobility even at 90 wt.% of BPE added. Interestingly, the devices fabricated from a highly diluted solution of conjugated polymer with BPE (98 wt.%) were shown to maintain good charge transport properties, in contrast to no working devices obtained for diluted solution of pure conjugated polymer before thermal annealing. This result confirms the contribution of BPE additive on the electronic properties of P(DPPTVT) semiconducting polymer. Moreover, a novel BPE/P(DPPTVT) polymer blend is a promising candidate for the large-scale fabrication of OFET devices with reduced amount of active material by 90 wt.% and without any presence of insulating materials, maintaining the same charge transport mobility.

In addition to the characterization of the solid-state morphology and electronic properties of DPP-based polymer/BPE blends, the investigation of the effect of BPE additive on the mechanical properties of P(DPPTVT) semiconducting polymer was also performed. Based on the obtained XRD results, BPE act as a plasticizer, thus preventing the formation of large crystalline phases which leads to a drastic decrease in crystallinity. Incorporation of 90 wt.% BPE to the

conjugated polymer led to a drastic increase in crack onset strain reaching the value of 75% strain, while the crack onset strain of pure conjugated polymer, containing 0 wt.% BPE, is 20% strain. The improvement of stretchability is shown by the reduction of the crack width under strain as a result the film consists mostly of numerous small cracks rather than various large cracks.

Overall, the findings confirm that BPE is an effective additive for fine-tuning the solid-state morphology without sacrificing performance in organic electronics and can have an important impact on the fabrication of OFETs with lower amounts of conjugated polymer and without the use of toxic additives. Moreover, BPE acts as plasticizer, improving the mechanical properties of conjugated polymers which is very promising for stretchable and flexible electronic devices.

## **5.2. Future Work and Perspectives**

In moving forward, the next steps of this research are to study the effect of other PE additives on the electronic and mechanical properties of conjugated polymers and to investigate the effect of different molecular weights of BPE additive on the morphology and phase separation of semiconducting polymers. Also, the fabrication of a fully stretchable device will be a great application in the field of stretchable and flexible electronics. One of the most important future steps of this work will involve the use of BPE additive for large-scale printing of OFET devices. Since BPE additive possesses the advantage of being completely removed upon thermal annealing it allows to get rid of insulating material in the large-scale fabricated devices, consequently, not affecting the performance of the fabricated devices.

The field of flexible and stretchable electronic devices has grown considerably in recent years. We have highlighted the advances and progress including main approaches, design of new

semiconducting material and their application areas. The development of desired materials with enhanced electronic and mechanical properties has a promising potential for the fabrication of large-scaled flexible and stretchable devices. However, a lot of challenges remained to be addressed in order to fully develop new flexible and stretchable devices using physical blending approach. Even though physical blending of semiconducting polymers with soft additives has found to be less time-consuming approach comparing to other strategies, it possesses some challenges, mainly miscibility of conjugated polymers with additives. Moreover, the phase separation that occurs during blending is a complex phenomenon that is still not fully studied. It can be affected by many factors such as solubility issues, solvent evaporation rate, solvent effect, interactions of the substrate and the polymer film blend, the surface free energy of each component and the film thickness. The minor obstacle that have been faced working in particular with BPE additive is impossibility to use characterization techniques containing high vacuum since BPE additive is very volatile and is being removed under these conditions even before running the experiments. Additionally, BPE additive has a plasticizing effect on the conjugated polymers, drastically reducing the crystallinity of polymer blends and making them softer and more amorphous which in turn makes it harder to obtain AFM images at high weight percentages of BPE due to the softness of the thin films.

Looking into the future, the field of flexible and stretchable electronics provides researchers to explore new and interesting concepts. We believe the results included in this thesis will contribute to the development of novel materials and approaches to conformable electronics, ultimately helping to make a step forward for novel organic electronic devices to be used in our daily lives.

## APPENDICES

### APPENDIX A. CHAPTER III SUPPORTING INFORMATION

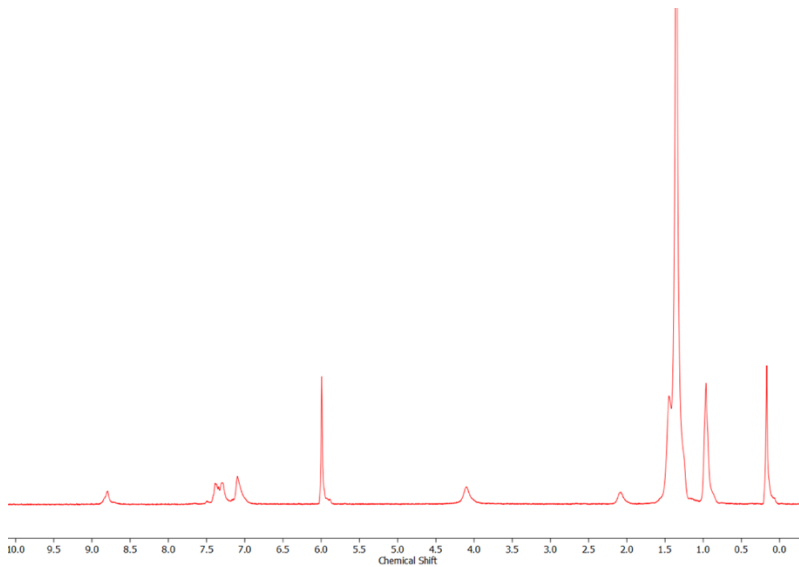


Figure A1.  $^1\text{H}$  NMR spectrum of P(DPPTVT) in  $\text{TCE-d}_2$  at  $120^\circ\text{C}$



Sample	Number-average Molecular weight (Da)	Boiling Point [ $^\circ\text{C}$ ]
Linear Polyethylene (LPE)	1700	>200
Branched Polyethylene (BPE)	500	135

Figure A2. Boiling point of LPE and BPE additives, measured by the capillary tube method.

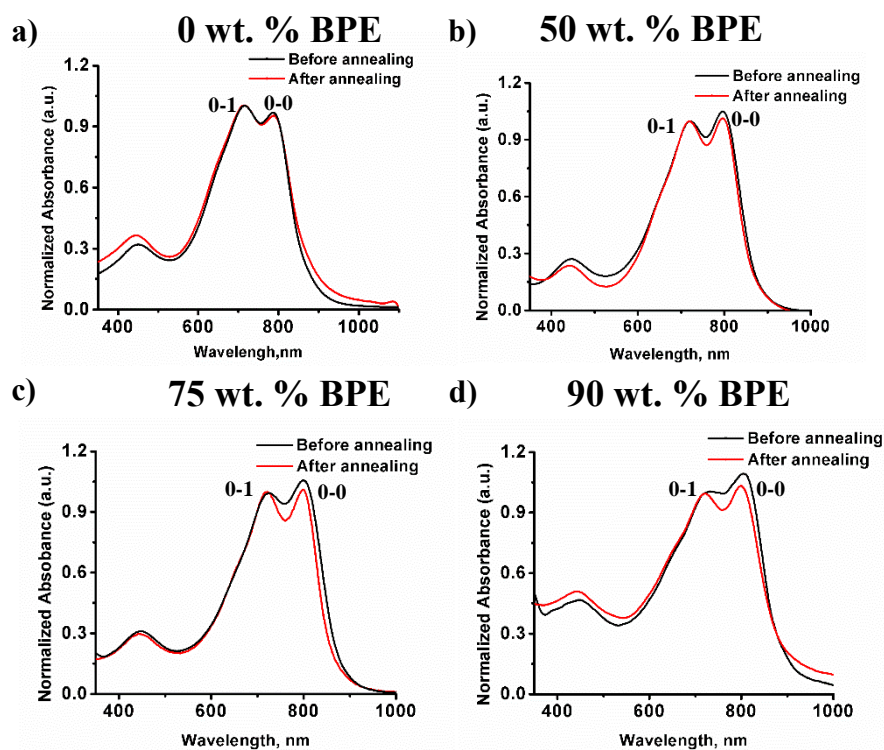


Figure A3. UV-Vis spectra of P(DPPTVT) blended with a) 0 wt.% BPE, b) 50 wt.% BPE, c) 75 wt.% HBPE and d) 90 wt.% BPE before and after thermal annealing for blending systems (thin films).

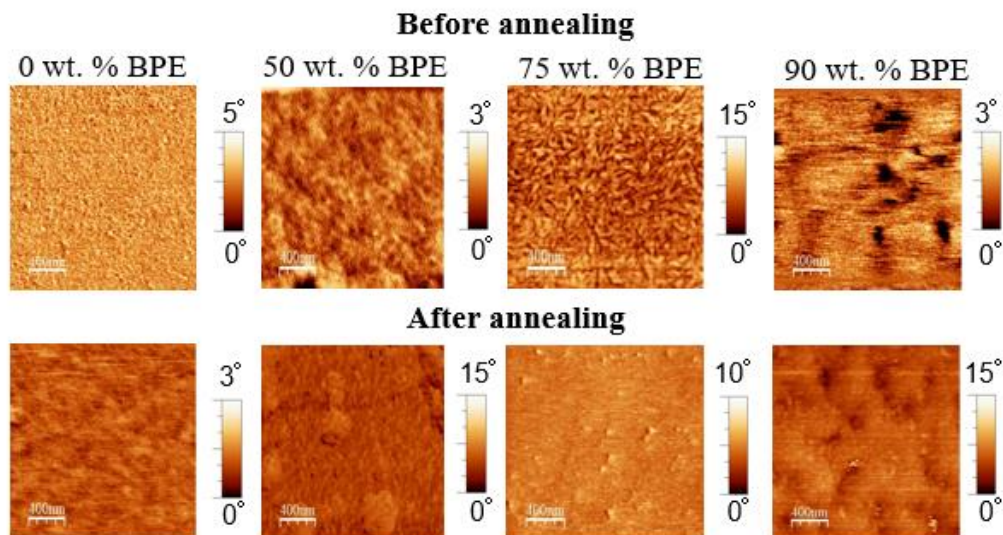


Figure A4. Atomic force microscopy images (phase) of 0, 50, 75 and 90 wt. BPE/P(DPPTVT) blends, before and after thermal annealing (170°C). Scale bar is 400 nm.

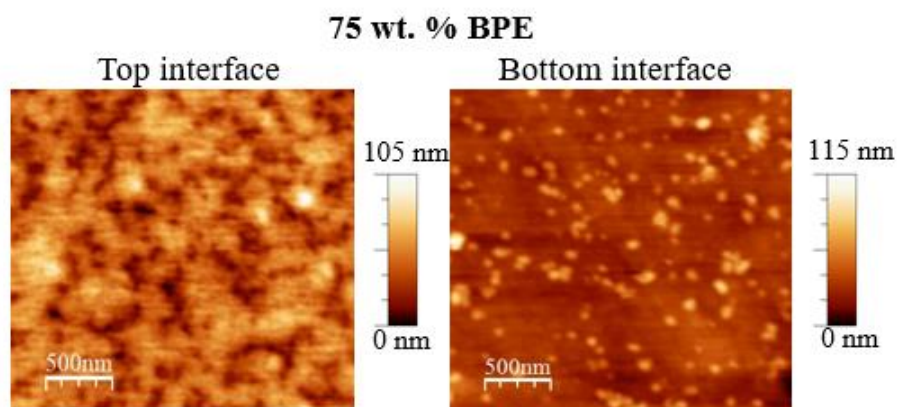


Figure A5. Atomic force microscopy images (height) of the top and bottom interfaces of the P(DPPTVT) film blended with 75 wt% BPE. Scale bar is 500 nm.

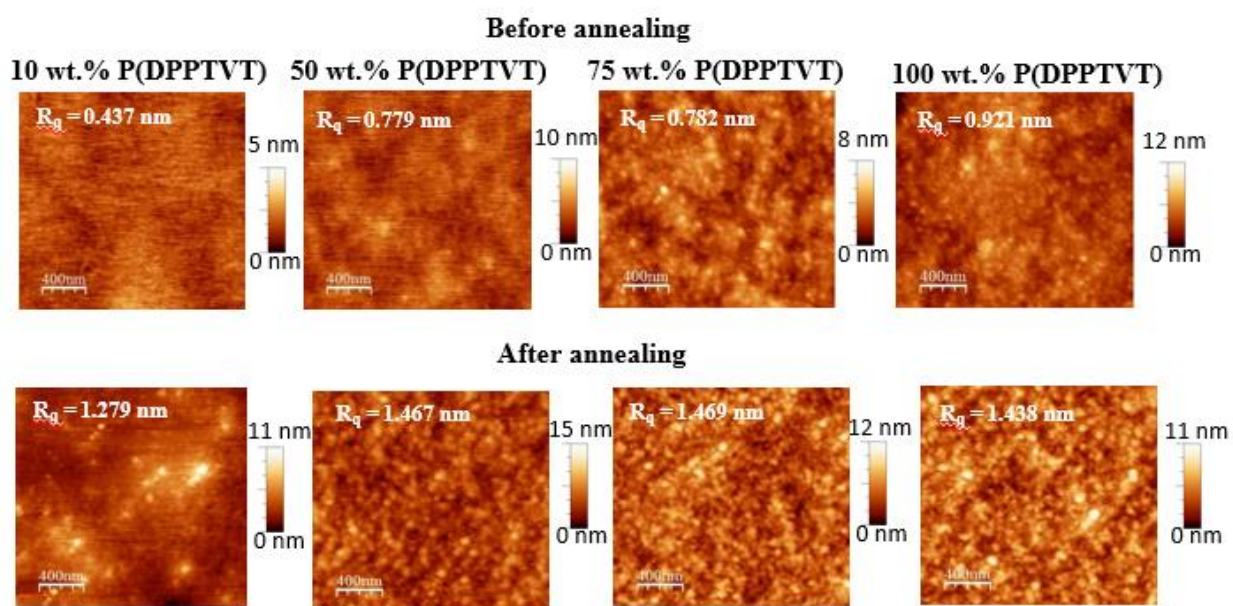


Figure A6. Atomic force microscopy images (height) of 100 to 10 wt.% P(DPPTVT) solution in chlorobenzene (CB), before and after thermal annealing (200°C). Scale bar is 400 nm.

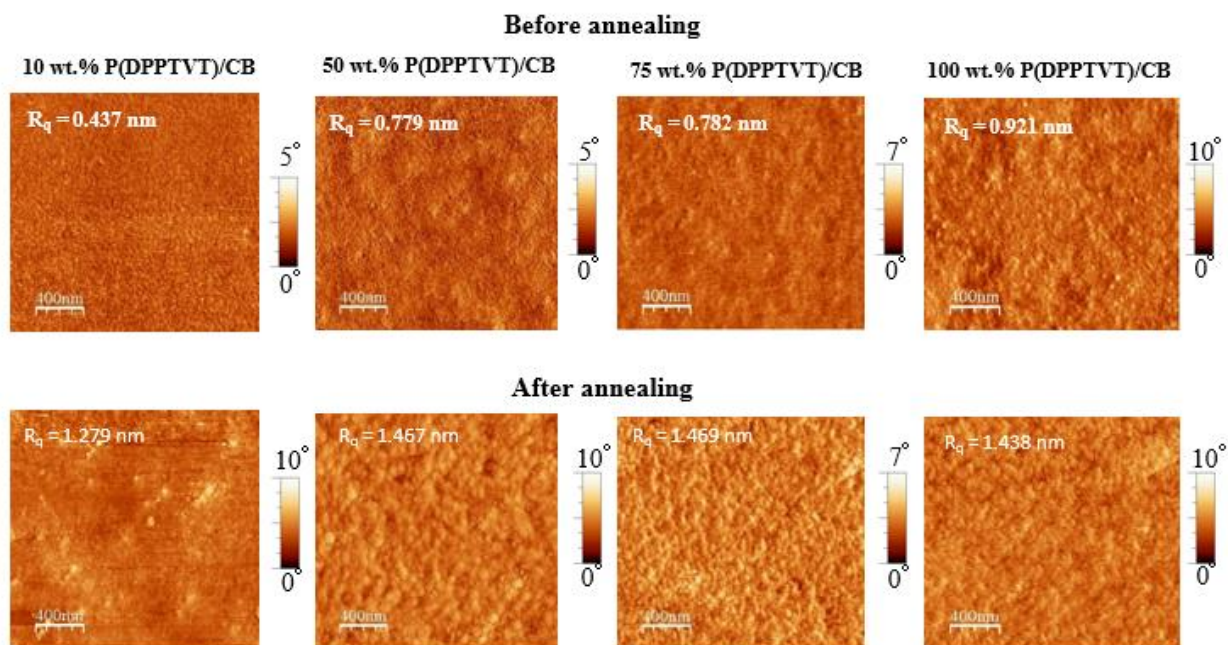


Figure A7. Atomic force microscopy images (phase) of 100 to 10 wt.% P(DPPTVT) solution in chlorobenzene (CB), before and after thermal annealing (200°C). Scale bar is 400 nm.

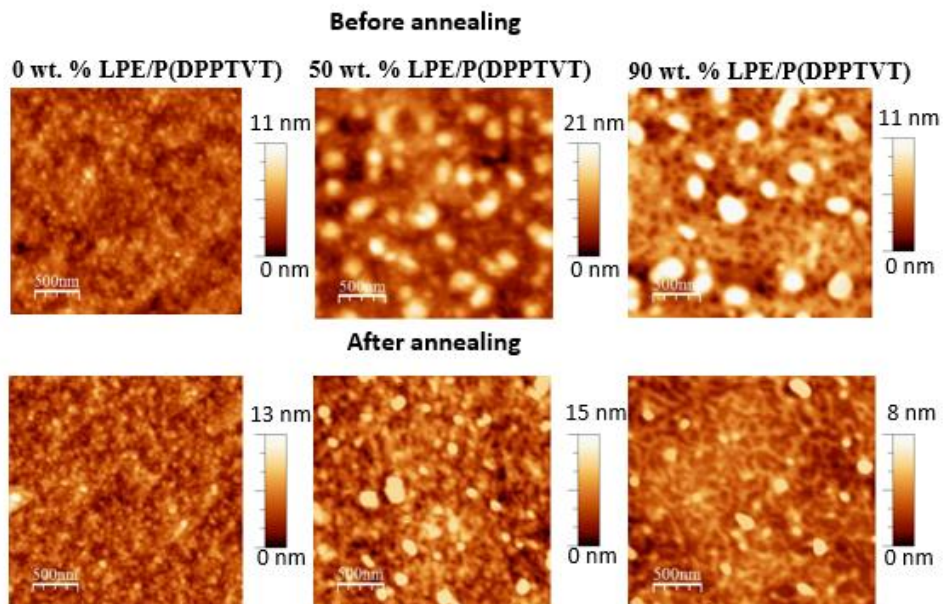


Figure A8. Atomic force microscopy images (height) of 0, 50 and 90 wt. LPE/P(DPPTVT) blends, before and after thermal annealing (170°C). Scale bar is 500 nm.



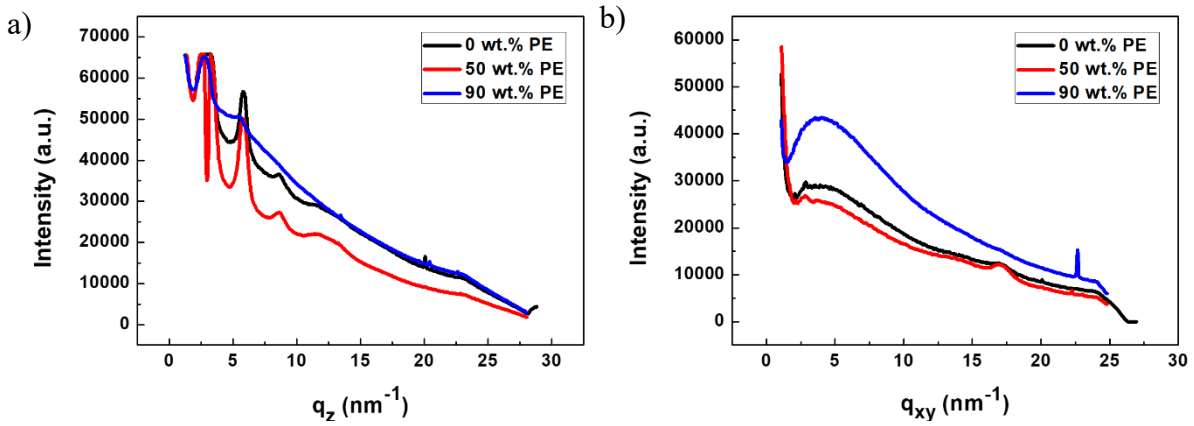


Figure A9. Wide-angle grazing incident X-Ray diffractogram (GIXRD) of P(DPPTVT) blended with 0 to 90 wt.% BPE in a) z axis, and b) x-y axis.

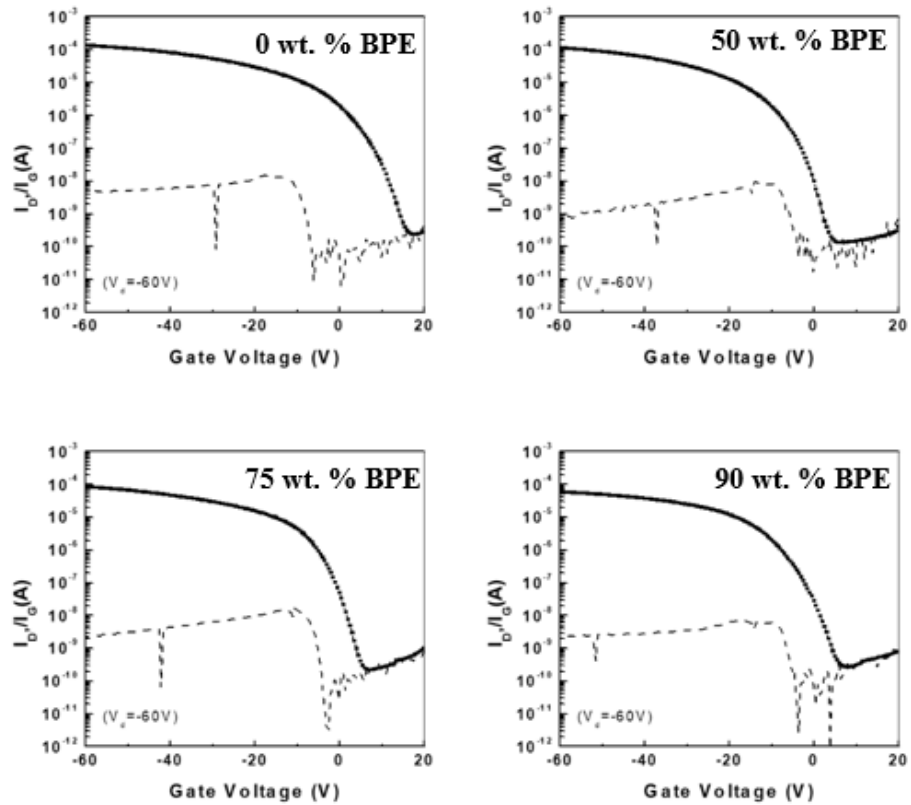


Figure A10. Transfer curves for OFET devices built from 0 wt.% BPE to 90 wt.% BPE, before thermal annealing.  $V_d = -60V$

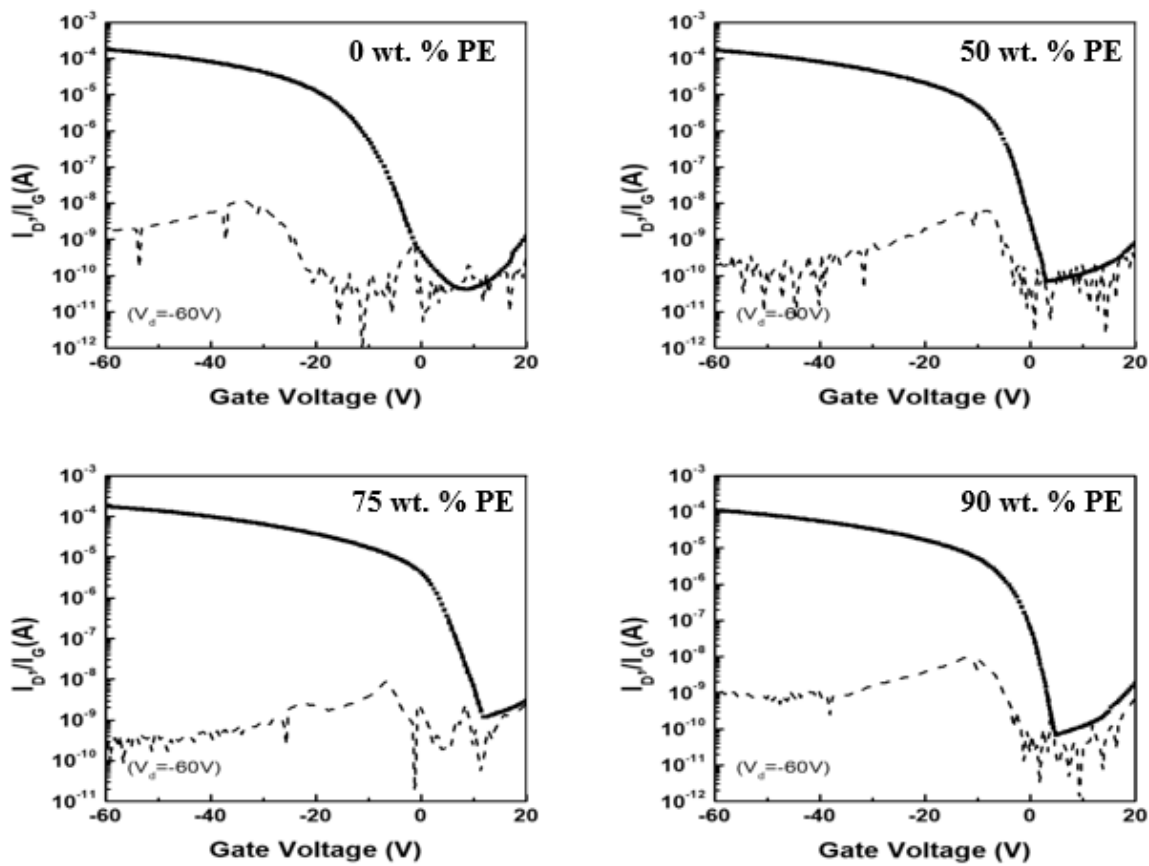


Figure A11. Transfer curves for OFET devices built from 0 wt.% BPE to 90 wt.% BPE, after thermal annealing.  $V_d = -60V$ .

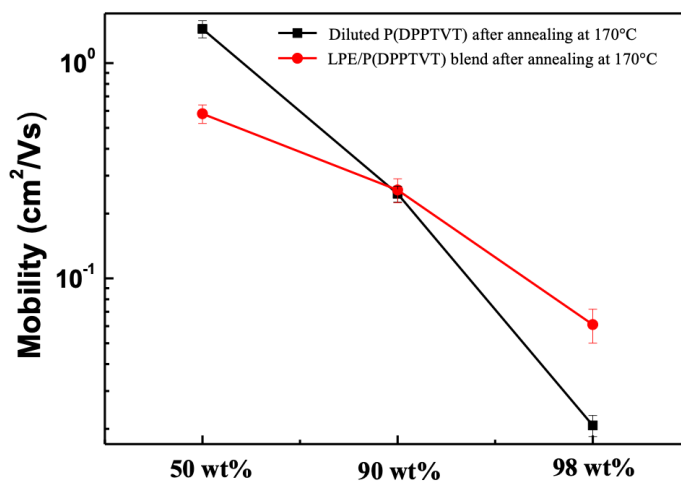


Figure A12. Charge mobility of P(DPPTVT) diluted in chlorobenzene after annealing at 170°C (black curve) and P(DPPTVT) blended with LPE at different ratios (red curve).

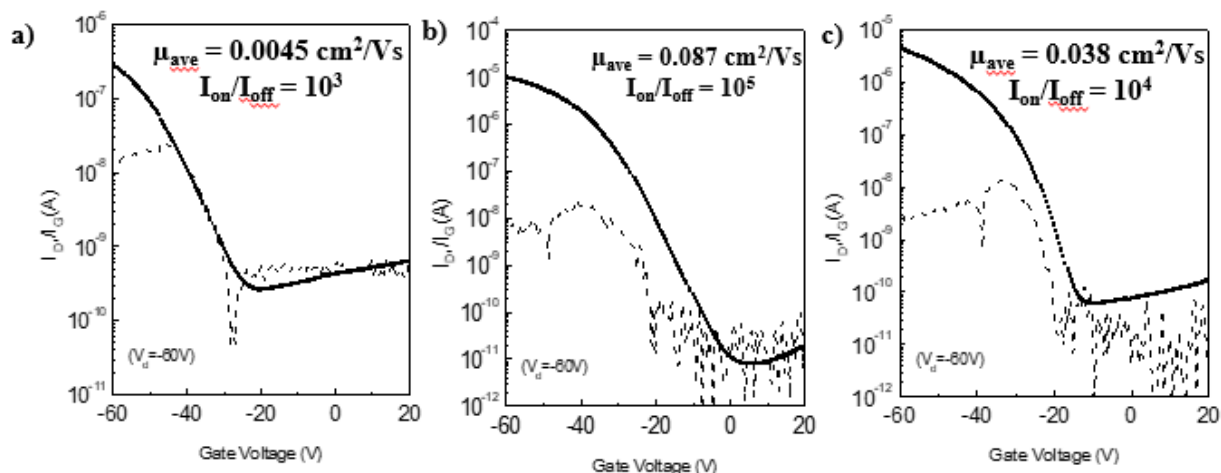


Figure A13. Transfer curves for OFET devices built from a) highly diluted solution of P(DPPTVT) in chlorobenzene, annealed at 170 °C; b) 98 wt.% BPE, annealed at 100 °C, and c) 98 wt.% BPE annealed at 170 °C.  $V_d = -60V$ .

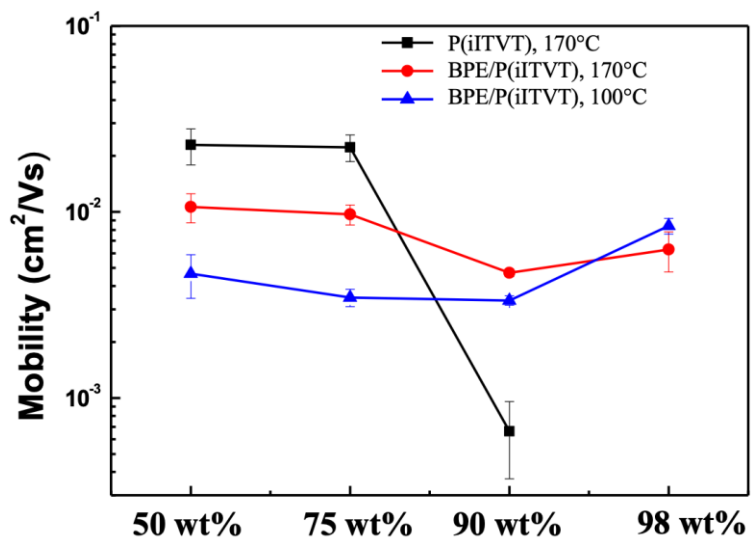


Figure A14. Charge mobility of P(iITVT) diluted in chlorobenzene after annealing at 170°C (black curve), P(iITVT) blended with BPE at different ratios (red curve) annealed at 170°C, and P(iITVT) blended with BPE at different ratios (blue curve) annealed at 100°C.

Table A1. Average and maximum hole mobility ( $\mu_h^{\text{ave}}$ ,  $\mu_h^{\text{max}}$ ), threshold voltages ( $V_{\text{th}}$ ),  $I_{\text{on}}/I_{\text{off}}$ , and ratios for OFETs fabricated from diluted solution of various conjugated polymers blended with 98 wt.% BPE before and after thermal annealing. The device performances were averaged from 12 devices, from three different batches.

Sample	Annealing Temperature [°C]	W/L	Thickness (nm)	$\mu_h^{\text{ave}} / \mu_h^{\text{max}}$ [ $\text{cm}^2 \text{V}^{-1} \text{s}^{-1}$ ]	$I_{\text{ON}}/I_{\text{OFF}}^{\text{ave}}$	$V_{\text{th}}^{\text{ave}}$ [V]
Diluted P(iTTVT) in chlorobenzene	as cast	20		Not determined		
	170			Not determined		
98 wt.% BPE/P(iTTVT)	170	20	13.4	$0.0063 \pm 0.0015 / 0.0087$	$10^3$	-44.97
	100		28.5	$0.0084 \pm 0.0008 / 0.0095$	$10^3$	-41.32

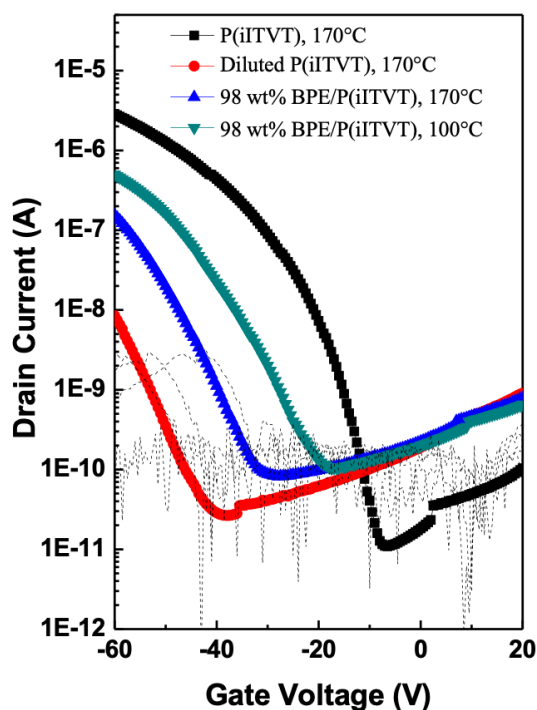


Figure A15. Transfer curves for OFET devices built from pure P(iITVT) annealed at 170°C (black curve), 0.05 wt.% P(iITVT) in chlorobenzene annealed at 170°C (red curve), 98 wt.% BPE/P(iITVT) after thermal annealing at 170°C, 98 wt.% BPE/P(iITVT) after thermal annealing at 100°C.

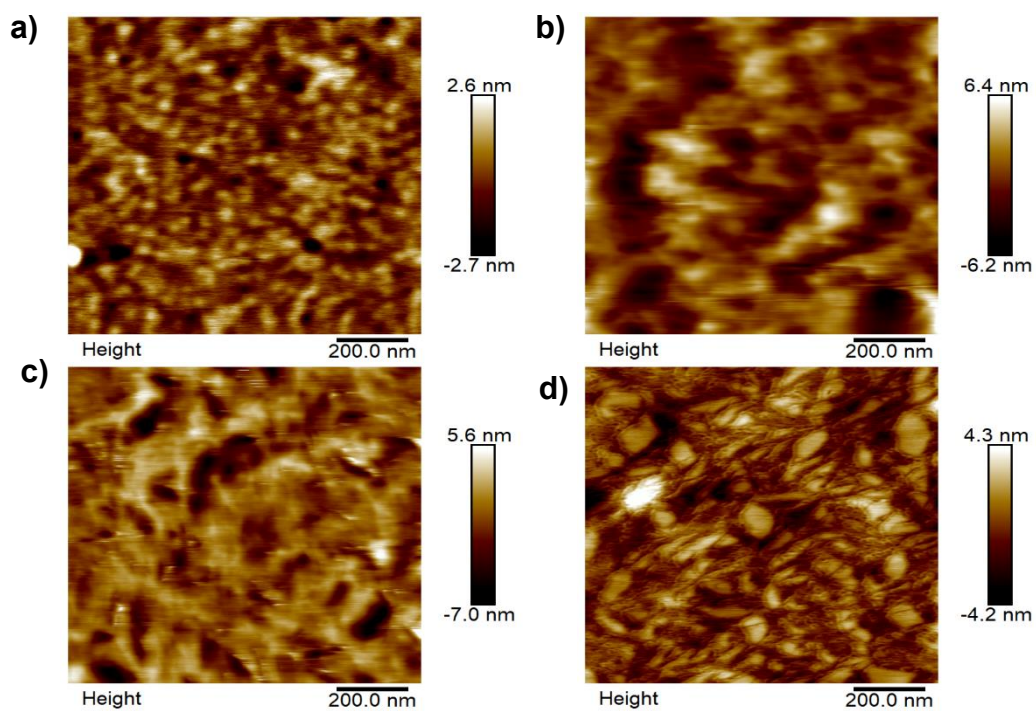


Figure A16. Atomic force microscopy height images of thin film of P(DPPTVT) a) 2 wt.% solution in chlorobenzene; b) blended with 98 wt.% BPE without annealing, c) blended with 98 wt.% BPE after annealing at 100 °C, and d) blended with 98 wt.% BPE after annealing at 170 °C.

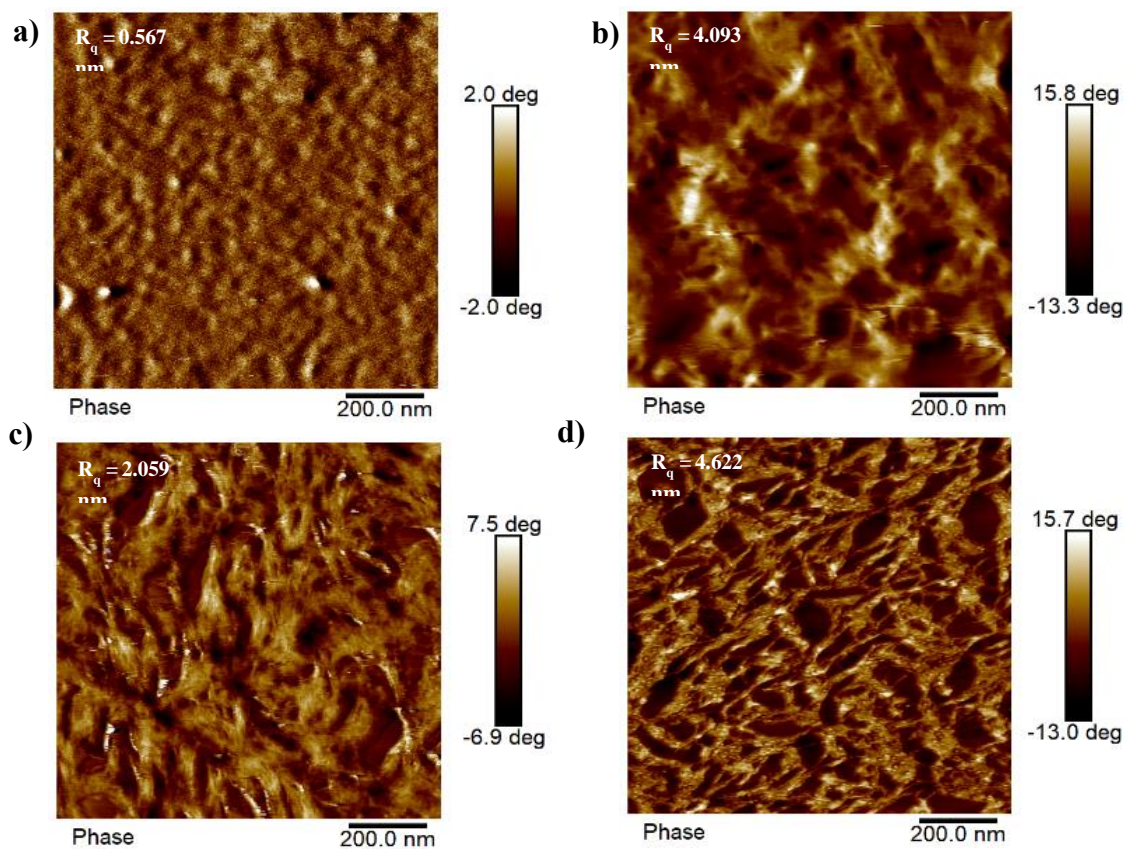


Figure A17. Atomic force microscopy phase images of thin film of P(DPPTVT) a) 2 wt.% solution in chlorobenzene; b) blended with 98 wt.% BPE without annealing, c) blended with 98 wt.% BPE after annealing at 100 °C, and d) blended with 98 wt.% BPE after annealing at 170 °C.

## APPENDIX B. CHAPTER IV SUPPORTING INFORMATION

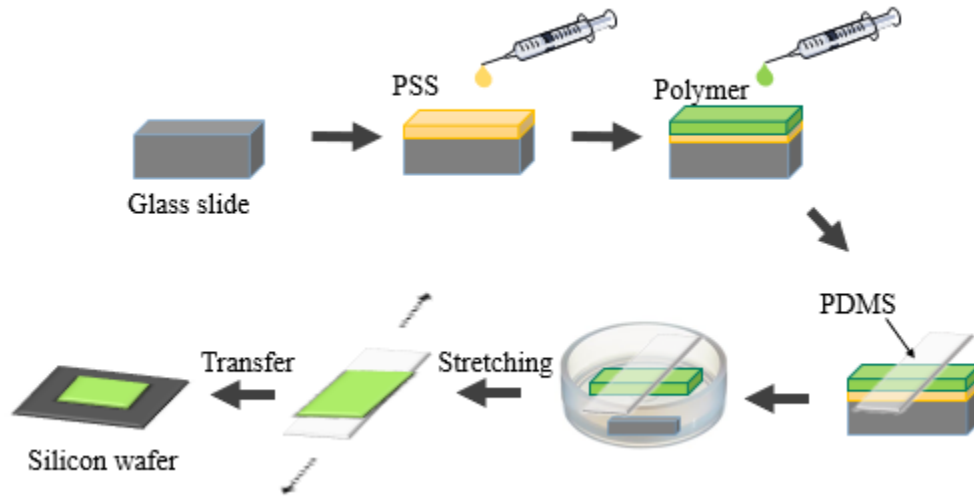


Figure B1 A schematic illustration of preparing a DPP-based polymer/BPE thin film under strain through film-on-water (FOW) method.

Table B1. Average and maximum hole mobility ( $\mu_h^{\text{ave}}$ ,  $\mu_h^{\text{max}}$ ), threshold voltages ( $V_{\text{th}}$ ),  $I_{\text{on}}/I_{\text{off}}$ , and ratios for OFETs fabricated from polymer blends of 0 wt.% to 90 wt.% BPE before and after thermal annealing. The device performances were averaged from 12 devices, from three different batches. Thickness was evaluated by profilometry.

Sample	Annealing Temperature [°C]	W/L	Thickness (nm)	$\mu_h^{\text{ave}} / \mu_h^{\text{max}}$ [ $\text{cm}^2\text{V}^{-1}\text{s}^{-1}$ ]	$I_{\text{ON}}/I_{\text{OFF}}^{\text{ave}}$	$V_{\text{th}}^{\text{ave}}$ [V]
0 wt.% BPE	as cast	20	25.8	$0.27 \pm 0.04 / 0.50$	$10^6$	$-0.1 \pm 4.90$
	170		30.8	$0.75 \pm 0.16 / 0.97$	$10^6$	$-9.8 \pm 4.04$
50 wt.% BPE	as cast	20	34.1	$0.33 \pm 0.09 / 0.52$	$10^5$	$-1.9 \pm 4.82$
	170		29.6	$0.64 \pm 0.09 / 0.89$	$10^6$	$-3.5 \pm 6.87$
75 wt.% BPE	as cast	20	33.1	$0.32 \pm 0.08 / 0.47$	$10^6$	$-1.8 \pm 4.10$
	170		30.7	$0.79 \pm 0.09 / 1.04$	$10^6$	$-2.6 \pm 5.24$
90 wt.% BPE	as cast	20	29.5	$0.29 \pm 0.10 / 0.46$	$10^5$	$-5.8 \pm 2.52$
	170		33.2	$0.53 \pm 0.10 / 0.84$	$10^6$	$-2.6 \pm 4.41$

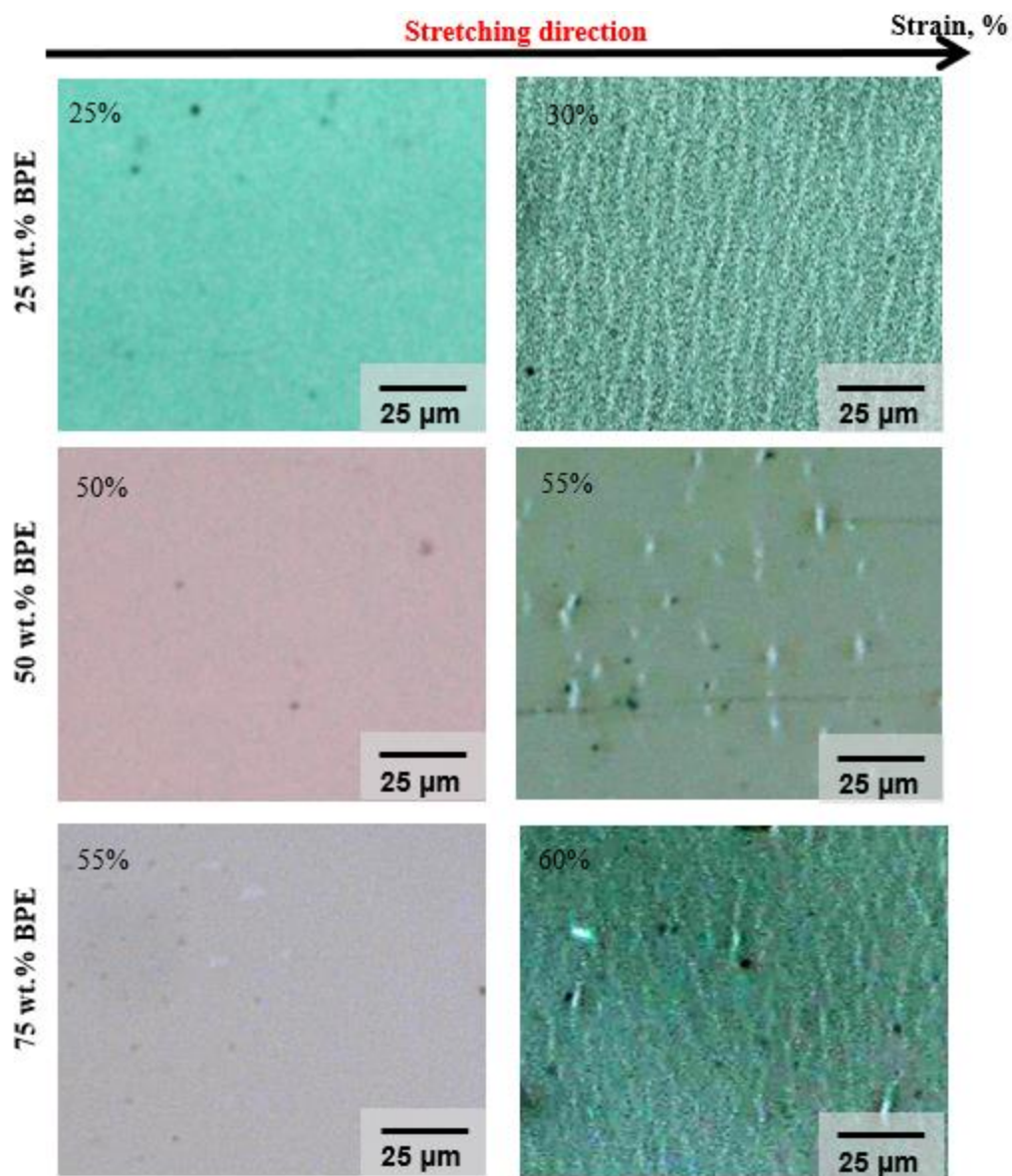


Figure B2. Crack on-set strain of P(DPPTVT)/BPE blends containing from 25 wt.% to 75 wt.% of BPE obtained by observing the formation of cracks under optical microscope (right) and before appearance of cracks (left). Scale bars are 50 $\mu$ m.



Table B2. Parameters used for AFM-IR imaging of the polymer blends

Sample	Scan Rate	IR Power	Setpoint	Integral Gain	Drive Strength	Wavenumber (cm <sup>-1</sup> )
25% BPE	0.5 Hz	65%	2.6 V	0.1	0.28%	1660
50% BPE	0.5 Hz	65%	2.8 V	0.1	6%	1660
75% BPE	0.5 Hz	65%	3.0 V	0.10	10%	1660
90% BPE	0.5 Hz	80%	1.1 V	0.75	15%	1660

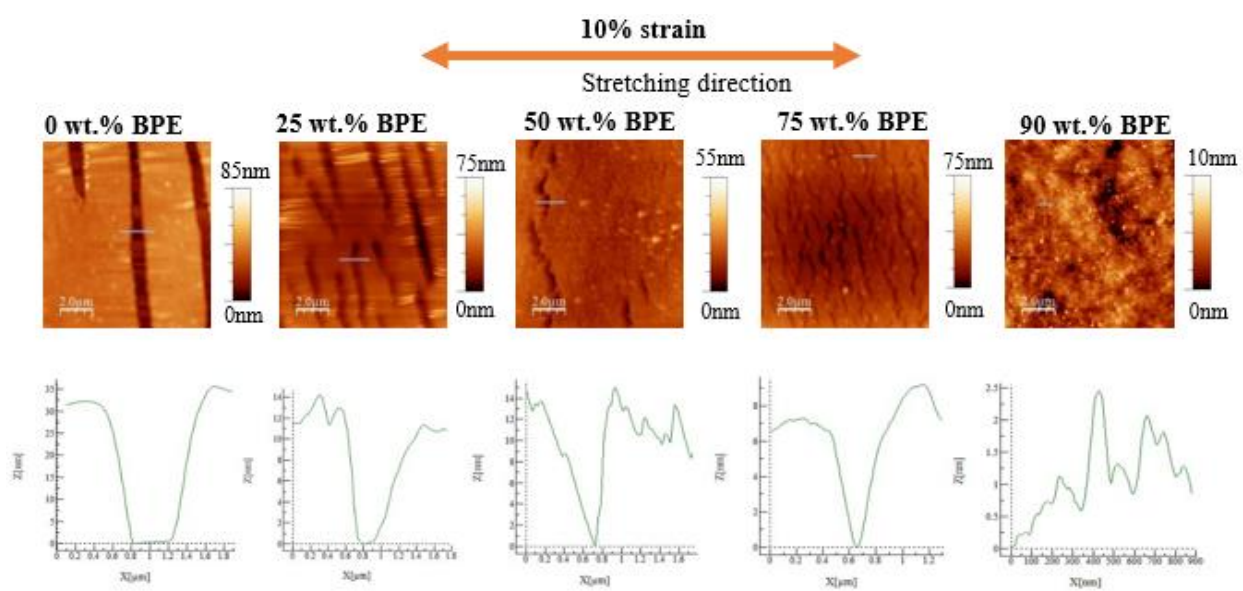


Figure B3. Atomic force microscopy images (height) of BPE/P(DPPTVT) blends containing 0 to 90 wt.% BPE at 10% strain before thermal annealing.

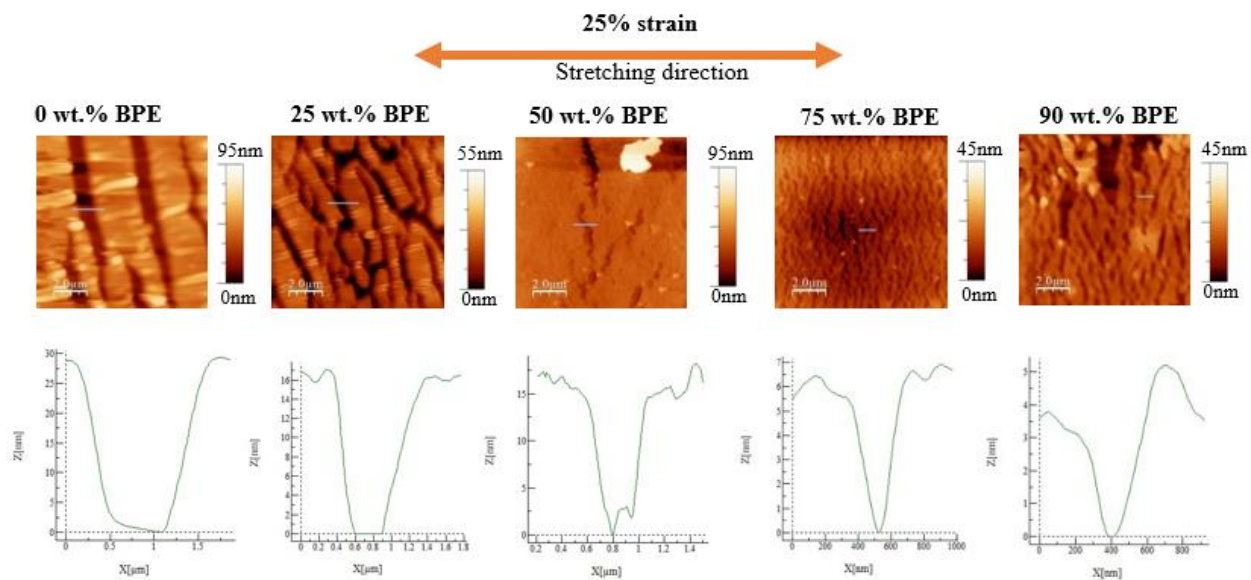


Figure B4. Atomic force microscopy images (height) of BPE/P(DPPTVT) blends containing 0 to 90 wt.% BPE at 25% strain before thermal annealing.

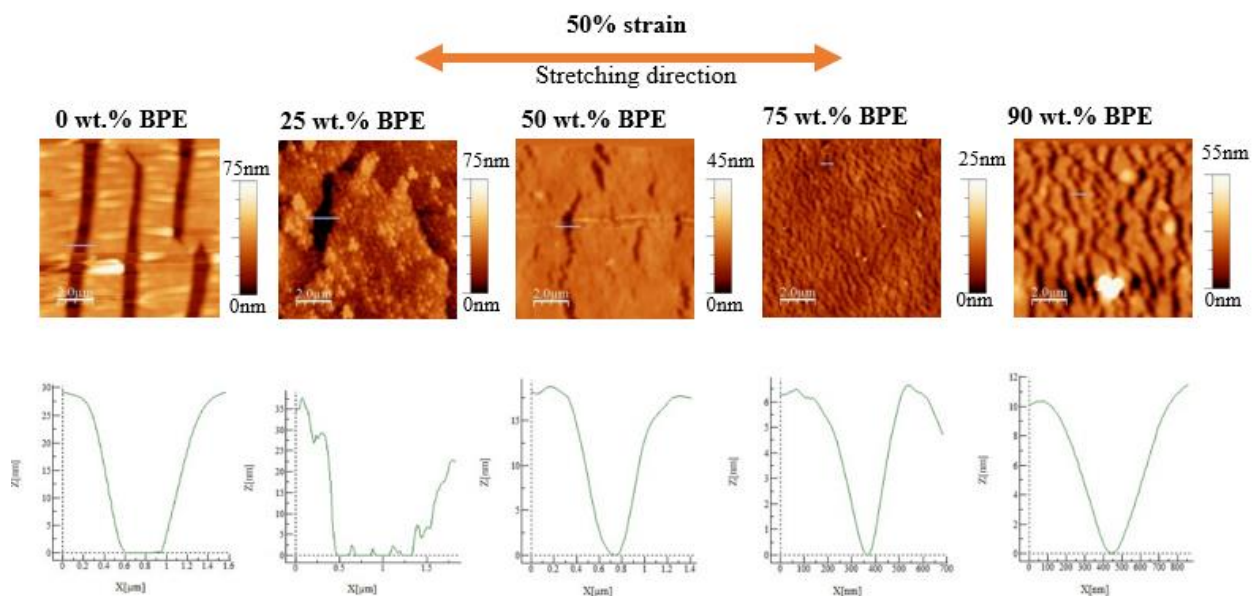


Figure B5. Atomic force microscopy images (height) of BPE/P(DPPTVT) blends containing 0 to 90 wt.% BPE at 50% strain before thermal annealing.

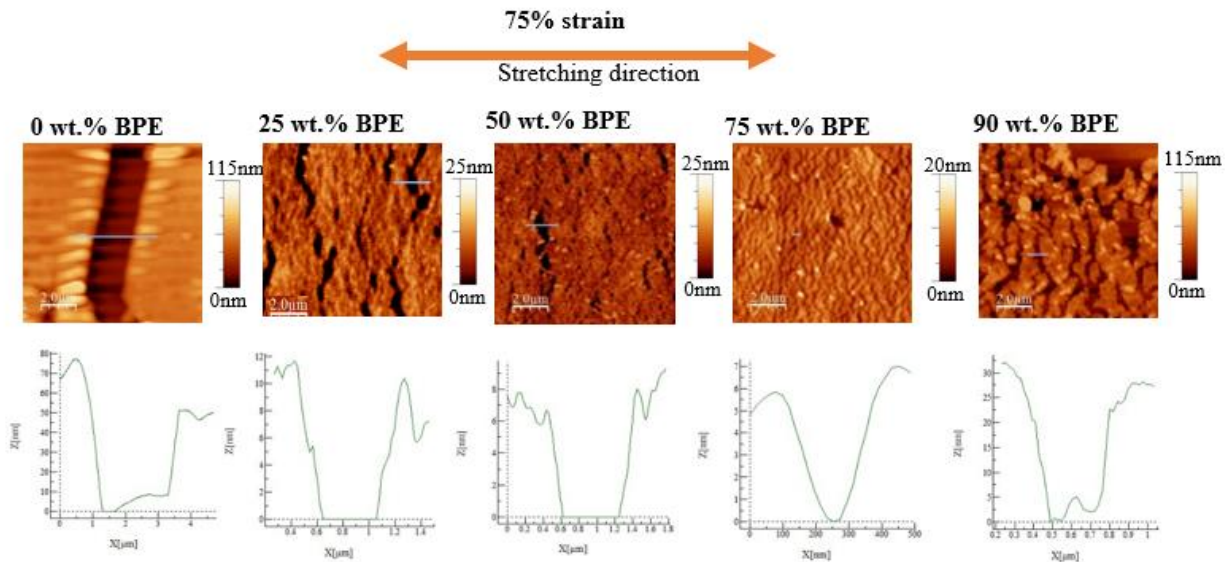


Figure B6. Atomic force microscopy images (height) of BPE/P(DPPTVT) blends containing 0 to 90 wt.% BPE at 75% strain before thermal annealing.

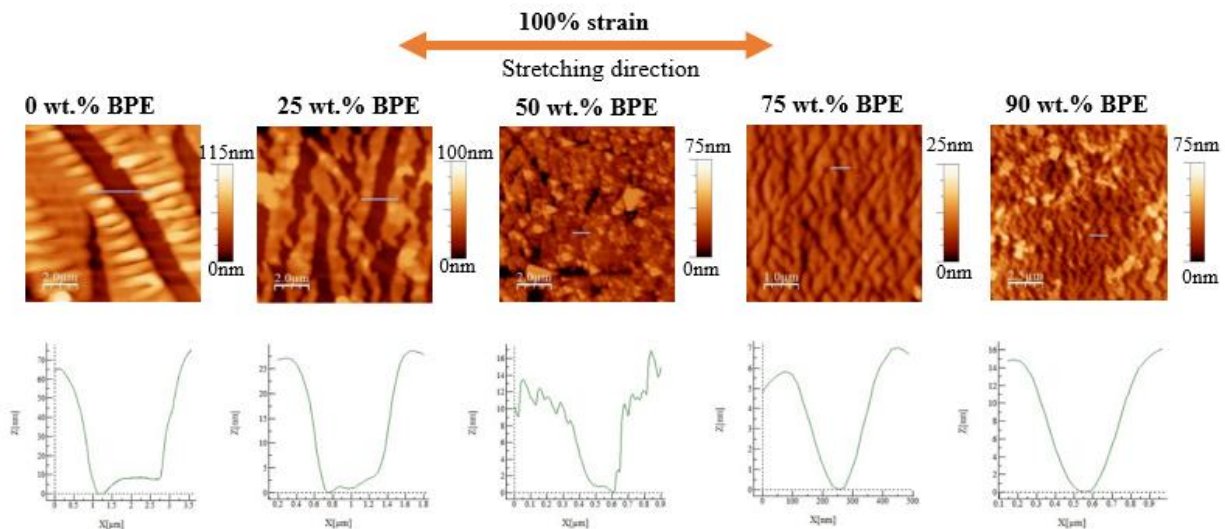


Figure B7. Atomic force microscopy images (height) of BPE/P(DPPTVT) blends containing 0 to 90 wt.% BPE at 100% strain before thermal annealing.

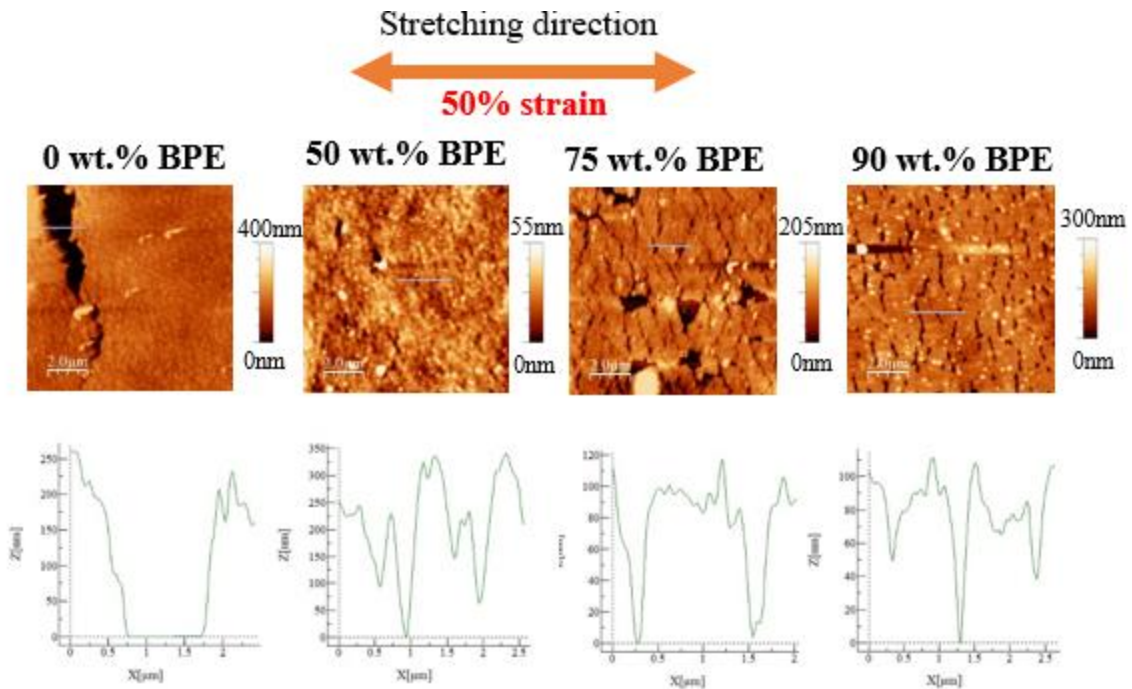


Figure B8. Atomic force microscopy images (height) of BPE/P(DPPTVT) blends containing 0 to 90 wt.% BPE at 50% strain after thermal annealing.

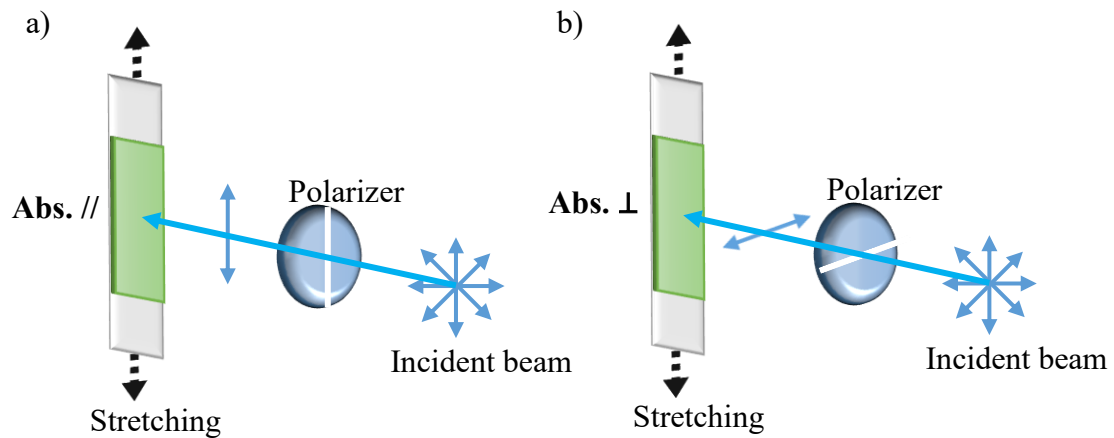


Figure B9. Schematic diagram of polarized UV-vis characterization on stretched polymer blend films with the polarization direction of light a) parallel and b) perpendicular to the stretching direction.

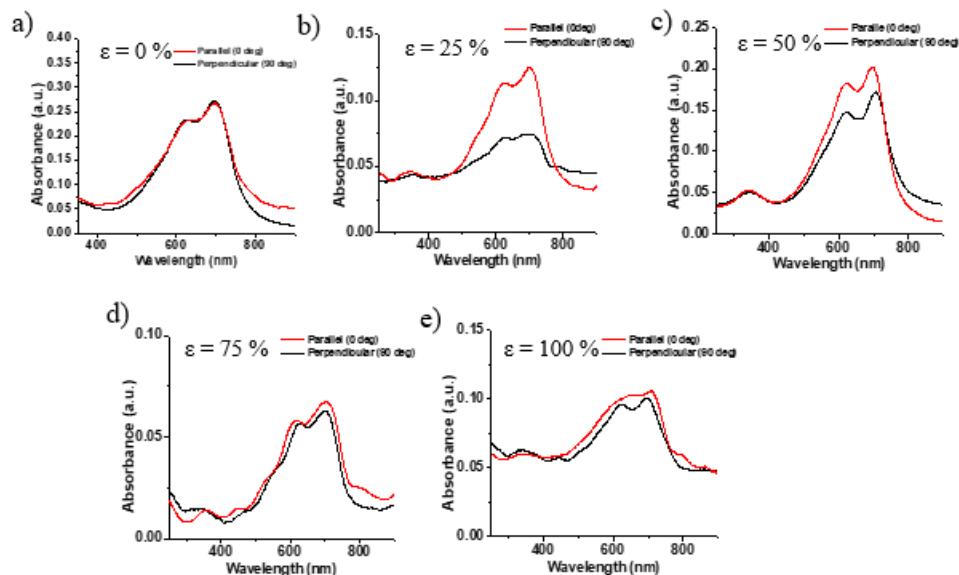


Figure B10. Polarized UV-vis spectra of BPE/P(DPPTVT) blended system with 0 wt.% BPE stretched at different percent strains, with the polarization direction of light parallel ( $0^\circ$ , red curve) and perpendicular ( $90^\circ$ , black curve) to the stretching direction.

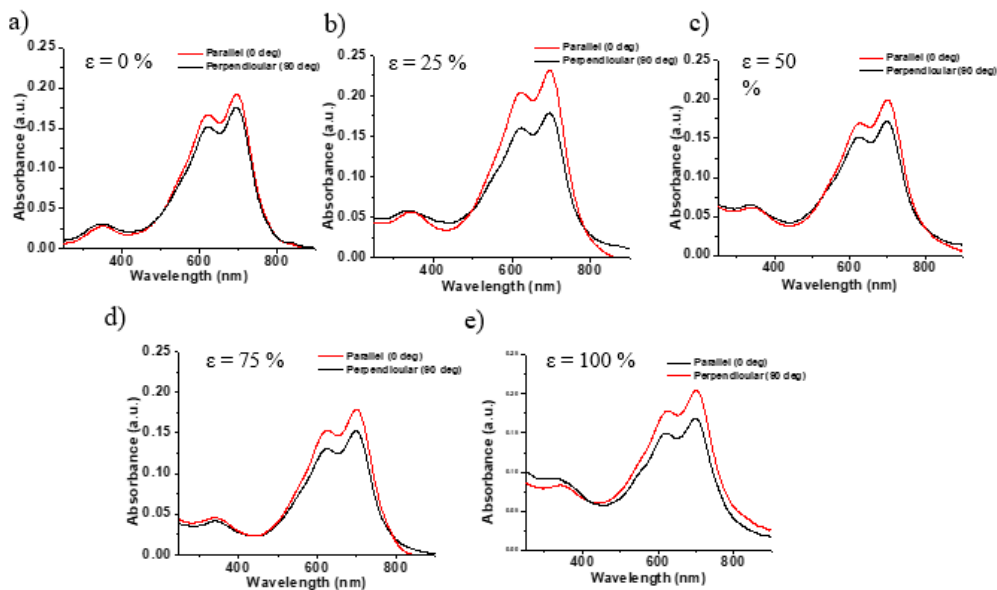


Figure B11. Polarized UV-vis spectra of BPE/P(DPPTVT) blended system with 25 wt.% BPE stretched at different percent strains, with the polarization direction of light parallel ( $0^\circ$ , red curve) and perpendicular ( $90^\circ$ , black curve) to the stretching direction.

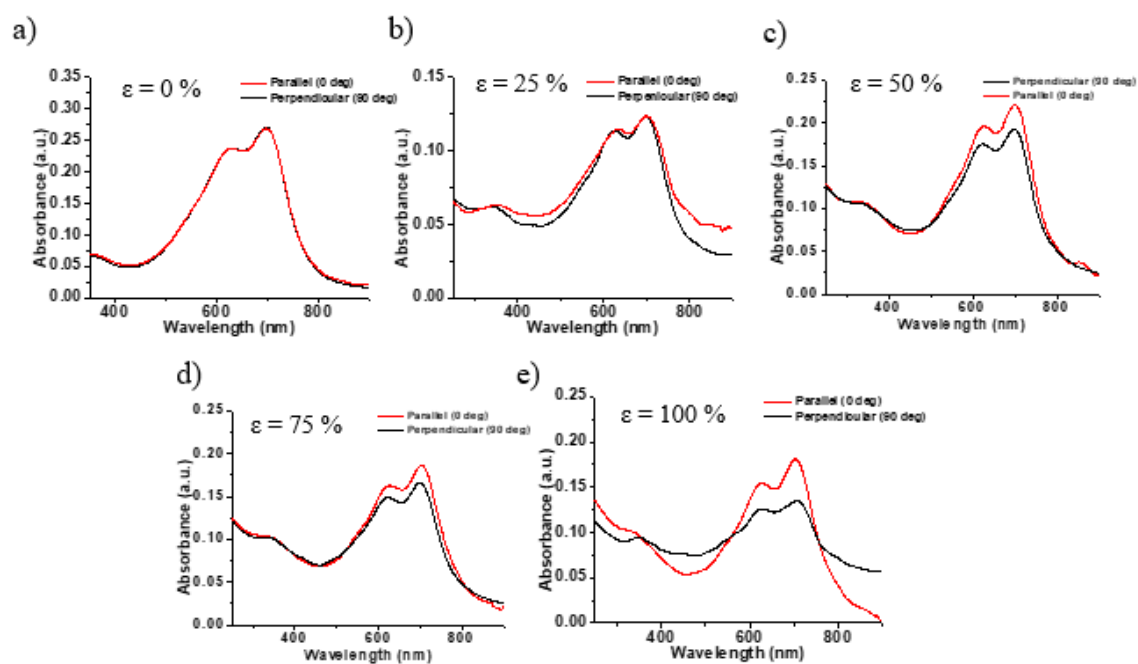


Figure B12. Polarized UV-vis spectra of BPE/P(DPPTVT) blended system with 50 wt.% BPE stretched at different percent strains, with the polarization direction of light parallel ( $0^\circ$ , red curve) and perpendicular ( $90^\circ$ , black curve) to the stretching direction.

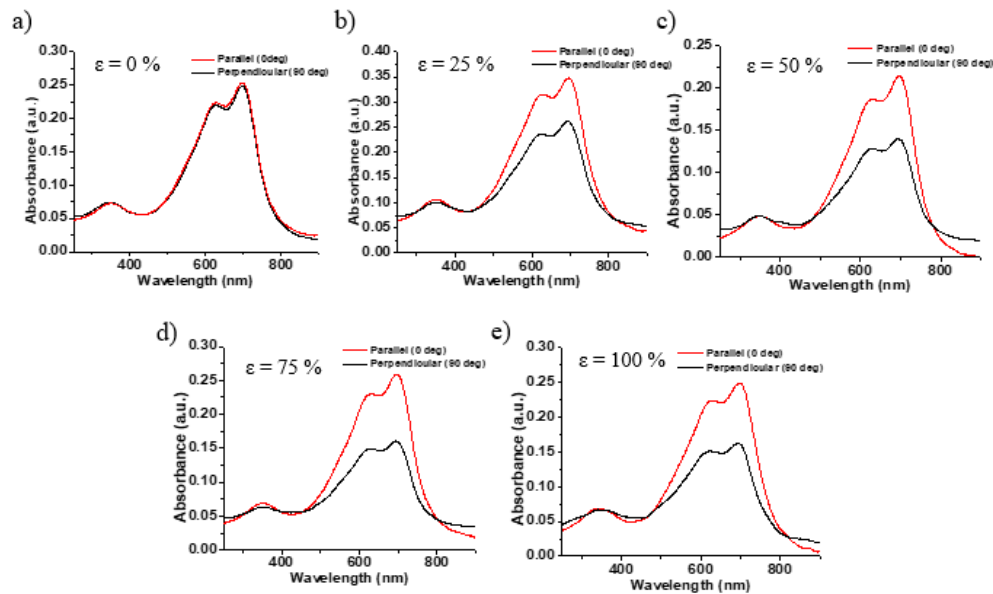


Figure B13. Polarized UV-vis spectra of BPE/P(DPPTVT) blended system with 75 wt.% BPE stretched at different percent strains, with the polarization direction of light parallel ( $0^\circ$ , red curve) and perpendicular ( $90^\circ$ , black curve) to the stretching direction.

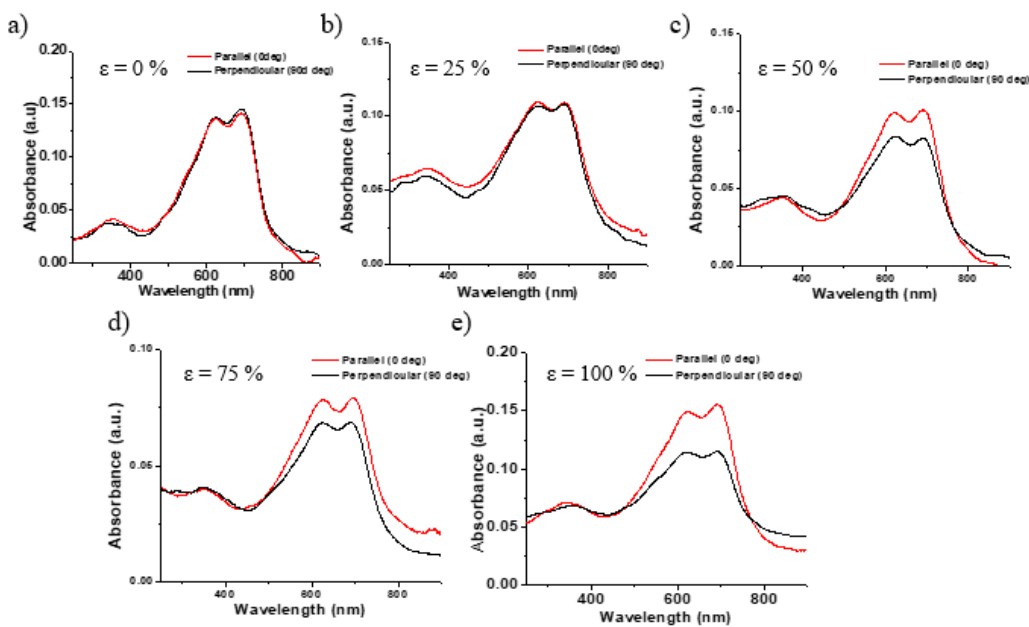


Figure B14. Polarized UV-vis spectra of BPE/P(DPPTVT) blended system with 90 wt.% BPE stretched at different percent strains, with the polarization direction of light parallel ( $0^\circ$ , red curve) and perpendicular ( $90^\circ$ , black curve) to the stretching direction.

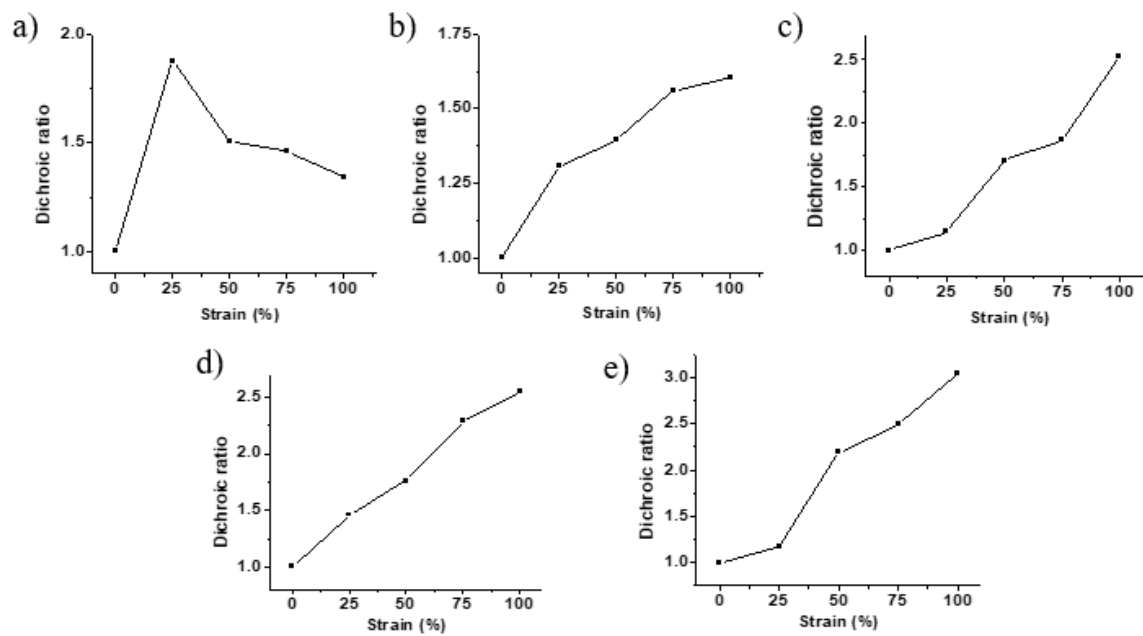


Figure B15. Dichroic ratios of the BPE/P(DPPTVT) blends containing a) 0 wt.%; b) 25 wt.%; c) 50 wt.%; d) 75 wt.%; and e) 90 wt.% of BPE in function of strain determined by polarized UV-Vis spectroscopy

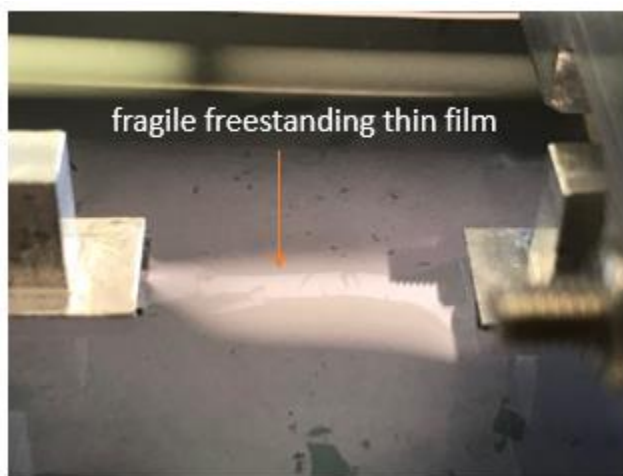


Figure B16. Observations of a brittle freestanding thin film above 25 wt.% BPE obtained by Film-On-Water tensile test.



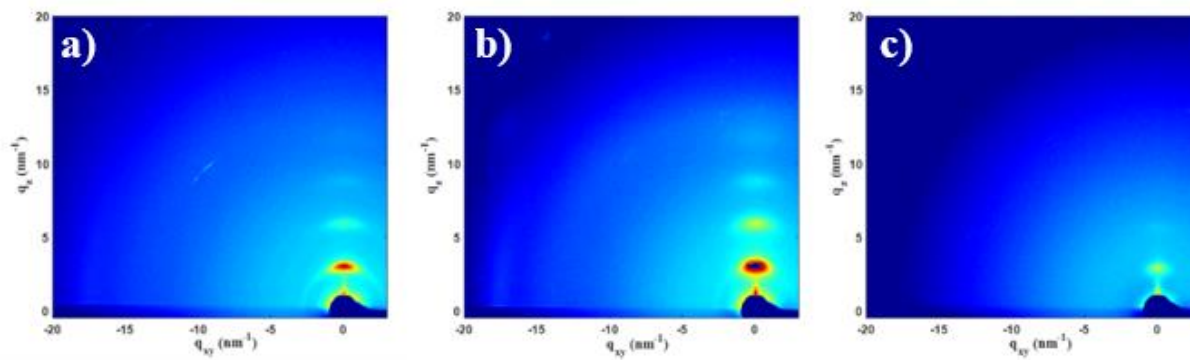


Figure B17. Wide-angle grazing incident X-Ray diffractogram (GIXRD) of a) P(DPPTVT), b) P(DPPTVT) + 50 wt.% BPE, and c) P(DPPTVT) + 90 wt.% BPE.

## APPENDIX C. COPYRIGHT PERMISSIONS

### SPRINGER NATURE LICENSE TERMS AND CONDITIONS

Aug 27, 2019

---

This Agreement between University of Windsor -- Mariia Selivanova ("You") and Springer Nature ("Springer Nature") consists of your license details and the terms and conditions provided by Springer Nature and Copyright Clearance Center.

License Number	4657160386120
License date	Aug 27, 2019
Licensed Content Publisher	Springer Nature
Licensed Content Publication	Nature Materials
Licensed Content Title	A general relationship between disorder, aggregation and charge transport in conjugated polymers
Licensed Content Author	Rodrigo Noriega, Jonathan Rivnay, Koen Vandewal, Felix P. V. Koch, Natalie Stingelin et al.
Licensed Content Date	Aug 4, 2013
Licensed Content Volume	12
Licensed Content Issue	11
Type of Use	Thesis/Dissertation
Requestor type	academic/university or research institute
Format	print and electronic
Portion	figures/tables/illustrations
Number of figures/tables/illustrations	1
High-res required	no
Will you be translating?	no
Circulation/distribution	<501
Author of this Springer Nature content	no
Title	Design and Preparation of Stretchable Semiconductors through Polymer Blending
Institution name	n/a
Expected presentation date	Aug 2019
Order reference number	40
Portions	Figure 1.6.

**JOHN WILEY AND SONS LICENSE  
TERMS AND CONDITIONS**

Aug 27, 2019

---

This Agreement between University of Windsor -- Mariia Selivanova ("You") and John Wiley and Sons ("John Wiley and Sons") consists of your license details and the terms and conditions provided by John Wiley and Sons and Copyright Clearance Center.

License Number	4657200670564
License date	Aug 27, 2019
Licensed Content Publisher	John Wiley and Sons
Licensed Content Publication	Macromolecular Rapid Communications
Licensed Content Title	Probing the Viscoelastic Property of Pseudo Free-Standing Conjugated Polymeric Thin Films
Licensed Content Author	Xiaodan Gu, Simon Rondeau-Gagné, Dongshan Zhou, et al
Licensed Content Date	May 11, 2018
Licensed Content Volume	39
Licensed Content Issue	14
Licensed Content Pages	8
Type of use	Dissertation/Thesis
Requestor type	University/Academic
Format	Print and electronic
Portion	Figure/table
Number of figures/tables	1
Original Wiley figure/table number(s)	Figure 1
Will you be translating?	No
Order reference number	60
Title of your thesis / dissertation	Design and Preparation of Stretchable Semiconductors through Polymer Blending
Expected completion date	Aug 2019
Expected size (number of pages)	153

**SPRINGER NATURE LICENSE  
TERMS AND CONDITIONS**

Aug 27, 2019

---

This Agreement between University of Windsor -- Mariia Selivanova ("You") and Springer Nature ("Springer Nature") consists of your license details and the terms and conditions provided by Springer Nature and Copyright Clearance Center.

License Number	4657170292921
License date	Aug 27, 2019
Licensed Content Publisher	Springer Nature
Licensed Content Publication	Science China Chemistry
Licensed Content Title	Constructing vertical phase separation of polymer blends via mixed solvents to enhance their photovoltaic performance
Licensed Content Author	Qingqing Yang, Jiantai Wang, Xiaoqin Zhang et al
Licensed Content Date	Jan 1, 2014
Licensed Content Volume	58
Licensed Content Issue	2
Type of Use	Thesis/Dissertation
Requestor type	academic/university or research institute
Format	print and electronic
Portion	figures/tables/illustrations
Number of figures/tables/illustrations	1
Will you be translating?	no
Circulation/distribution	<501
Author of this Springer Nature content	no
Title	Design and Preparation of Stretchable Semiconductors through Polymer Blending
Institution name	n/a
Expected presentation date	Aug 2019
Order reference number	136
Portions	Figure 1.10.

**JOHN WILEY AND SONS LICENSE  
TERMS AND CONDITIONS**

Aug 27, 2019

---

This Agreement between University of Windsor -- Mariia Selivanova ("You") and John Wiley and Sons ("John Wiley and Sons") consists of your license details and the terms and conditions provided by John Wiley and Sons and Copyright Clearance Center.

License Number	4657200812458
License date	Aug 27, 2019
Licensed Content Publisher	John Wiley and Sons
Licensed Content Publication	FEBS Letters
Licensed Content Title	Measuring elasticity of biological materials by atomic force microscopy
Licensed Content Author	Giorgio Semenza, Anja Vinckier
Licensed Content Date	Dec 18, 1998
Licensed Content Volume	430
Licensed Content Issue	1-2
Licensed Content Pages	5
Type of use	Dissertation/Thesis
Requestor type	University/Academic
Format	Print and electronic
Portion	Figure/table
Number of figures/tables	1
Original Wiley figure/table number(s)	Figure 1
Will you be translating?	No
Order reference number	76
Title of your thesis / dissertation	Design and Preparation of Stretchable Semiconductors through Polymer Blending
Expected completion date	Aug 2019
Expected size (number of pages)	153

**JOHN WILEY AND SONS LICENSE  
TERMS AND CONDITIONS**

Aug 28, 2019

---

This Agreement between University of Windsor -- Mariia Selivanova ("You") and John Wiley and Sons ("John Wiley and Sons") consists of your license details and the terms and conditions provided by John Wiley and Sons and Copyright Clearance Center.

License Number	4657770852480
License date	Aug 28, 2019
Licensed Content Publisher	John Wiley and Sons
Licensed Content Publication	Small
Licensed Content Title	Optimized Structural Designs for Stretchable Silicon Integrated Circuits
Licensed Content Author	John A. Rogers, Yongwei Zhang, Keh-chih Hwang, et al
Licensed Content Date	Dec 14, 2009
Licensed Content Volume	5
Licensed Content Issue	24
Licensed Content Pages	7
Type of use	Dissertation/Thesis
Requestor type	University/Academic
Format	Print and electronic
Portion	Figure/table
Number of figures/tables	1
Original Wiley figure/table number(s)	Figure 3
Will you be translating?	No
Order reference number	78
Title of your thesis / dissertation	Design and Preparation of Stretchable Semiconductors through Polymer Blending
Expected completion date	Aug 2019
Expected size (number of pages)	153

**JOHN WILEY AND SONS LICENSE  
TERMS AND CONDITIONS**

Aug 27, 2019

---

This Agreement between University of Windsor -- Mariia Selivanova ("You") and John Wiley and Sons ("John Wiley and Sons") consists of your license details and the terms and conditions provided by John Wiley and Sons and Copyright Clearance Center.

License Number	4657200967616
License date	Aug 27, 2019
Licensed Content Publisher	John Wiley and Sons
Licensed Content Publication	Advanced Electronic Materials
Licensed Content Title	Stretchable and Transparent Organic Semiconducting Thin Film with Conjugated Polymer Nanowires Embedded in an Elastomeric Matrix
Licensed Content Author	Eunjoo Song, Boseok Kang, Hyun Ho Choi, et al
Licensed Content Date	Oct 29, 2015
Licensed Content Volume	2
Licensed Content Issue	1
Licensed Content Pages	8
Type of use	Dissertation/Thesis
Requestor type	University/Academic
Format	Print and electronic
Portion	Figure/table
Number of figures/tables	1
Original Wiley figure/table number(s)	Figure 1
Will you be translating?	No
Order reference number	80
Title of your thesis / dissertation	Design and Preparation of Stretchable Semiconductors through Polymer Blending
Expected completion date	Aug 2019
Expected size (number of pages)	153



**Title:** Amide-Containing Alkyl Chains in  
Conjugated Polymers: Effect on  
Self-Assembly and Electronic  
Properties  
**Author:** Michael U. Ocheje, Brynn P.  
Charron, Yu-Hsuan Cheng, et al  
**Publication:** Macromolecules  
**Publisher:** American Chemical Society  
**Date:** Feb 1, 2018  
Copyright © 2018, American Chemical Society

Logged in as:  
Maria Selivanova  
University of Windsor  
Account #: 3001507830

[LOGOUT](#)

### PERMISSION/LICENSE IS GRANTED FOR YOUR ORDER AT NO CHARGE

This type of permission/license, instead of the standard Terms & Conditions, is sent to you because no fee is being charged for your order. Please note the following:

- Permission is granted for your request in both print and electronic formats, and translations.
- If figures and/or tables were requested, they may be adapted or used in part.
- Please print this page for your records and send a copy of it to your publisher/graduate school.
- Appropriate credit for the requested material should be given as follows: "Reprinted (adapted) with permission from (COMPLETE REFERENCE CITATION). Copyright (YEAR) American Chemical Society." Insert appropriate information in place of the capitalized words.
- One-time permission is granted only for the use specified in your request. No additional uses are granted (such as derivative works or other editions). For any other uses, please submit a new request.



**JOHN WILEY AND SONS LICENSE  
TERMS AND CONDITIONS**

Aug 27, 2019

---

This Agreement between University of Windsor -- Mariia Selivanova ("You") and John Wiley and Sons ("John Wiley and Sons") consists of your license details and the terms and conditions provided by John Wiley and Sons and Copyright Clearance Center.

License Number	4657201089197
License date	Aug 27, 2019
Licensed Content Publisher	John Wiley and Sons
Licensed Content Publication	Advanced Functional Materials
Licensed Content Title	Tough, Semiconducting Polyethylene-poly(3-hexylthiophene) Diblock Copolymers
Licensed Content Author	N. Stingelin-Stutzmann, P. Smith, H. Sirringhaus, et al
Licensed Content Date	Aug 23, 2007
Licensed Content Volume	17
Licensed Content Issue	15
Licensed Content Pages	6
Type of use	Dissertation/Thesis
Requestor type	University/Academic
Format	Print and electronic
Portion	Figure/table
Number of figures/tables	1
Original Wiley figure/table number(s)	Figure 1
Will you be translating?	No
Order reference number	88
Title of your thesis / dissertation	Design and Preparation of Stretchable Semiconductors through Polymer Blending
Expected completion date	Aug 2019
Expected size (number of pages)	153

**THE AMERICAN ASSOCIATION FOR THE ADVANCEMENT OF SCIENCE LICENSE  
TERMS AND CONDITIONS**

Aug 27, 2019

---

This Agreement between University of Windsor -- Mariia Selivanova ("You") and The American Association for the Advancement of Science ("The American Association for the Advancement of Science") consists of your license details and the terms and conditions provided by The American Association for the Advancement of Science and Copyright Clearance Center.

License Number	4657191290096
License date	Aug 27, 2019
Licensed Content Publisher	The American Association for the Advancement of Science
Licensed Content Publication	Science
Licensed Content Title	Highly stretchable polymer semiconductor films through the nanoconfinement effect
Licensed Content Author	Jie Xu,Sihong Wang,Ging-Ji Nathan Wang,Chenxin Zhu,Shaochuan Luo,Lihua Jin,Xiaodan Gu,Shucheng Chen,Vivian R. Feig,John W. F. To,Simon Rondeau-Gagné,Joonsuk Park,Bob C. Schroeder,Chien Lu,Jin Young Oh,Yanming Wang,Yun-Hi Kim,He Yan,Robert Sinclair,Dongshan Zhou,Gi Xue,Boris Murmann,Christian Linder,Wei Cai,Jeffery B.-H. Tok,Jong Won Chung,Zhenan Bao
Licensed Content Date	Jan 6, 2017
Licensed Content Volume	355
Licensed Content Issue	6320
Volume number	355
Issue number	6320
Type of Use	Thesis / Dissertation
Requestor type	Scientist/individual at a research institution
Format	Print and electronic
Portion	Figure
Number of figures/tables	1
Order reference number	110
Title of your thesis / dissertation	Design and Preparation of Stretchable Semiconductors through Polymer Blending
Expected completion date	Aug 2019
Estimated size(pages)	153

ELSEVIER LICENSE  
TERMS AND CONDITIONS

Aug 27, 2019

---

This Agreement between University of Windsor -- Mariia Selivanova ("You") and Elsevier ("Elsevier") consists of your license details and the terms and conditions provided by Elsevier and Copyright Clearance Center.

License Number	4657240693857
License date	Aug 27, 2019
Licensed Content Publisher	Elsevier
Licensed Content Publication	Polymer
Licensed Content Title	Backbone orientation in semiconducting polymers
Licensed Content Author	Itaru Osaka, Kazuo Takimiya
Licensed Content Date	Feb 24, 2015
Licensed Content Volume	59
Licensed Content Issue	n/a
Licensed Content Pages	15
Start Page	A1
End Page	A15
Type of Use	reuse in a thesis/dissertation
Intended publisher of new work	other
Portion	figures/tables/illustrations
Number of figures/tables/illustrations	2
Format	both print and electronic
Are you the author of this Elsevier article?	No
Will you be translating?	No
Order reference number	13
Original figure numbers	Figure 1 and Figure 2
Title of your thesis/dissertation	Design and Preparation of Stretchable Semiconductors through Polymer Blending
Expected completion date	Aug 2019
Estimated size (number of pages)	153



**Title:** Morphology and Electronic Properties of Semiconducting Polymer and Branched Polyethylene Blends  
**Author:** Mariia Selivanova, Ching-Heng Chuang, Blandine Billet, et al  
**Publication:** Applied Materials  
**Publisher:** American Chemical Society  
**Date:** Apr 1, 2019  
Copyright © 2019, American Chemical Society

Logged in as:

Mariia Selivanova  
University of Windsor[LOGOUT](#)**PERMISSION/LICENSE IS GRANTED FOR YOUR ORDER AT NO CHARGE**

This type of permission/license, instead of the standard Terms & Conditions, is sent to you because no fee is being charged for your order. Please note the following:

- Permission is granted for your request in both print and electronic formats, and translations.
- If figures and/or tables were requested, they may be adapted or used in part.
- Please print this page for your records and send a copy of it to your publisher/graduate school.
- Appropriate credit for the requested material should be given as follows: "Reprinted (adapted) with permission from (COMPLETE REFERENCE CITATION). Copyright (YEAR) American Chemical Society." Insert appropriate information in place of the capitalized words.
- One-time permission is granted only for the use specified in your request. No additional uses are granted (such as derivative works or other editions). For any other uses, please submit a new request.

## **VITA AUCTORIS**

Name: Mariia Selivanova

Place of Birth: Horodok, Khmelnytskyi Oblast

Year of Birth: 1996

Education: National University of Kyiv-Mohyla Academy (NaUKMA), Kyiv, Ukraine

B.Sc. (2013-2017)

University of Windsor, Windsor, Ontario

M.Sc. (2017-2019)